Theses and Dissertations   Graduate School

2017

Investigation of Polymeric Composites for Controlled Drug Release

Hsi-wei Yeh

Investigation of Polymeric Composites for Controlled Drug Release

A dissertation submitted in partial fulfillment of the requirements for the degree of Doctor of Philosophy at Virginia Commonwealth University.

by

Hsi-wei Yeh
Doctor of Philosophy
Department of Mechanical and Nuclear Engineering, 2017

Director: Da-ren Chen, Ph.D.
Professor and Floyd D. Gottwald, Sr. Chair
Department of Mechanical and Nuclear Engineering

Virginia Commonwealth University
Richmond, Virginia
June, 2017

Acknowledgment

TABLE OF CONTENTS

List of Tables

List of Figures

xi

Abstract

INVESTIGATION OF POLYMERIC COMPOSITES FOR CONTROLLED DRUG RELEASE

By Hsi-wei Yeh, Ph.D.

A dissertation submitted in partial fulfillment of the requirements for the degree of Doctor of Philosophy at Virginia Commonwealth University.

Virginia Commonwealth University, 2017.

Major Director: Da-ren Chen, Ph.D., Professor and Floyd D. Gottwald, Sr. Chair, Department of Mechanical and Nuclear Engineering

The Electrospray (ES) technique is a promising particle generation method for drug delivery due to its capabilities of producing monodisperse PLGA composite particles with unique configurations and high drug encapsulation efficiency. In the dissertation work, the coaxial dual capillary ES was used to generate drug-loaded core-shell PLGA particles to study the effects of particle filling materials, drug loading locations and particle shell thicknesses on the resultant *in vitro* release behaviors of the hydrophilic and/ or hydrophobic model drugs. The work can be divided into two parts: 1) the extended release of the combination of a highly hydrophilic compound (Theophylline, THY) and a highly hydrophobic compound (Budesonide, BUD) and 2) the extended and sequential release of the combination of a hydrophilic large-molecule compound (Bovine Serum Albumin, BSA) and a hydrophobic small-molecule compound (Paclitaxel, PTX). In the part 1 research work, the coaxial dual capillary ES was employed to generate core-shell PLGA particles (particle size: 400 nm and 1 μm) loaded with THY and/ or BUD to study the critical factors for extended release of both drugs. The results suggest that the PLGA with a lower molecular weight is suitable for slowing down the release rate of THY due

to its lower porosity. The particle shell thickness is also essential to further decrease the release rate of THY, and co-encapsulation of BUD and THY in the particle core was confirmed to be the most effective drug loading strategy for extended release of both drugs. In the part 2 research work, PLGA (Mw: 7,000-17,000 g/mol, LA/GA: 50/50) was selected as the particle filling material. Release rate of BSA could be decreased by increased particles shell layer thicknesses. The sequential release of BSA and PTX was achieved with 400-nm PLGA particles by loading the two drugs together in the particle core because the BSA release rate was accelerated by the presence of PTX in the particle core. The formulation strategy obtained in this study can be in principle generalized for biopharmaceutical applications of extended release and sequential release in fixed-dose combination therapy.

Chapter 1

Introduction

1.1 Significance of Extended Release Drug Delivery Systems

Surgery, psychotherapy, physical therapy, radiation, and pharmacotherapy are methods usually used to treat illnesses and diseases clinically. Among them, pharmacotherapy (treatment with drugs) is the most frequently used technique because it is, generally speaking, the most cost-effective and preferred method with the broadest range of applications to the greatest variety of disease states. With the advancement of modern pharmaceutical technology, pharmacotherapy can even be considered as the first line therapy against certain diseases that were conventionally treated by other forms of treatment.

Over the past 120 years, health regulations and amendments have been promulgated by the government of the United States of America to control quality, safety and efficacy of drugs/ products and to ensure that they undergo strict review and approval processes before listed into the market. The IND (Investigational New Drug) application and review were also included into the pharmaceutical product development process to further assure adequate protection for subjects recruited into human clinical trials [Banker and Rhodes, 2002]. However, there is still room for further improvement to provide patients with better life quality when administrated with pharmacotherapy.

Figure 1.1 is a typical pharmacokinetic level-time curve of a non-intravenous systemic drug delivery system describing the relationship between the concentration of the active pharmaceutical ingredient of a drug product in the plasma and the time after it is administered to a patient. The therapeutic window denoted in Figure 1.1 (A) represents the range of the plasma drug concentration when the drug product

administered is efficacious but non-toxic to the patient during its duration. Figure 1.1 (B) shows the real situation of the multiple dose treatment that the dose accumulation phenomenon is usually seen after the same drug product is repeatedly administered to a patient. The dose accumulation could impose a risk that allows the drug plasma concentration to exceed the level of minimum toxic concentration (MTC) and to bring toxicity and side effects to patients even though the advised dosing frequency is fully complied. These side effects are not always in acceptable levels to patients, especially for drug molecules with very high potency, such as cancer drugs. Furthermore, repeated dosing is inconvenient to patients especially for those with dementia diseases or for those have to constantly go back to hospitals for drug administration. That is why the goals of modern pharmaceutical technology are to pursue the prolonged duration, the maintenance of the drug plasma concentration level within its therapeutic window, the reduced dosing frequency to avoid dose accumulation and to enhance the patient compliance. Such goals can be achieved by the application of extended (or sustained) drug release technology to modify the drug release rate.
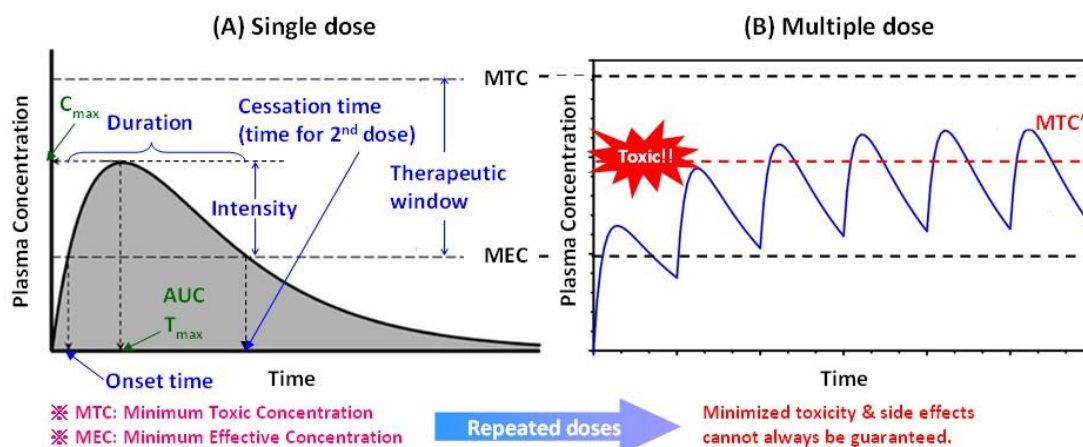
Figure 1.1. A typical pharmacokinetic level-time curve of a non-intravenous systemic drug delivery system after it is administered to a patient: (A) the single dose case, (B) the multiple dose case.

1.2 Extended Release Drug Delivery Systems Controlled by Diffusion

Extended release is a term for a dosage form that is modified to protract the release rate of its active pharmaceutical ingredient compared to that observed for an immediate-release dosage form according to the definition by the United States Pharmacopeia Chapter 1151. Drug release from extended release dosage forms is rate-controlled by diffusion, dissolution or osmotic pressure. By judiciously utilizing these control mechanisms, pharmaceutical companies have successfully put various extended release drug products on the market to treat diseases or to be used for other clinical applications, such as cancer, hepatitis, central nervous system diseases, urologic diseases, intestinal diseases, pain management, and contraceptive applications according the U.S. FDA website. Among the three types of mechanisms controlling drug release from an extended release drug product, the diffusion-controlled mechanism is considered the most promising one because of its relatively precise control over release rates for both hydrophobic and hydrophilic drug

4

molecules, its biodegradable property as therapy without surgical operations, and its acceptable price to patients [Nair and Laurencin, 2006]. Statistical data (Figure 1.2) further indicates that it is widely applied to investigational new drugs with the highest activity of currently ongoing human clinical trials among modified drug delivery systems [Anselmo and Mitragotri, 2014].
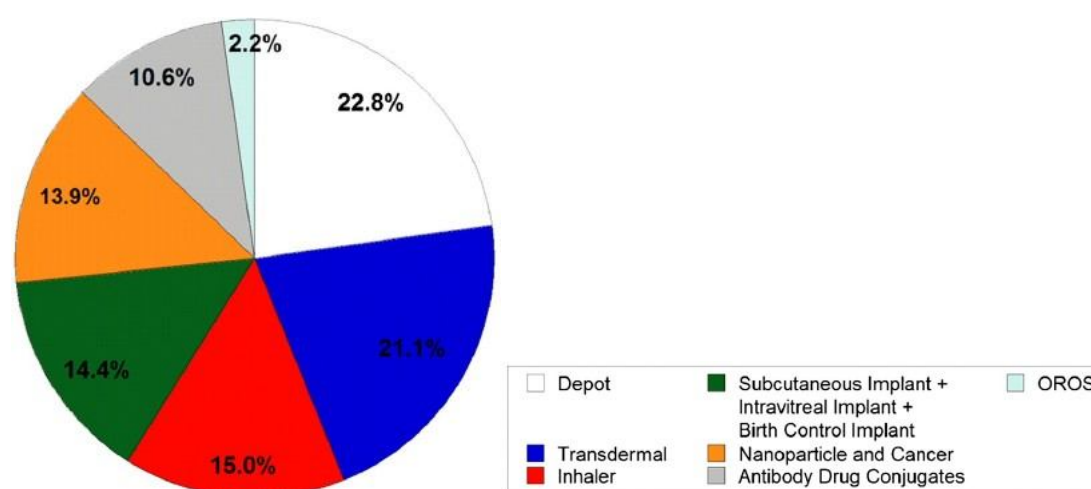
Figure 1.2. Normalized pie chart for clinical trial search on **clinicaltrials.gov** that counts the hits for clinical trials that are active and currently ongoing [Anselmo and Mitragotri, 2014].

Matrix-type and core-shell type biodegradable polymeric microspheres are the most common formulations used in commercialized extend release dosage forms controlled by diffusion. They are often made of poly(lactic-co-glycolic acid) (i.e. PLGA) or polylactic acid (i.e. PLA), two FDA-approved biodegradable synthetic polymers without safety concerns to human bodies, to release drugs for longer period of time [Nair and Laurencin, 2006; Kerimoğlu and Alarçin, 2012; Nagavarma et al., 2012; Rytting et al., 2008; Yang and Pierstorff, 2012; Danhier et al., 2012].

Considering the routes they are administered, usually subcutaneous (SC) injection or intramuscular (IM) injection [Nair and Laurencin, 2006], these drug-containing particles are usually with the sizes no greater than the micron scale. Table 1.1 summarizes the approved pharmaceutical products containing PLGA-based micro-particulate formulations [Kerimoğlu and Alarçin, 2012]. They are mostly given to patients as depots to slowly and continuously supply drug molecules into the systemic blood circulation, and there are currently no drug products containing PLGA-based nanoparticulate formulations in the market [Sah and Sah, 2015].

Product name	Active ingredient	Company	Application
Lupron Depot®	Leuprolide acetate	TAP	Prostate cancer
Nutropin Depot®	Growth hormone	Genetech	Pediatric growth hormone deficiency
Suprecur® MP	Buserelin acetate	Aventis	Prostate cancer
Decapeptyl®	Triptorelin pamoate	Ferring	Prostate cancer
Sandostatin LAR® Depot	Octreotide acetate	Novartis	Acromegaly
Somatuline® LA	Lanreotide	Ipsen	Acromegaly
Trelstar™ Depot	Triptorelin pamoate	Pfizer	Prostate cancer
Arestin®	Minocycline	Orapharma	Periodontal disease
Risperidal® Consta™	Risperidone	Johnson & Johnson	Antipsychotic

Table 1.1. PLGA-based microparticles available on the market [Kerimoğlu and Alarçin, 2012].

PLGA nanoparticles have been considered potential for intravenous drug delivery systems [Muthu, 2009]. Like liposomal particulate formulations, the enhanced permeability and retention effect (EPR effect) and the internalization of PLGA nanoparticles into cells via endocytosis make PLGA nanoparticles promising to be applied to anticancer and antibiotic therapy [Danhier et al., 2012; Davis et al., 2008]. Table 1.2 summarizes the major pharmaceutical and biopharmaceutical characteristics shared by PLGA nanoparticles and liposomal nanoparticles and those possessed by PLGA nanoparticles only, suggesting that more research work on PLGA

nanoparticles is demanding for their wider clinical applications [Nair and Laurencin, 2006; Davis et al., 2008; Sipai et al., 2012; Cao et al., 2014; Leonard et al., 2012; Ali et al., 2014; Zhang et al., 2008; Beletsi et al., 2005].

In view of non-invasive route of drug administration, PLGA formulations are promising for local therapies of pulmonary diseases via inhalation drug delivery [Ungaro et al., 2012; Ozeki and Tagami , 2014]. With the large pulmonary surface area and extensive blood supply in the alveolar region of the lung, pulmonary drug administration is thus also promising for systemic drug delivery, capable of bypassing the hepatic first pass metabolism and achieving rapid onset of action with lower doses and side effects. However, the intrinsic mucociliary clearance in airways and macrophages in alveolar regions hamper the retention of drugs to utilize the bronchial circulation for drug absorption. Inhaled PLGA particles smaller than 1 μm have potential to reach higher particle deposition percentage in the alveolar region than those greater than 6 μm in diameter [HEYDER et al., 1986]. Compared with PLGA microspheres, these PLGA nanoparticles are with slower clearance rate by alveolar macrophages and minimized elimination by mucociliary clearance, making them promising to achieve longer retention time in the deep lung for greater bioavailability [Smyth and Hickey, 2011].

	Liposomes	Polylactide-co-glycolide (PLGA) particles
Capabilities	- Encapsulation of hydrophilic, hydrophobic, and biological molecules. - Facilitating drug absorption at the site of action. - Enhancing the retention time of drug molecules at the target site. - Prolonging half-life of drug molecules within blood circulation by PEGylation technique. - Targeting cancer cells by the EPR effect. - Protecting physical, chemical, and biological properties of drug molecules under physiological conditions.	- Encapsulation of hydrophilic, hydrophobic, and biological molecules. - Facilitating drug absorption at the site of action. - Enhancing the retention time of drug molecules at the target site. - Prolonging half-life of drug molecules within blood circulation by PEGylation technique. - Targeting cancer cells by the EPR effect. - Protecting physical, chemical, and biological properties of drug molecules under physiological conditions. - Sustaining drug blood concentration level and minimizing peak drug concentration by IM/ SC administrations.

Table 1.2. Pharmaceutical and biopharmaceutical characteristics of PLGA and liposomal nanoparticles.

1.3 Methods for the Generation of PLGA Particles

Various techniques have been used in published literatures to generate PLGA nanoparticles to conduct *in vitro* or *in vivo* drug release experiments in order to study their potential applications in nanomedicine. Among these techniques, solvent evaporation technique, nanoprecipitation technique, and spray drying technique are the most frequently used methods, and each of them has its pros and cons. Solvent evaporation is a process used to fabricate PLGA nanoparticles by evaporation of the water-immiscible organic solvent from droplets generated by emulsifying drug solution or drug dispersion in the continuous phase containing surfactants [O'Donnell and McGinity, 1997]. Though it has been used to encapsulate either hydrophobic or hydrophilic medicaments, encapsulation efficiency of PLGA nanoparticles generated with this process is usually low, especially for drug molecules with greater

hydrophilicity [Hao et al., 2014; O'Donnell and McGinity, 1997; Popa and Dumitriu, 2013]. Moreover, the broad size distribution of the prepared particles is another shortcoming of this process, which affects drug release behaviors of PLGA nanoparticles and their interactions with cells [Sah and Sah, 2015]. Slightly different from solvent evaporation technique, a nanoprecipitation process involves evaporation of the organic solvent after injecting the drug-containing polymer solution into a stirred continuous phase containing surfactants. Fast diffusion of the water-miscible solvent then causes deposition of PLGA at the interface between water and the organic solvent and instantaneous formation of nanoparticles [Nagavarma et al., 2012]. Compared with the solvent evaporation process, the nanoprecipitation process is a relatively mild one since high energy input is not required. The process can be accomplished without any surfactants added into the continuous phase by using suitable benign solvents, which greatly minimize the concerns with toxicity caused by solvents and surfactants. However, removal of benign organic solvents is challenging because of their low volatility. Despite some attempts to improve the drug loading, the encapsulation efficiency of PLGA nanoparticles generated via the nanoprecipitation technique, especially for hydrophilic drug compounds, is usually low [Schubert et al., 2011]. Spray drying is another method often used to generate PLGA nanoparticles. Its first application comes from the year 1860 and is adaptable in an industrial scale as continuous and automatic control [Guterres et al., 2009; Cal and Sollohub, 2010; Mu and Feng, 2001]. Generally speaking, spray drying is to transform the feed in a fluid state into the product in a dried particulate form by spraying the feed into a gaseous drying medium [Patel et al., 2009; Cal and Sollohub, 2010]. Like solvent evaporation,

the spray drying technique can be used to encapsulate hydrophilic and hydrophobic drug compounds into PLGA nanoparticles [Mu and Feng, 2001; Guterres et al., 2009]. However, the conventional spray drying technique is incapable of generating PLGA particles with special internal structures to provide diverse biopharmaceutical applications [Patel et al., 2009].

In view of the facts mentioned above, the electrospray (ES) technique is considered excellent to be used to generate PLGA nanoparticles because it possesses all advantages and overcomes all disadvantages of aforementioned techniques. By applying the electrospray technique, monodisperse PLGA nanoparticles can be generated in a large scale via a single step process which is potential for industrial applications in the future [Lee et al., 2010; Sridhar and Ramakrishna, 2013]. The electrospray process can encapsulate drug molecules into PLGA nanoparticles with significantly higher encapsulation efficiency compared with conventional particle generation processes regardless of hydrophilicity and molecular weight of the loaded drug molecules [Bock et al., 2012; Lee et al., 2010; Hao et al., 2014]. Furthermore, it can also be used to generate PLGA nanoparticles with unique structures for less extent initial burst release compared with those generated via conventional particle generation techniques [Lee et al., 2010]. Content of residual solvents used during the particle generation process is relatively lower than conventional particle generation processes in the liquid phase, leading to less safety concerns for potential biopharmaceutical applications [Bock et al., 2012, Bai and Yang, 2013; Rezvanpour et al., 2010].

According to aforementioned background information, the motivation of this

study is therefore to employ the electrospray technique to generate biocompatible PLGA nanocomposite with unique configurations to deliver drugs. Because of the increasing importance of the fixed-dose combination therapy to patients requiring multiple therapies for simplified disease management and enhanced medication concordance, drug release behaviors of co-encapsulated combination drugs with significant differences in hydrophilicity and molecular weights from matrix-type and core-shell type PLGA nanoparticles are investigated, and release profiles of the single active agent encapsulated in a single dosage formulation are also studied as a reference for the combination PLGA nanoparticulate formulations. Through this research, we expect to provide general principles from systematic release profile studies for sustained release and/ or sequential release of fixed-combined hydrophilic and hydrophobic active ingredients from PLGA nanoparticles for their potential biopharmaceutical applications in inhalation therapy and cancer therapy.

1.4 Review of Drug Delivery with ES PLGA Nanoparticles

1.4.1   Matrix-type PLGA Nanoparticles Generated by the Single Capillary ES

Though electrospray technique has been studied for more than 100 years, it has begun to be applied to generate micro-/nano-structured materials since 1990s [Xie et al., 2015]. Due to the progress of nanomedicine and the limitations of employing conventional methods to produce PLGA nanoparticles, electrospray has brought to the attention for its advantages to generate PLGA nanoparticles for encapsulation and extended release of therapeutics since 2000s.

Challenges of formulating hydrophobic medicaments according to modern

pharmaceutical science reveal the fact that PLGA micro-/nano-particles could be a useful formulation to deliver drugs with low water solubility. Xie et al. (2006) [Xie et al., 2006] reported that Paclitaxel, a highly hydrophobic small molecule used for cancer treatment, can be encapsulated into PLGA particles with size ranging from 355 nm to 1.2 μm by adjusting the feed flow rate of spray liquid and the concentration of PLGA. They also found that a higher PLGA concentration is helpful to generate PLGA particles with smooth surface and spherical morphologies. Though they didn't test the encapsulation efficiency of the PLGA particles generated in their research, their results demonstrated that PLGA nanoparticles can be used to encapsulate hydrophobic drug molecules. Similar research was done later by Valo et al. in 2009 [Valo et al., 2009] that both hydrophilic and hydrophobic model drugs, Salbutamol sulfate and Beclomethasone dipropionate respectively, were successfully encapsulated in 200-nm PLA particles with narrow size distribution. Drug encapsulation efficiency was higher than 50% regardless of hydrophilicity of the drug, demonstrating that electrospray is more efficient than conventional techniques based on liquid phases to encapsulate both hydrophilic and hydrophobic drugs. They also claimed that electrospray can be used to co-encapsulate a hydrophilic and a hydrophilic drug molecule in matrix-type PLGA nanoparticles. However, they didn't actually prove the feasibility of their claim with data. The above two published scientific articles reported the capability of electrospray to encapsulate small molecule drugs, yet they didn't address how drugs are released from the vehicles.

In 2011, Almería et al. [Almería et al., 2011] utilized the single nozzle electrospray technique, the multiplexed electrospray technique, and the solvent

evaporation technique to encapsulate three molecules with different hydrophilicity, which were Rhodamine B (RHO_B), Rhodamine B octadecyl ester perchlorate (RHO_{BOEP}) and Doxorubicin hydrochloride (DOX). Through a series of comparisons, they concluded that release rates of the hydrophilic and the hydrophobic drug molecules were both greater when encapsulated in matrix-type electrospray nanoparticles with smaller particle size. Higher drug release rate was observed for the drug with greater hydrophilicity due to the less affinity between the drug and PLGA. They also confirmed that the technique used to produce PLGA nanoparticles didn't significantly affect drug release profiles for the same drug compound regardless of the hydrophilicity of the loaded drug. Through systematic studies, the results of this research help us learn the effects of particle size, particle generation methods, and the hydrophilicity of drug on drug release profiles of PLGA nanoparticles.

Drugs classified as Class 1 according to the Biopharmaceutical Classification System (BCS) defined by U.S. FDA are suitable to be formulated into conventional immediately release dosage forms because of the high water solubility and the easiness to cross biological membranes to be absorbed. However, they are also easy to be excreted by Kidney, except for antibody therapeutics with extremely high molecular weights, meaning that t.i.d. or q.i.d. dosing frequencies are usually needed especially for BCS Class 1 drugs with short half-lives in human body. That is why extended release formulations for hydrophilic drugs having short half-lives are with great values.

N-Acetylcysteine (NAC) is a hydrophilic small molecule drug containing a thiol group. It possesses antioxidant and mucolytic properties and is often used to treat

neuroinflammation, fibrosis, cartilage erosion and acetaminophendetoxification. Its low oral bioavailability and high plasma protein binding tendency after intravenous administration make it suitable to be encapsulated with PLGA nanoparticles as protection away from plasma proteins. Previous studies performed by Zarchi et al. (2015) [Zarchi et al., 2015] showed that NAC can be efficiently encapsulated, with encapsulation efficiency greater that 50%, in PLGA particles smaller than 150 nm by employing optimized electrospray process parameters. The resultant nanoparticles performed extended release of NAC for greater than 2 days *in vitro*, suggesting the potentials of PLGA nanoparticles smaller than 150 nm to be applied to hydrophilic small molecule drug delivery.

Due to the successful research results of the matrix-type PLGA nanoparticles generated via electrospray to encapsulate and to slowly release both hydrophilic and hydrophobic drugs *in vitro*, further studies have been done for its application in targeted drug delivery systems for high potency drugs. Bai et al. (2014) [Bai and Liu, 2014] proposed to use a single nozzle electrospray process to generate polyethylene glycol-poly(lactic-co-glycolic acid) (PEG-PLGA) nanoparticles. Compared with conventional methods requiring bioconjugation reactions to synthesize PEG-PLGA first before particle generation procedures, results of FTIR and NMR confirmed the maleimide moiety of PEG intact as incorporated into resultant nanoparticles after the electrospray processing. The intact maleimide moiety ensures the successful coupling of CD44 antibody through a chemical reaction between its thiol group and the maleimide moiety of PEG-PLGA nanoparticles. *In vitro* cell studies showed significant effectiveness of the Cisplatin-loaded CD44-PEG-PLGA nanoparticles on

antiproliferation of CP70 and SKOV ovarian cancer cell lines. Based on our literature review, this is the first study to generate antibody-PEG-PLGA nanoparticles with the electrospray technique and to confirm their anticancer effectiveness via *in vitro* cell studies, even though they didn't study *in vitro* drug release profiles of the as-produced nanoparticles.

1.4.2 Core-shell Type PLGA Nanoparticles Generated by the Coaxial Dual Capillary ES

Like Section 1.4.1, numerous studies have been done to learn drug encapsulation, drug release and biological effectiveness of core-shell type PLGA nanoparticles generated via the coaxial dual capillary electrospray (ES) technique.

The polymer concentration of the outer liquid in a dual capillary electrospray process affects size of the particles. Generally speaking, a higher polymer concentration in outer polymer coating solution leads to larger particle size and vice versa. With this principle, Enayati et al. (2010) [Enayati et al., 2010] generated core-shell type PLGA particles with the size ranging from 120 nm to a few micrometers via adjusting the PLGA concentration of the spray liquid in the outer layer. Estradiol, a hydrophobic sex hormone with low oral bioavailability, was encapsulated in the core of these nanoparticles with encapsulation efficiency close to 70% and continuously released up to 20 days *in vitro*. The size effect was also reported in their research. Among the particles studied, drug release rate of Estradiol was faster from PLGA nanoparticles with smaller particle sizes because of their higher surface area to volume ratio. Nonetheless, drug release profiles were biphasic

regardless of the sizes of particles been studied.

To compare the performances of different types of formulations, Bai et al. (2013) [Bai and Yang, 2013] formulated Niclosamide, a hydrophobic compound used for the treatment of tapeworm infections, into electrosprayed Niclosamide, matrix-type PLGA nanoparticles, and core-shell type PLGA nanoparticles. The conventional Niclosamide solution formulation, dissolving Niclosamide in DMSO, was prepared and studied as the control group. Their results showed that the electrosprayed Niclosamide performed fastest drug release rate among all the formulations within 500 hours of test time because of its extremely high surface area to volume ratio and the uncontrolled release behaviors without PLGA in the formulation. During the same period of time, the drug release rate of the core-shell nanoparticles was always lower than that of the matrix-type nanoparticles yet the two-stage release profile could be clearly observed for the case of core-shell particles. Though both matrix-type and core-shell type PLGA nanoparticles exhibited greater drug release rates than electrosprayed Niclosamide due to the dose dumping phenomenon after the 500th hour of the release studies, such a finding was considered with limited use in reality by the author. The results of *in vitro* cell studies confirmed the greatest antiproliferation effectiveness of the electrosprayed matrix-type PLGA nanoparticles against ovarian cancer cells among all the tested formulations because of its large surface area to volume ratio and easiness to be incorporated into cells. The antiproliferation effectiveness of the electrosprayed core-shell type PLGA nanoparticles was surprisingly the lowest because of the slowest drug release rate controlled by particle structure.

Similar research was done by Lee et al. (2010) [Lee et al., 2010] to address the size effect and the structure effect of PLGA nanaparticles on drug release behaviors. Unlike the aforementioned studies, they employed the coaxial dual capillary electrospray technique and the solvent evaporation technique to encapsulate Budesonide, a hydrophobic drug compound, into the cores of the core-shell type PLGA nanoparticles and the matrix-type PLGA nanoparticles, respectively. In their results, particles smaller than 200 nm were successfully generated via electrospray with around 89.9% encapsulation efficiency, which was confirmed to be significantly higher than that of particles generated via the solvent evaporation technique. Due to the lesser surface loaded drugs, the core-shell type nanoparticles performed less severe initial burst release and continuously released Budesonide for more than two days. Particles with sizes ranging from 165 nm to 1.2 μm were generated by optimized electrospray process parameters through a thorough study on the effects of electric conductivity and polymer concentration of the outer spray liquid. Particles with smaller sizes were confirmed to release encapsulated Budesonide with a higher release rate than larger particles, which was concluded to be associated with pin holes formed on the surface of smaller particles as a result of the infusion of the surrounding release media into the particles. The encapsulation of epigallocatechin gallate (EGCG), a hydrophilic compound, into the matrix-type and the core-shell type PLGA nanoparticles was also studied in their research. Though the drug release profiles of EGCG were not studied, a significantly higher encapsulation efficiency of EGCG in electrospray core-shell PLGA nanoparticles than that in matrix-type PLGA nanoparticles produced by the solvent evaporation technique was reported.

Further research on coaxial dual capillary electrospray technique for hydrophilic drug delivery has been done after Lee's research published in 2010 for cancer treatment. 5-Aminolevulinic acid (ALA) is a natural amino acid synthesized by animal and plant mitochondria. It is often applied to the Photodynamic Therapy (PDT) as an important approach to treat solid tumors. Under physiological conditions, ALA is metabolized into Protoporphyrin IX (PpIX) by the heme biosynthesis. The resultant PpIX inherently tends to target tumors and requires much more time to be degraded in cancer cells than in normal cells. By applying photo excitation of light with special wavelength, the reactive oxygen species (ROX) is generated to perform anti-tumor activities. Due to the poor stability in the physiological environment, biodegradable drug carriers are considered promising to the delivery of ALA. Gual et al. (2015) [Guan et al., 2015] encapsulated ALA into core-shell structure PLGA nanoparticles with sizes ranging from 200 nm to 1 μm by adjusting the outer and the inner flow rate ratio. The reported encapsulation efficiencies of all the particles in their study were higher than 60% to slowly release ALA for more than 7 days. For nanoparticles, their results suggest that the smaller particle size did not necessarily result in greater drug release rate. Higher drug encapsulation efficiency in larger nanoparticles could also lead to faster drug release rate than that of smaller nanoparticles when these smaller particles were with lower encapsulation efficiency. Higher fluorescent intensity of intracellular PpIX in HSC-3 cells confirmed that the 200-nm electrosprayed PLGA nanoparticles were capable of delivering ALA into cells compared with the control group that no treatment was applied to HSC-3 cells.

The layered structure of PLGA nanoparticles makes them suitable to deliver

more than one medicament simultaneously. Due to the overly expressed efflux pumps usually seen in cancer cells, the coaxial dual capillary electrospray technique is promising to generate core-shell type PLGA nanoparticles for combination chemotherapy. Cao et al. (2014) [Cao et al., 2014] co-encapsulated Combretastatin A4 (CA4, a hydrophobic anti-angiogenesis agent) and Doxorubicin (DOX, a relatively hydrophilic drug molecule compared with CA4) in the shell and core of the nanoparticles, respectively. They also added biodegradable/ biocompatible polymers with different hydrophobic properties, i.e., the hydrophilic polyvinylpyrrolidone (PVP) and the hydrophobic poly(3-caprolactone) (PCL), in inner drug solution during the electrospray process to tailor release profiles of these dual drug loaded particles. Due to the high intermolecular affinity between CA4 and PLGA, slower release rate was always observed for CA4 even though it was encapsulated in the shell region regardless of the hydrophobicity of polymers in the core region. In addition, a higher release rate was observed for both CA4 and DOX when PVP was formulated in the core region resulted from greater influx of the surrounding release media into particles. Results of cell studies also demonstrated the melanoma cells B16-F10 and human umbilical vein endothelial cells (HUVECs) were sequentially targeted and killed by DOX and CA4 sequentially released from the particles.

In view of the importance of biomolecules in clinical applications and the potentials of core-shell type PLGA nanoparticles for combination chemotherapy, Wang et al. (2015) [Wang et al., 2015] employed the electrospray technique to encapsulate Bone morphogenetic protein 2 (BMP-2) and Vascular endothelial growth factor (VEGF) in the core and shell of the PLGA nanoparticles, respectively. Because

of the PLGA and PLA formulated in the core and shell, respectively, in these particles, drug release profiles of both BMP-2 and VEGF were better controlled than same drugs co-encapsulated into matrix-type PLGA nanoparticles produced via the single nozzle electrospray technique. Moreover, drug release behaviors of co-encapsulated BMP-2 and VEGF were independent with each other by comparing their release profiles from core-shell structure PLGA nanoparticles containing BMP-2 or VEGF individually. Results of *in vitro* cell studies and *in vivo* animal studies confirmed the effectiveness of the proposed core-shell PLGA nanoparticles on cell proliferation and the growth of bone tissues and blood vessels. This study indicated that core-shell type PLGA nanoparticles loaded with BMP-2 and VEGF could stimulate angiogenesis and osteogenesis to be applied to post-surgical repair of large bone defects.

As a conclusion of our literature review, great efforts have been made through previous studies to identify the key process parameters of electrospray and how these parameters affect size, size distribution and morphology of the resultant PLGA nanoparticles. Factors affecting rates of drug release from electrosprayed PLGA nanoparticles have also been identified as a reference to tailor their drug release behaviors for potential biopharmaceutical applications. Compared with conventional particle generation methods based on liquid phase, electrospray can often maintain the activity of the loaded drug and reach significant higher drug encapsulation efficiency regardless of the hydrophilicity of the loaded drugs, which is crucial prerequisite for extended drug release. Due to the simplicity of an electrospray process, key moiety for chemical reactions can be directly incorporated into PLGA nanoparticles, which greatly ensures successful coupling of antibody to particles for the applications of the

target therapy. Comparisons regarding *in vitro* drug release profiles and effectiveness through cell studies have been done for both hydrophilic and hydrophobic drugs encapsulated into PLGA nanoparticles with different internal configurations by either the electrospray technique or the solvent evaporation technique. However, limited studies have been done to systematically characterize *in vitro* drug release profiles of combination therapy encapsulated in PLGA nanoparticles with unique configurations. Because electrospray is a one-step process capable of generating particles with different conformations, we utilize the electrospray process in this dissertation work to produce drug-loaded PLGA nanoparticles with unique configurations and systematically investigate their resultant drug release behaviors. Key factors influencing drug release behaviors from PLGA nanoparticles are also identified to learn how to slowly release loaded drugs from ES PLGA nanoparticles for their biopharmaceutical application in combination therapy.

1.5 Research Objectives

The aim of this dissertation work is to advance our knowledge of *in vitro* drug release of one or two pharmacologic agents with varied hydrophilicity and molecular weights from PLGA nanoparticles with unique structures. Accordingly, the objective of this work is to investigate *in vitro* release profiles of drug-loaded PLGA nanoparticles to identify key factors that are critical for extended drug release and sequential drug release.

Chapter 2

Methods

2.1 Preparation of Drug-loaded PLGA Nanoparticles

Electrospray (also called electrohydrodynamic spray) is a liquid atomization phenomenon caused by electrical forces [Bock et al., 2012; Jaworek and Sobczyk, 2008]. Figure 2.1 is a schematic representation of a typical electrospray setup with the point-to-plate configuration [Hao et al., 2014]. An electrospray (ES) process begins with the deformation of the interface of a liquid droplet exiting a capillary by the electric field created by the applied high voltage on the capillary. The resultant electric charges generate electrostatic forces to compete and eventually to balance with surface tension of the droplet to reach the cone-jet mode operation. A thin jet is then ejected from the apex of the cone, and smaller micro-/nano-charged droplets are formed via jet breakup by coulomb repulsion to dissipate excess charges. Finally, ejected droplets are dried via evaporation of the spray solvent, and dry particles are collected on surface of the grounded substrate [Hao et al., 2014; Bock et al., 2012; Xie et al., 2006].

Dripping mode, silver bullet mode, pulsating mode, cone-jet mode, and multijet mode are the five modes that are usually seen during the operation of an electrospray process. Among them, the cone-jet mode holds a conspicuous position because it can be used to generate monodisperse particles [Chen et al., 1995; Mei and Chen, 2008]. Key process parameters of an electrospray process, such as the feed flowrate, the electric conductivity and the polymer concentration of the spray liquid, for PLGA micro-/nano-particle generation have been investigated and identified by previous studies. The results have been discussed in previous literature review sections on sustained drug release with PLGA particles produced by the electrospray technique.

Except for the key process parameters, spray solvent and the tip-to-collector (TTC) distance of the electrospray setup also affect morphology and monodispersity of the as-produced PLGA particles [Bock et al., 2012; Park and Lee, 2009]. Increasing the TTC and selecting a solvent, or a combination solvent system, with slower evaporation rate help enhance monodispersity and spherical morphologies of the resultant PLGA particles for favorable release behaviors [Bock et al., 2012; Park and Lee, 2009].
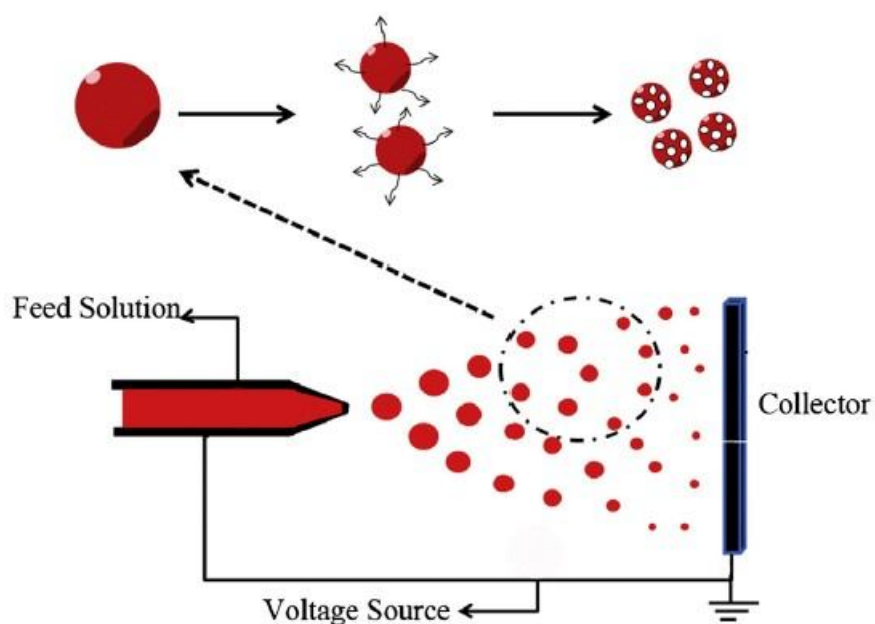
Figure 2.1. A schematic representation of a typical electrospray setup with the point-to-plate configuration [Hao et al., 2014].

In this dissertation work, an electrospray setup with the point-to-plate configuration was employed to generate and collect PLGA nanoparticles as shown in Figure 2.2. During the electrospray process, spray solutions, containing PLGA and/ or loaded drugs, were injected in the flow channels of the nozzle by programmable

syringe pumps (Harvard, Model PHD 2000). A positive DC voltage, via DC high voltage power supply (Bertan 230), was applied to the nozzle to help overcome surface tension of the spray liquids for generating monodisperse PLGA nanoparticles under cone-jet mode operation, monitored via a video microscope (Infinity, Model: K2 DistaMax) and a digital camera (Edmund optics, Model: 2013C LE). Mildly heated compressed dry air was also applied in our electrospray system to facilitate the evaporation of the solvents in sprayed droplets. A grounded substrate was placed under the nozzle at a proper distance away from its tip to collect the as-produced particles. The setup of the single capillary electrospray open system and the coaxial dual capillary electrospray open system are similar but different in type of the nozzle and the number of flow channels and syringe pump included in the process setup.

25
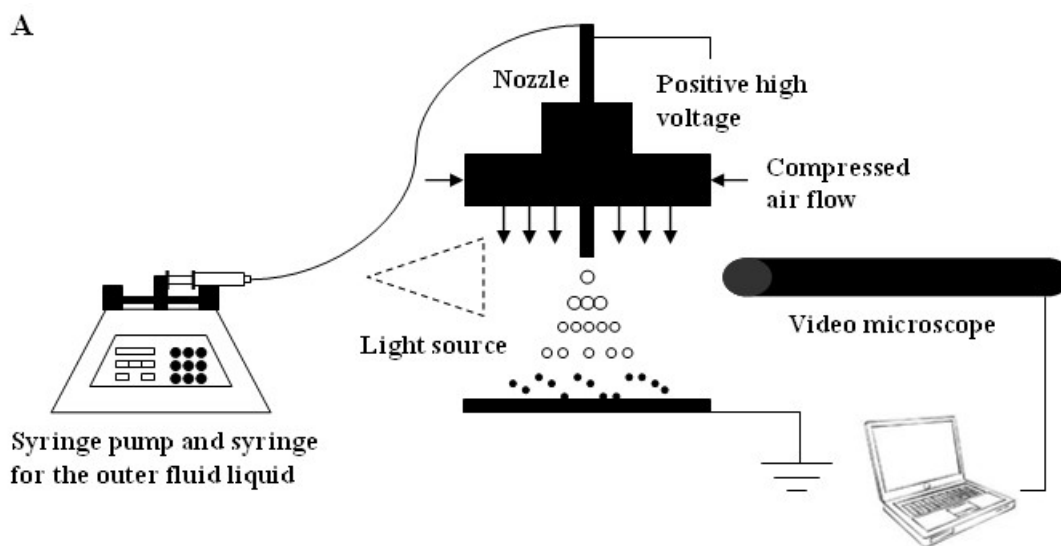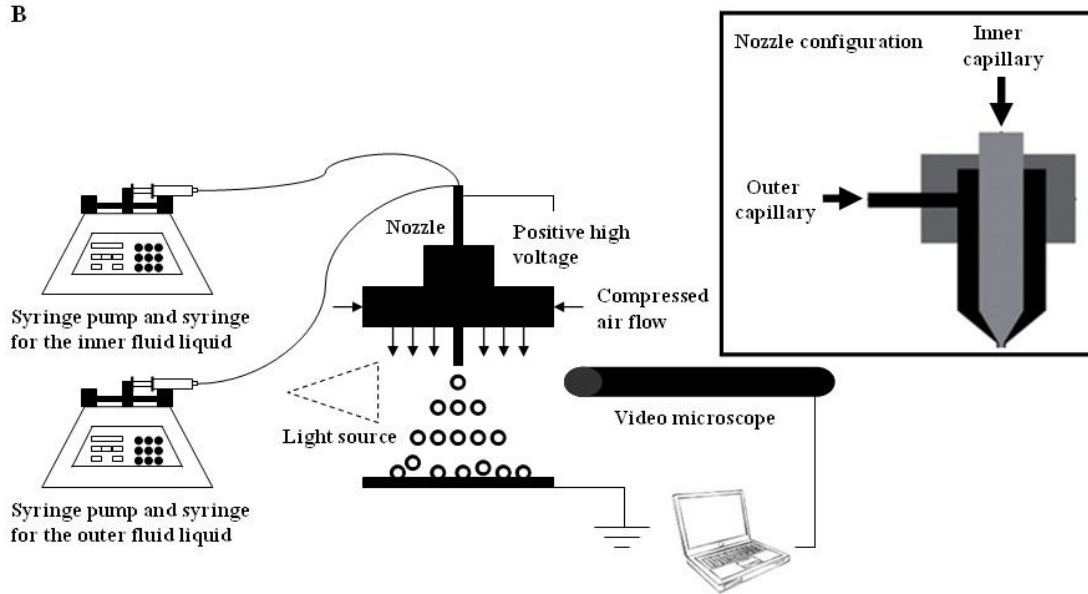
Figure 2.2. Schematic diagrams of (A) the single capillary electrospray process setup and (B) the coaxial dual capillary electrospray process setup used to generate matrix-type and core-shell type PLGA nanoparticles, respectively.

2.2 Characterization of Morphology and Size Distributions of PLGA Particles

The size distribution of prepared particles were primarily measured by either a scanning mobility particle sizer, SMPS (TSI Model 3081) for particles in the sizes ranging from 3 nm to 700 nm in diameter or an optical particle sizer, OPS (TSI Model 3330) for particles in the sizes ranging from 100 nm to 10 μm. Instead of an open system, a close electrospray system with a charge reduction chamber was connected with particle sizing instruments and used in this part of characterization. The differences between the electrospray open system and the close system are the grounded electrode and the charge reduction scheme applied to the close system only. In the close system, an aluminum orifice with 0.25 inches in diameter is placed at approximately 15 mm below tip of the nozzle as the grounded electrode. The carry air

flow of 10 liters per minute is used to transport the sprayed particles into the charge reduction chamber, where electrical charges of sprayed particles are minimized with four radioactive sources (Po210; MOD: P-2042) to reduce particle loss in the system. The charge-reduced particles are then sent into particle sizers for the characterization of their size distributions. Data from particle sizers were recorded in a PC for further analysis. The schematic diagram of the coaxial dual capillary electrospray close system along with a SMPS is illustrated in Figure 2.3 for the characterization of size distributions of core-shell type PLGA particles in the sizes ranging from 3 nm to 700 nm in diameter. The nozzle in the close electrospray system and the particle sizer are both replaceable for characterizing either matrix-type or core-shell type PLGA nanoparticles in different size ranges. The morphology of the prepared drug-loaded PLGA particles was also characterized by SEM (Hitachi, Model: SU-70 FE-SEM). Prior to SEM, the particle samples were sputtered with Platinum for 90 seconds (Denton Vacuum, Model: Desk V). The magnification of the SEM is 20x-800,000x.
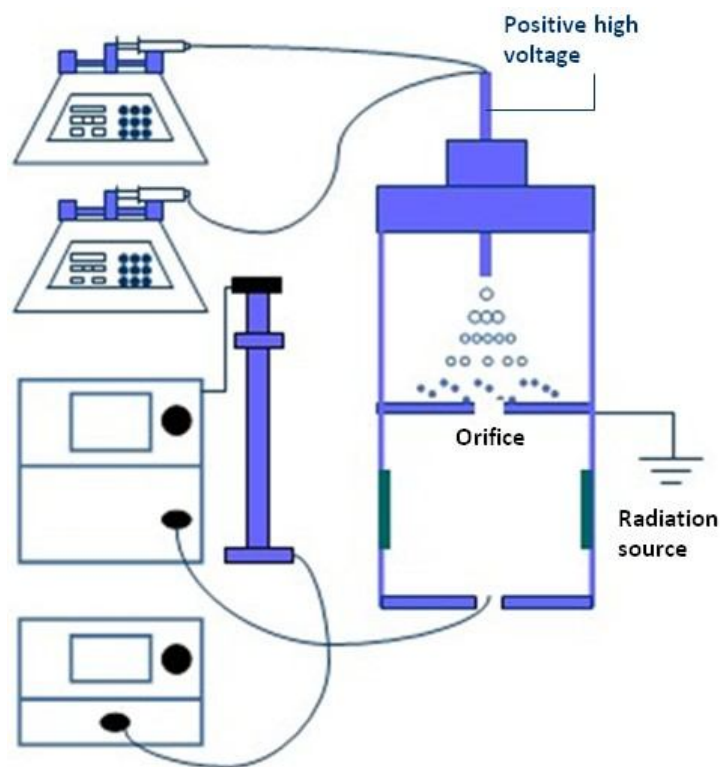
Figure 2.3. A schematic diagram of the electrospray close system along with a Scanning Mobility Particle Sizer (SMPS) to characterize size distributions of ES PLGA nanoparticles.

2.3 *In vitro* Drug Release Testing Procedures

In vitro drug release testing, or dissolution testing, is a commonly used tool in preclinical research within the pharmaceutical industry to study the performance of developing dosages and to monitor batch-to-batch quality control for mass production. It has been employed to investigate *in vitro* drug release behaviors of the myriad of dosage forms, such as transdermal patches, suspensions and chewing gums, though it was recommended for solid oral dosage forms in the beginning [Betageri et al., 2011]. Currently available mainstream methods to study release kinetics from nanoparticulate drug carriers are (i) dialysis; (ii) sampling and separation by using centrifugation [Betageri et al., 2011]. Both methods have been widely used previously,

generating *in vitro* drug release data for nanoparticles with the dialysis method and the centrifugation method in nearly forty and fifty cases of about ninety published literature articles, respectively, in 2011 [Zambito et al., 2012]. In order to establish a standardized procedure of the *in vitro* drug release testing on drug-loaded PLGA nanoparticles for this dissertation work, feasibility of the dialysis method for drug release testing was first studied in the following Section 2.3.1.

2.3.1 Investigation of the Dialysis Method

The application of colloidal drug carriers in drug delivery is getting greater attention recently. However, the separation of nanoparticles from the release media is challenging due to the very small size of the particles. Stronger centrifugal forces are therefore used in order to cleanly separate particles from the media, which often leads to inaccurate drug release results because the integrity of the nanoparticles is affected [Abdel-Mottaleb and Lamprecht, 2011]. Moreover, the accuracy of drug release results is also impacted because drug carriers are still releasing the encapsulated drugs during the centrifugation process.

Because the diffusion of drugs across the dialysis membrane can be the rate-limiting step of dialysis, feasibility of the dialysis method as a standardized procedure for *in vitro* drug release testing was assessed by studying the diffusion of Budesonide (the hydrophobic model drug) across the dialysis membrane with the apparatus shown in Figure 2.4. The dialysis bag (Spectrum®, Float-A-Lyzer, Molecular weight cutoff: 0.5-1 kD) had been pretreated by sequentially soaked in 40 ml 10% ethanol, DI water and PBS for 10 minutes, 20 minutes and overnight,

respectively, before dialysis was initiated. To learn whether Budesonide can diffuse from the donor phase (i.e., inside the dialysis bag) into the receiving phase (i.e., outside the dialysis bag), 10 μg Budesonide were dissolved in the 1-ml phosphate buffered saline (PBS, 0.02 M, pH 7.4), and the 1-ml Budesonide PBS solution was put in the dialysis bag. The bag was then put into a 50-ml glass beaker containing 40 ml PBS as the receiving phase with gentle stir. During the dialysis study, 1.5 ml PBS solution was sampled from the receiving phase along with equal volume of fresh PBS filled to the receiving phase at each sampling time. In the end of the 12-hour dialysis study, Budesonide concentrations in the dialysis bag and in the PBS sampled at pre-determined time intervals from the receiving phase were measured by HPLC. The cumulative mass of Budesonide in the receiving phase is displayed in Figure 2.5, evidencing the fact that the amount of Budesonide diffusing from the donor phase to the receiving phase was extremely small at each sampling time during the dialysis process. However, Budesonide concentrations in the donor phase before and in the end of the dialysis study were 10 μg/ml and 0.17 μg/ml, respectively, suggesting the fact that around 9.83 μg of Budesonide was leaving the donor phase during the dialysis process. The above finding implies potential interactions between Budesonide and the dialysis membrane. Therefore, the dialysis method is not a capable methodology to be used for *in vitro* drug release testing in the present dissertation study.
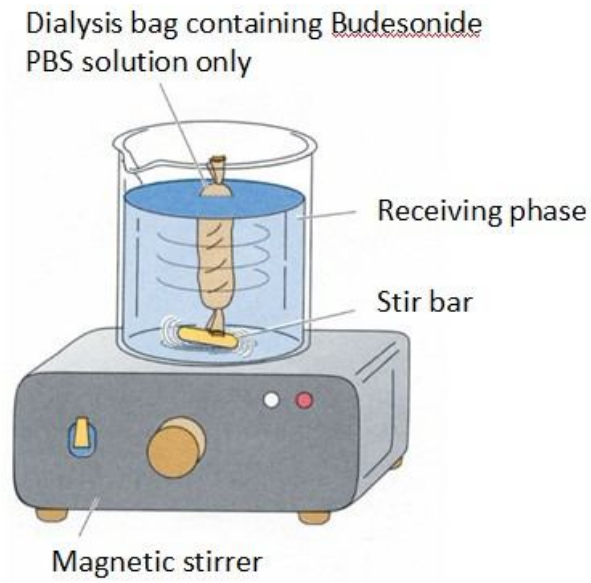
Figure 2.4. A schematic diagram of the dialysis apparatus for studying diffusion of Budesonide across

the dialysis membrane.
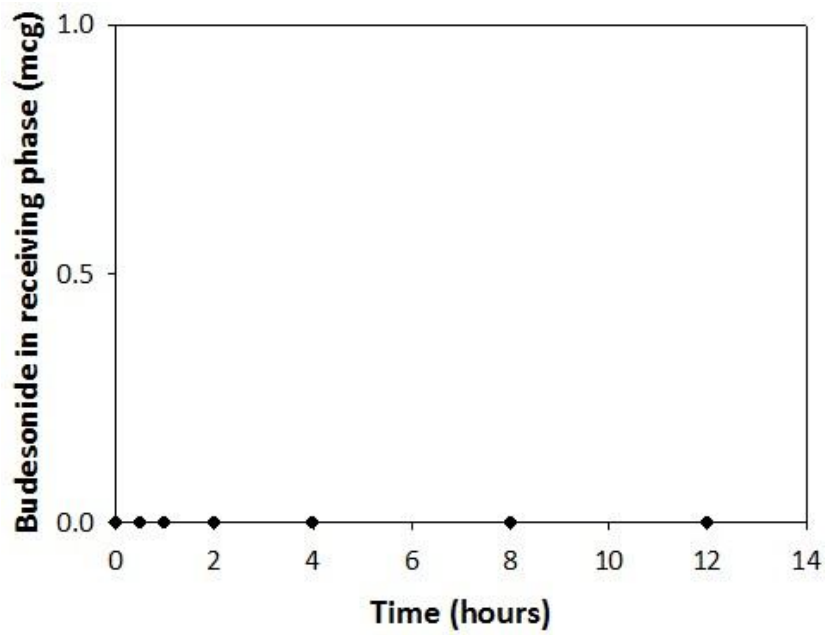
Figure 2.5. Cumulative mass of Budesonide detected in the 40-ml receiving phase (0.02 M PBS, pH 7.4)

during the 12-hour dialysis study.

2.3.2 Drug Release Testing Procedures with the Centrifugation Method

Previous research has proven that the dialysis method is not necessarily discriminating to generate descriptive data for significant comparison between different formulation parameters of nanoparticulate drug carriers [Zambito et al., 2012; Abdel-Mottaleb and Lamprecht, 2011]. Our earlier studies in Section 2.3.1 also indicated that the dialysis method is not an appropriate method for *in vitro* drug release testing for the tested model drugs.

In the present dissertation work, we utilized the centrifugation method to characterize drug release considering the fact that physical or chemical interactions between the test drugs and the dialysis membranes could affect the resultant release profiles. Moreover, the method also endued us with greater research flexibility to select drug compounds to be studied instead of been restricted by currently available dialysis membranes on the market. The procedures of the centrifugation method and the recipe of the release media are as follows:

<u>Procedures of the centrifugation method:</u>

(1) Incubated PLGA particles attached on the surface of an aluminum foil in a 15-ml plastic centrifugation tube containing 10 ml 0.02 M PBS (pH=7.4, [NaCl]=0.15 M) as the release media with the Shaker Water Bath (Thermo Scientific, Model: Precision 2870, setting: 40 RPM, 36.5 $^{\circ}$C). The optimized volume of the release media (i.e., 10 ml PBS) for the thesis study was determined by performing *in vitro* drug release testing on Budesonide encapsulated in 70-80 nm ES matrix-type PLGA (Mw: 7,000-17,000 g/mol, LA/GA: 50/50) nanoparticles (Budesonide-to-PLGA mass ratio: 2:10) and

comparing the resultant drug release profiles in various volumes of release media (i.e., 4 ml, 10 ml and 40 ml). Figure 2.6 depicts the Budesonide release profiles in different volumes of the release media. The result indicates that the drug release rate in greater volume of release media was higher on account of the greater driving force for drug diffusion. In view of our currently available bench-top centrifuge used to collect release media during drug release experiments, we chose 10 ml 0.02 M PBS ([NaCl]=0.15 M, pH=7.4) as the release media throughout the thesis work.

(2) Removed the aluminum foil from the plastic centrifugation tube at the pre-determined time intervals.

(3) Centrifugalized the tube with a bench-top centrifuge (eppendorf, Model: 5417C) at 14,000 RPM for 20 minutes to collect all release media and to minimize the loss of detached particles from the aluminum foil.

(4) Put the aluminum foil back into the plastic centrifugation tube and refilled the tube with fresh release media.

(5) Incubated the tube in a Shaker Water Bath till the next pre-determined time interval for another sampling.

(6) Quantified the amount of the released drug in the release media sampled at pre-determined time intervals by HPLC (Agilent, Model: 1260) or by a protein assay detected by an ELISA plate reader (BioTek, Model: Synergy H1).

Recipe and preparation protocol of the release media:

Step 1: Dissolved the following compounds in 600 ml distilled water.

NaH$_2$PO$_4$: 0.54 g.

Na$_2$HPO$_4$: 1.06 g.

NaCl: 5.26 g.

Step 2: Adjusted pH to 7.4.
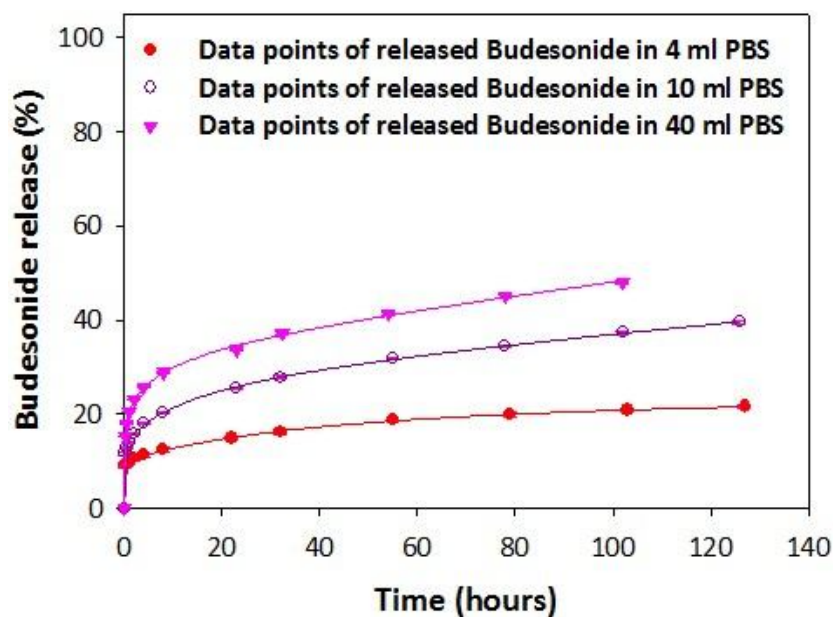
Figure 2.6. Budesonide release profiles of 70-80 nm PLGA (Mw: 7000-17000 g/mol, LA/GA: 50/50) particles in different volumes of release media (0.02 M PBS, [NaCl] = 0.15 M, pH = 7.4).

2.4 Analytical Method Development for Quantification of the Loaded Drugs

2.4.1 HPLC Analytical Method Development for the Quantification of the Small-molecule Model Drugs

In order to quantify the amount of drugs released from PLGA nanoparticles in the release media, reliable HPLC analytical methods of small-molecule model drugs have been developed based on our lab facilities. This was done in order to

characterize drug release profiles for the tested nanoparticulate formulations. The Agilent 1260 HPLC system composed of a quaternary pump, a standard autosampler, a thermostatted column compartment, a ZORBAX SB-C18 2.1 x 150 mm, 3.5 μm column, and a diode-array detector was used throughout this research. Acetonitrile, Methanol, and pure water were the solvents for the mobile phase.

A literature review has been conducted for HPLC analytical methods of Budesonide [Gupta and Bhargava, 2006; Naikwade and Bajaj, 2008; United States pharmacopeia 35 (2012)], Theophylline [Kanakal et al., 2014; Oprea et al., 2012; Bispo et al., 2002] and Paclitaxel [Cho et al., 2004; Fonseca et al., 2002]. Through the optimization of HPLC parameters, such as the injection volume of each sample, UV wavelength setting of the detector, flow rate and composition of the mobile phase and the column compartment temperature, the finalized analytical methods are consolidated as below along with standard curves made by measuring samples of known concentrations with the optimized operation condition. All R-square values of standard curves in the analytical methods of Budesonide, Theophylline and Paclitaxel were greater than 0.999, confirming the accuracy of the methods that we have developed for our small-molecule model drugs. The developed HPLC analytical methods and the corresponding standard curves of the small-molecule model drugs are consolidated as follows:

HPLC parameters for Budesonide measurement:

✓ Mobile phase: Methanol/ H_2O (80/20)

✓ Flow rate: 0.25 ml/ min

✓ Column: Zorbax C-18 (2.1 x 150 mm, 3.5 μm)

✓ Detection UV wavelength: 244 nm

✓ Injection volume: 2 μl

✓ Column temperature: 20 °C
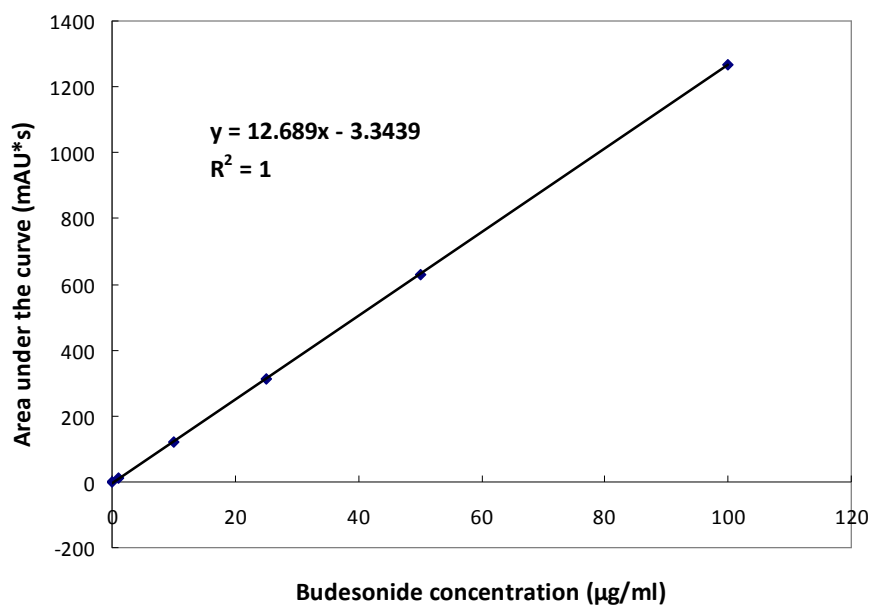
Figure 2.7. The standard curve of the HPLC analytical method of Budesonide.

HPLC parameters for Theophylline measurement:

✓ Mobile phase: H_2O/ Acetonitrile (90/10)

✓ Flow rate: 0.25 ml/ min

✓ Column: Zorbax C-18 (2.1 x 150 mm, 3.5 μm)

✓ Detection UV wavelength: 271 nm

✓ Injection volume: 2 μl

✓ Column temperature: 20 °C
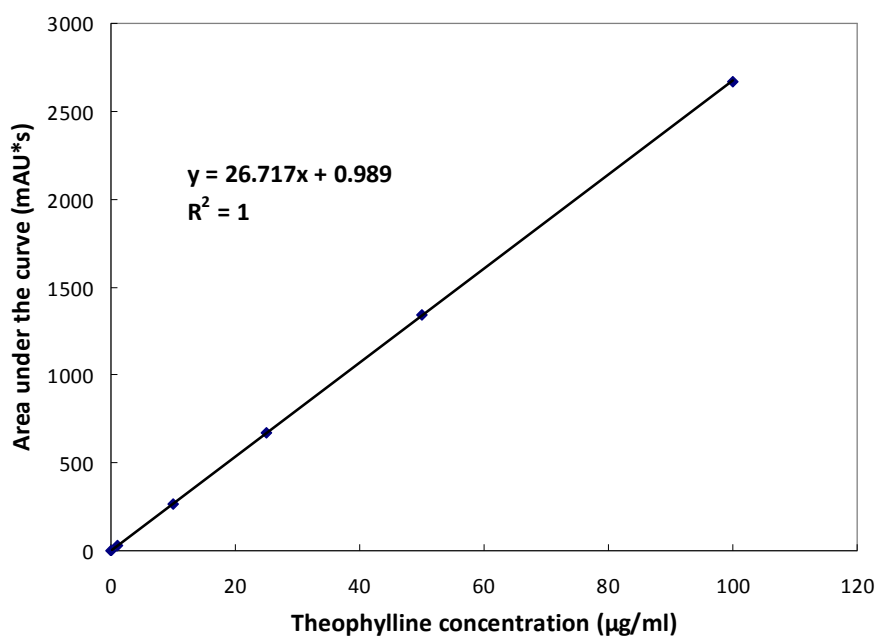
Figure 2.8. The standard curve of the HPLC analytical method of Theophylline.

HPLC parameters for Paclitaxel measurement:

- ✓ Mobile phase: H_2O/ Acetonitrile (45/55)

- ✓ Flow rate: 0.25 ml/ min

- ✓ Column: Zorbax C-18 (2.1 x 150 mm, 3.5 μm)

- ✓ Detection UV wavelength: 227 nm

- ✓ Injection volume: 3 μl

- ✓ Column temperature: 20 ^{o}C

$$y = 32.458x - 6.9359$$
$$R^2 = 1$$
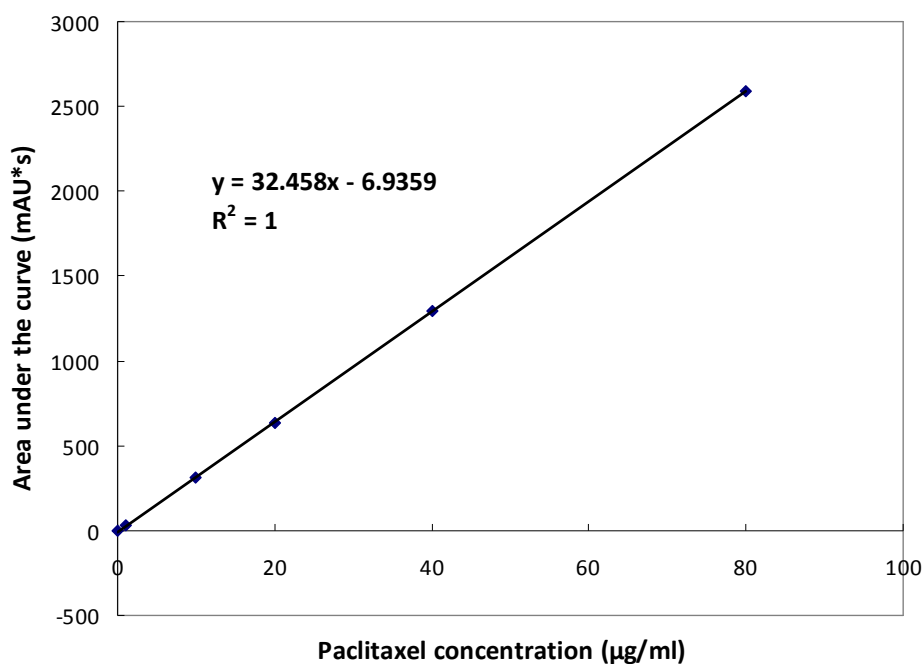
Figure 2.9. The standard curve of the HPLC analytical method of Paclitaxel.

2.4.2   The Protein Assay for the Quantification of Bovine Serum Albumin (BSA)

Protein assays are the methods used to estimate protein concentration. It has been extensively applied to molecular biology, cell biology, protein purification and many other applications in life science research. A myriad of protein assays are currently available in the market with different reliable protein concentration ranges of detection. Each of them has its own advantages and limitations, particularly considering their buffer compatibilities. None of the protein assays is capable of yielding absolutely accurate results on its own. Therefore, the suitability of a protein assay should be carefully considered according to its research applications [Ernst and Zor, 2010; Olson, 2016].

Herein, the NanoOrange® Protein Quantification Kit was used to measure the

concentration of Bovine Serum Albumin (BSA) in the release media. Compared to other assays for protein quantification in aqueous solutions, the NanoOrange assay is advantageous with lower protein-to-protein signal variability. Detection of the samples is not influenced by nucleic acids or reducing agents according to the product information. Samples can be read up to six hours after been prepared with extremely limited loss of sensitivity, making the assay convenient and reliable for lab use. By employing the 200 µl microplate assays, the linear working range of the assay are between 100 ng/ml and 10 μg/ml. The detailed operational protocol of the NanoOrange protein assay and its standard curve for the estimation of protein concentration are as follows:

Procedures of the NanoOrange® Protein Quantification Kit for quantification of BSA:

(1) Prepared 1X protein quantification diluent by mixing the concentrated NanoOrange® protein quantification diluent and diluting 10-fold in distilled water.

(2) Prepared 1X NanoOrange® reagent working solution by diluting the NanoOrange® protein quantification reagent (i.e., Component A of the Kit) 500-fold into the 1X protein quantification diluent from step (1). The as-prepared working solution needed to be protected from light. All the following steps were also performed in an environment without influencing by light.

(3) Mixed 10 µl BSA solution having unknown concentration with 240 µl working solution in an eppendorf with a Vortex Mixer. Incubated samples at

90-96°C for 10 minutes, protected from light.

(4) Cooled the samples at the room temperature for 20 minutes, protected from light.

(5) Centrifugalized the samples at 14,000 RPM with a bench-top centrifuge for 30 seconds. Transferred 200 μl solution from each eppendorf to a pre-determined well of the 96-well microplate for ELISA plate reading with proper wavelength settings (excitation wavelength: 485 nm; emission wavelength: 590 nm).

(6) Estimated BSA concentration of samples with unknown concentrations by using the standard curve plotted with the fluorescence values versus the concentrations of the BSA standard solutions.
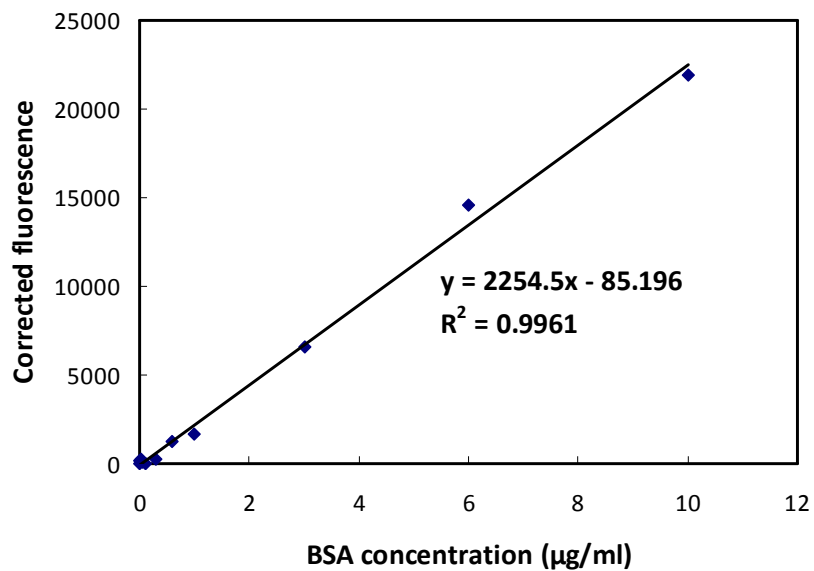
Figure 2.10. The standard curve of the NanoOrange® protein assay.

Chapter 3

In vitro Drug Release of Small-molecule Therapies from Matrix-type ES PLGA Particles

3.1 Experiment and Conditions of Matrix-type ES PLGA Nanoparticles Generated via a Single Capillary Nozzle

Theophylline, a bronchodilator with a narrow therapeutic window for symptom minimization of asthma, belongs to the methylxanthine group of the drugs. It is a hydrophilic compound and has been used to treat respiratory diseases, such as asthma and chronic obstructive pulmonary diseases, for decades [Kanakal et al., 2014; Oprea et al., 2012; Sundaran et al., 2013]. On the other hand, Budesonide is a hydrophobic small molecule for airway inflammation control and asthma attack prevention. It is an inhaled corticosteroid with high topical anti-inflammatory activity and hepatic first-pass metabolism, and is often used to prevent asthma attack and to treat inflammatory bowel disease [Gupta and Bhargava, 2006; Shendge and Sayyad, 2013]. According to former clinical studies, low dose Theophylline (THY) is an efficacious add-on therapy to Budesonide (BUD) for the treatment of asthma [Barnes, 2002], and they are chosen as the hydrophilic and the hydrophobic model drugs for our research to study the key influential factors for their sustained release from ES PLGA nanoparticles. The molecular structure and the selective physicochemical properties of Budesonide and Theophylline are summarized in Figure 3.1 [Bispo et al., 2002; Drug Bank Website].

Budesonide (BUD)

- Molecular weight: 430.53 g/mol
- Partition coefficient (logK$_D$): 2.73
- Aqueous solubility: 0.028 mg/ml
- pKa: 13.74
- Biological half-life: 2-3.6 hours

Theophylline (THY)

- Molecular weight: 180.16 g/mol
- Partition coefficient (logK$_D$): -0.17
- Aqueous solubility: 218 mg/ml
- pKa: 8.6
- Biological half-life: 5-6 hours

Molecular structure
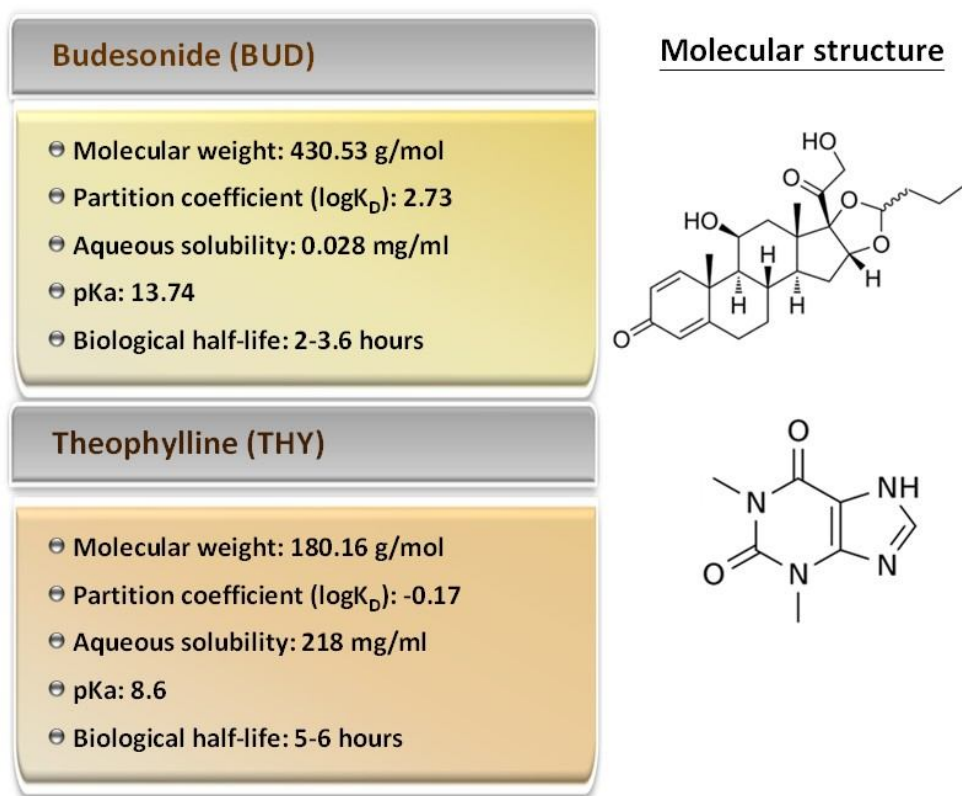
Figure 3.1. Molecular structures and selective physiological properties of Budesonide and Theophylline.

In the following Section 3.2, two types of nanoparticles, the 70-80 nm PLGA (Mw: 7,000-17,000 g/mol, LA/GA: 50/50) particles and the 130-140 nm PLGA (Mw: 24,000-38,000 g/mol, LA/GA: 50/50) particles, were produced by the single capillary ES technique. Key ES process parameters for generating PLGA particles with desired dimensions were determined by online measurement of particle size distributions with an electrospray close system connected to the SMPS. Particle morphology was also observed by SEM imaging. The key electrospray process parameters used for particle generation are summarized in Table 3.1-3.3 as follows.

Formulation ID	F1	F2	F3	F4
Spray solvent mixture	Acetonitrile/DMSO (75/25)	Acetonitrile/DMSO (75/25)	Acetonitrile/DMSO (75/25)	Acetonitrile/DMSO (75/25)
Electric conductivity of spray solvent	300 μS/cm	300 μS/cm	300 μS/cm	300 μS/cm
Feeding flowrate	0.3 μl/min	0.3 μl/min	0.3 μl/min	0.3 μl/min
Tip-to-collector (TTC) distance	5 cm	5 cm	5 cm	5 cm
PLGA molecular weight (LA/GA: 50/50)	7K-17K g/mol	7K-17K g/mol	7K-17K g/mol	7K-17K g/mol
PLGA concentration	10 mg/ml	10 mg/ml	10 mg/ml	10 mg/ml
Budesonide-to-PLGA mass ratio	1:10	2:10	5:10	8:10

Table 3.1. Process parameters of the single capillary ES for the generation of 70-80 nm matrix-type PLGA (Mw: 7K-17K g/mol, LA/GA: 50/50) particles to determine the optimized drug-to-polymer ratio for release profile characterization.

Formulation ID	F5	F6	F7
Spray solvent mixture	Acetonitrile/DMSO (75/25)	Acetonitrile/DMSO (75/25)	Acetonitrile/DMSO (75/25)
Electric conductivity of spray solvent	300 μS/cm	300 μS/cm	300 μS/cm
Feeding flowrate	0.3 μl/min	0.3 μl/min	0.3 μl/min
Tip-to-collector (TTC) distance	5 cm	5 cm	5 cm
PLGA molecular weight (LA/GA: 50/50)	7K-17K g/mol	7K-17K g/mol	7K-17K g/mol
PLGA concentration	10 mg/ml	10 mg/ml	10 mg/ml
Budesonide-to-PLGA mass ratio	1:10	1:10	1:10
Theophylline-to-PLGA mass ratio	1:10	5:10	8:10

Table 3.2. Process parameters of the single capillary ES for the generation of matrix-type PLGA (Mw: 7K-17K g/mol, LA/GA: 50/50) particles to study the effect of the loaded mass of Theophylline on drug release behaviors of the particles (size: 70-80 nm) loaded with both Budesonide and Theophylline.

44

Formulation ID	F8	F9	F10
Spray solvent mixture	Acetonitrile/DMSO (75/25)	Acetonitrile/DMSO (75/25)	Acetonitrile/DMSO (75/25)
Electric conductivity of spray solvent	120 μS/cm	120 μS/cm	120 μS/cm
Feeding flowrate	1.0 μl/min	1.0 μl/min	1.0 μl/min
Tip-to-collector (TTC) distance	5 cm	5 cm	5 cm
PLGA molecular weight (LA/GA: 50/50)	24K-38K g/mol	24K-38K g/mol	24K-38K g/mol
PLGA concentration	10 mg/ml	10 mg/ml	10 mg/ml
Budesonide-to-PLGA mass ratio	1:10	-	1:10
Theophylline-to-PLGA mass ratio	-	1:10	1:10

Table 3.3. Process parameters of the single capillary ES for the generation of matrix-type PLGA (Mw: 24K-38K g/mol, LA/GA: 50/50) particles (size: 130-140 nm) to study the effect of drug combination on release behaviors of the particles.

3.2 Results and Discussion

3.2.1 Generation of PLGA Particles Smaller than 150 nm in Diameter

According to the ES process parameters in Section 3.1, two types of PLGAs with the same lactic-to-glycolic ratio but with different molecular weights (i.e., 7,000-17,000 g/mol and 24,000-38,000 g/mol) were used to produce matrix-type PLGA nanoparticles in the sizes ranging between 70-80 nm and 130-140 nm via a single nozzle electrospray process. Size distributions of the as-produced PLGA nanoparticles are given in Figure 3.2. The geometric standard deviation (GSD) of synthesized nanoparticles was less than 1.40, suggesting excellent uniformity in sizes of the prepared PLGA particles. SEM imaging results shown in Figure 3.3 demonstrate the morphology and also confirm the particle size/ size distributions of as-produced particles to be in the desired size ranges for subsequent research work.

These particles were then used to encapsulate drugs according to the process parameters listed in Table 3.1, Table 3.2 and Table 3.3 to become the formulations as F1-F10 for testing to learn their drug release behaviors *in vitro*.
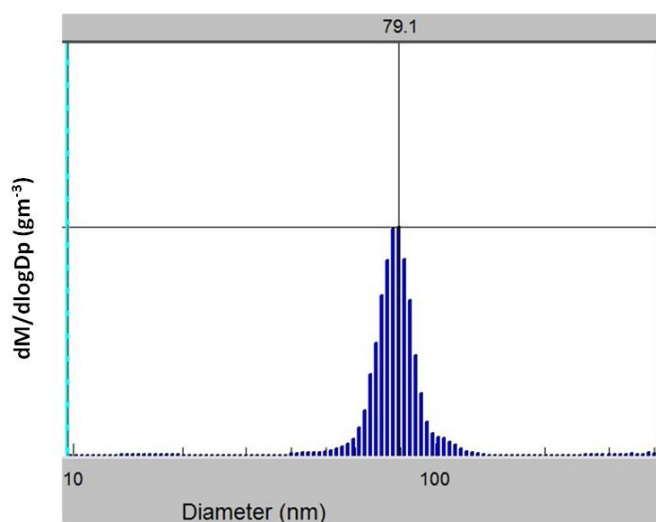
(A)
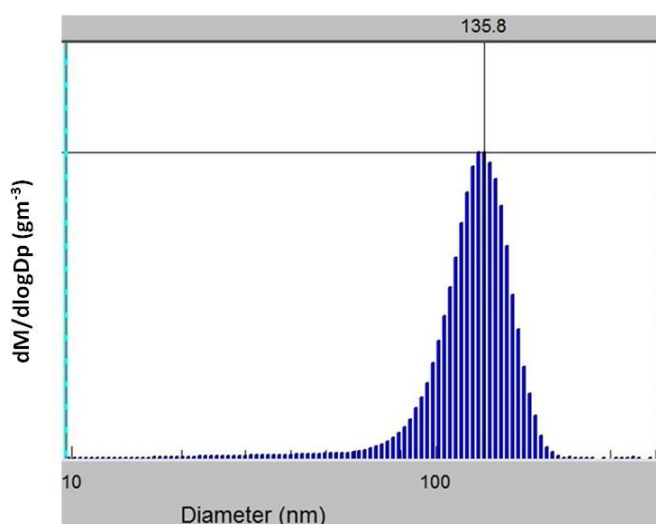
(B)

Figure 3.2. Size distributions of the matrix-type PLGA nanoparticles measured by SMPS: (A) 79.1 nm (GSD: 1.35) PLGA (Mw: 7K-17K g/mol, LA/GA: 50/50) particles, (B) 135.8 nm (GSD: 1.36) PLGA (Mw: 24K-38K g/mol, LA/GA: 50/50) particles.
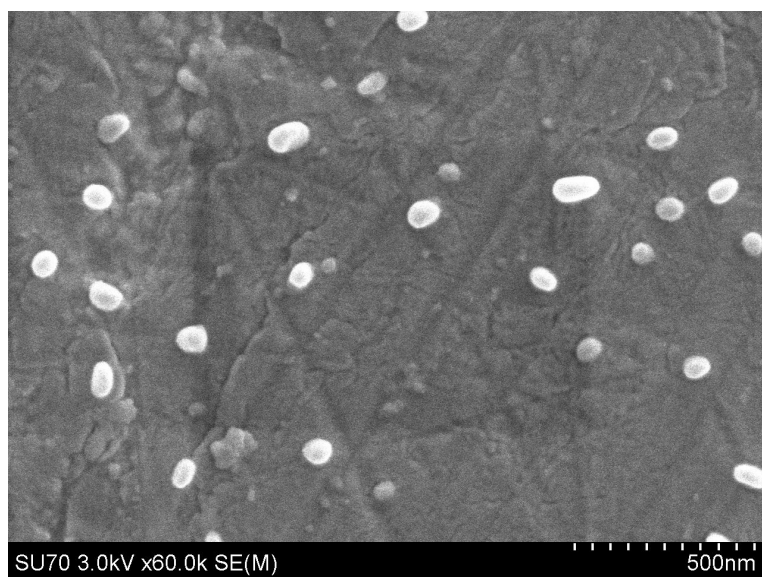
(A)
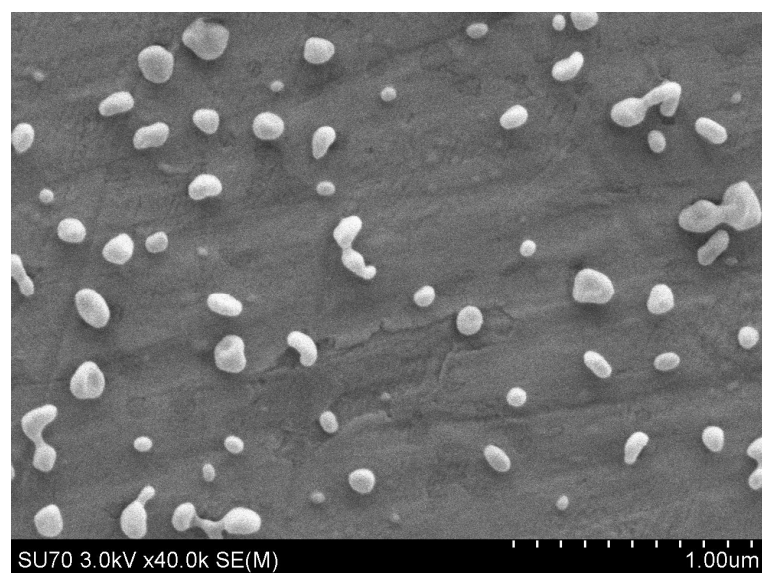
(B)

Figure 3.3. SEM images of: (A) 70-80 nm matrix-type PLGA (Mw: 7K-17K g/mol, LA/GA: 50/50) particles, (B) 130-140 nm matrix-type PLGA (Mw: 24K-38K g/mol, LA/GA: 50/50) particles.

3.2.2 Determination of the Loaded Drug-to-PLGA Ratio for Budesonide and Theophylline

As the highest drug release rate is anticipated to be seen from particles with smaller size, the 70-80 nm matrix-type PLGA (Mw: 7,000-17,000, LA/GA: 50/50) particles were employed to determine the drug-to-polymer ratio of Budesonide and Theophylline that should be used throughout the research work in Chapter 3 and Chapter 4. For determination of the Budesonide-to-PLGA ratio, a single capillary electrospray process was employed to generate the 70-80 nm matrix-type PLGA particles composed of different Budesonide-to-PLGA concentration ratios (1:10, 2:10, 5:10, and 8:10 as F1, F2, F3 and F4, respectively). *In vitro* drug release studies were then performed to determine the mass ratio of the encapsulated Budesonide to the polymer matrix based on the resultant release profiles shown in Figure 3.4. The slower Budesonide release rate observed from the data could be attributed to lower infusion rate of the media surrounding the particles, which eventually leaded to delayed drug dissolution and drug release. The 1:10 Budesonide-to-PLGA ratio was chosen also because particles generated with this drug-to-polymer ratio performed the sustained drug release behavior that allowed most of the encapsulated Budesonide to be released during the 102-hour drug release testing to minimize the impact of dose dumping. The 1:10 drug-to-polymer ratio also ensures that the released Budesonide can be accurately detected by HPLC, especially at the late stage of drug release when the amount of drug in the media is usually low.
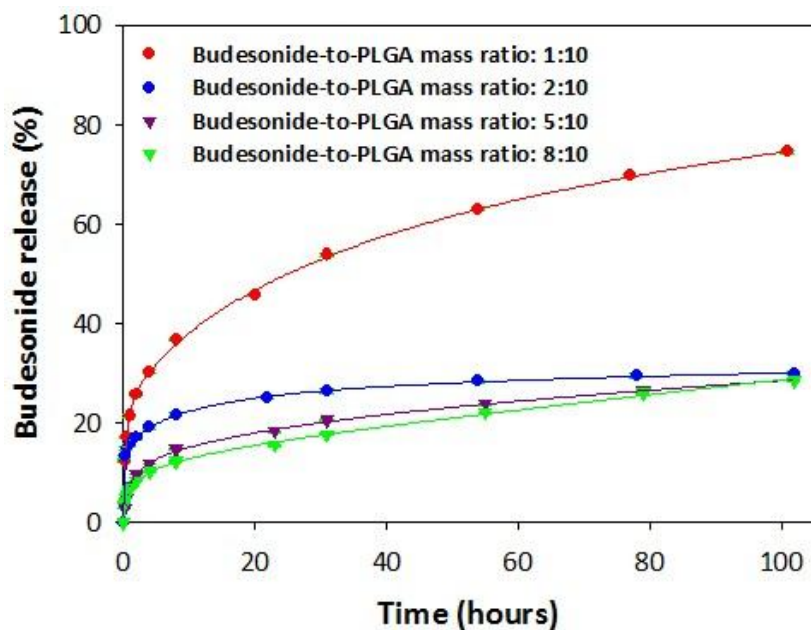
Figure 3.4. *In vitro* drug release profiles of Budesonide from the 70-80 nm matrix-type ES PLGA (Mw: 7K-17K g/mol, LA/GA: 50/50) particles encapsulating Budesonide in different drug-to-polymer mass ratios (formulations F1-F4).

Similar to Budesonide, the dose of Theophylline has also been determined via a series of drug release studies from 70-80 nm matrix-type PLGA (Mw: 7,000-17,000 g/mol, LA/GA: 50/50) particles loaded with Theophylline in different mass ratios of Theophylline-to-PLGA. Meanwhile, a fixed amount of Budesonide (Budesonide-to-PLGA mass ratio: 1:10) was co-encapsulated with Theophylline to ensure that the resultant particle formulations could perform sustained release over both Budesonide and Theophylline. The results in Figure 3.5 show that the release rate of Theophylline was always fast and with insignificant difference regardless of the amount of loaded Theophylline. However, greater amount of Theophylline in the formulation promoted the release rate of Budesonide. Such a finding could be

explained by the greater spaces left behind by the fast dissolution and release of Theophylline after the influx of release media into the particles. Therefore, it was expected that Budesonide molecules, except for those loaded near the surface of the particles, encountered weaker resistance against diffusion, leading to a higher Budesonide drug release rate. Based on above discussions, the 1:10 Theophylline-to-PLGA ratio was chosen for the following thesis work of Chapter 3 and the most part of Chapter 4.
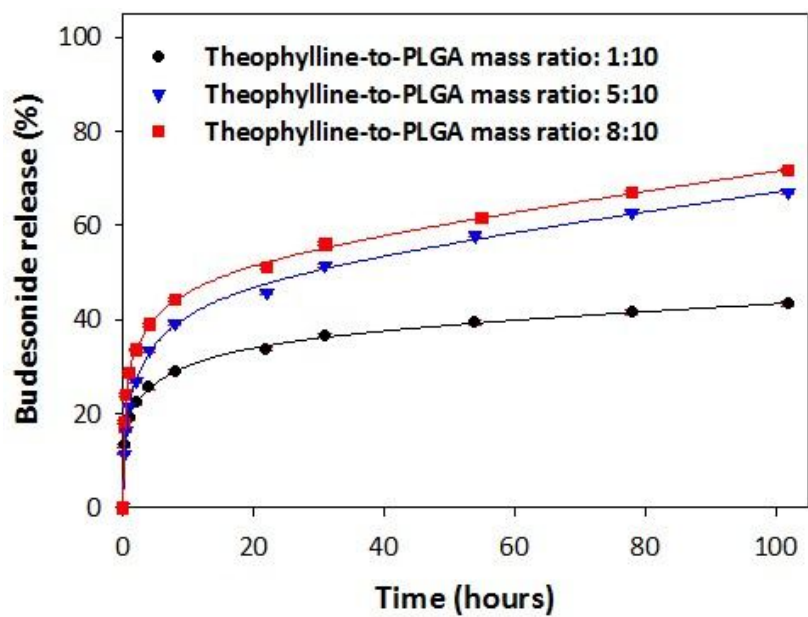
(A)
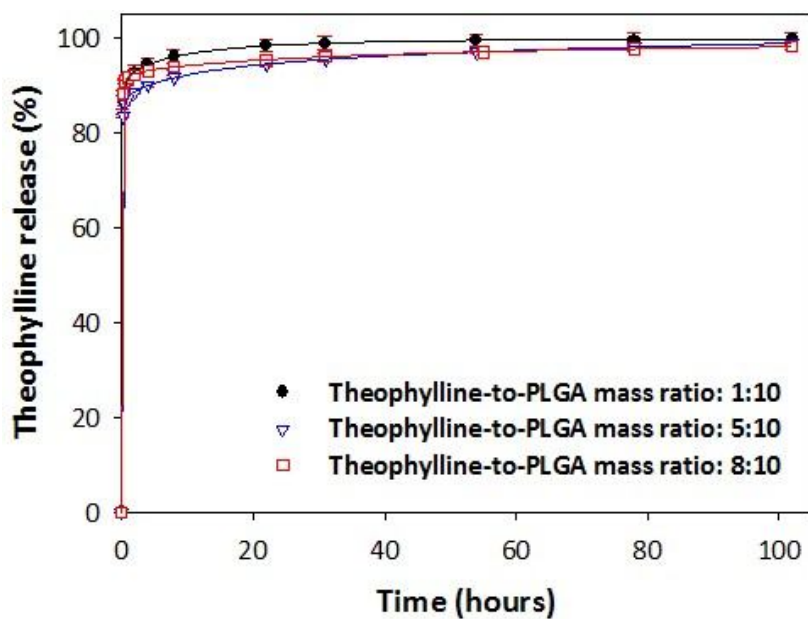
(B)

Figure 3.5. *In vitro* drug release profiles of (A) Budesonide and (B) Theophylline from the 70-80 nm

matrix-type ES PLGA (Mw: 7K-17K g/mol, LA/GA: 50/50) particles loaded with both drugs.

3.2.3   Effects of Drug Combination on Release Behaviors

The key objective of this work is to explore the feasibility of achieving the sustained release for both hydrophobic and hydrophilic drugs when both are loaded in ES PLGA nanoparticles (both matrix-type and core-shell type particles). Therefore, it is crucial to probe into how a singular active ingredient in a single dosage formulation is released from the nanoparticulate PLGA drug carriers. The influence of each loaded drug compound on the drug release behaviors of the other when both of them are simultaneously encapsulated in the nanoparticles can thus be further studied. Herein, three different PLGA (Mw: 24,000-38,000 g/mol, LA/GA: 50/50) nano-particulate formulations (i.e., F8, F9 and F10; particle size: 130-140 nm) loaded with Budesonide, Theophylline, and the combination of Budesonide and Theophylline as shown in Figure 3.6 were produced. The resultant drug release profiles of Budesonide and Theophylline are displayed in Figure 3.7. It is observed that the Budesonide release rate of F8 was not significantly different from that of F10. However, the Theophylline release rate of F10 was much higher than that of F9. The above observations may be associated with the void space left behind by the released drug molecules. Due to the higher molecular weight of Budesonide (430.53 g/mol) than Theophylline (180.16 g/mol), release of Budesonide created larger void spaces than release of Theophylline did in the polymer matrix. When Budesonide and Theophylline were co-encapsulated in the matrix-type PLGA particles, release of Budesonide promoted the Theophylline release via these larger void spaces and therefore accelerated its release rate by the enhanced infusion rate of the surrounding release media. Thus, Theophylline release rate was faster when co-encapsulated with Budesonide in PLGA nanoparticles than

the case when Theophylline was singly encapsulated in the same type of PLGA drug carrier. On the contrary, the void spaces created by the Theophylline drug release were smaller than those left behind by Budesonide drug release. That is why there was no significant difference between the Budesonide release rates of F8 and F10 from the perspective of void spaces in the polymer matrix. Figure 3.7 (C) indicates that over 80% of the loaded Theophylline was released within the first 30 minutes of the 2-day drug release testing. More efforts need to be made to slow down the release rate of Theophylline from ES PLGA nanoparticles. Relevant work will be performed, and the resultant data will be presented and discussed in the following sections.

Drug-to-polymer mass ratio = 1:10

❖ Formulation ID: F8
❖ Polymer:
   PLGA (Mw: 24K-38K
   g/mol; LA/GA: 50/50)
❖ Particle size: 135.8 nm

❖ Formulation ID: F9
❖ Polymer:
   PLGA (Mw: 24K-38K
   g/mol; LA/GA: 50/50)
❖ Particle size: 135.8 nm

❖ Formulation ID: F10
❖ Polymer:
   PLGA (Mw: 24K-38K
   g/mol; LA/GA: 50/50)
❖ Particle size: 135.8 nm
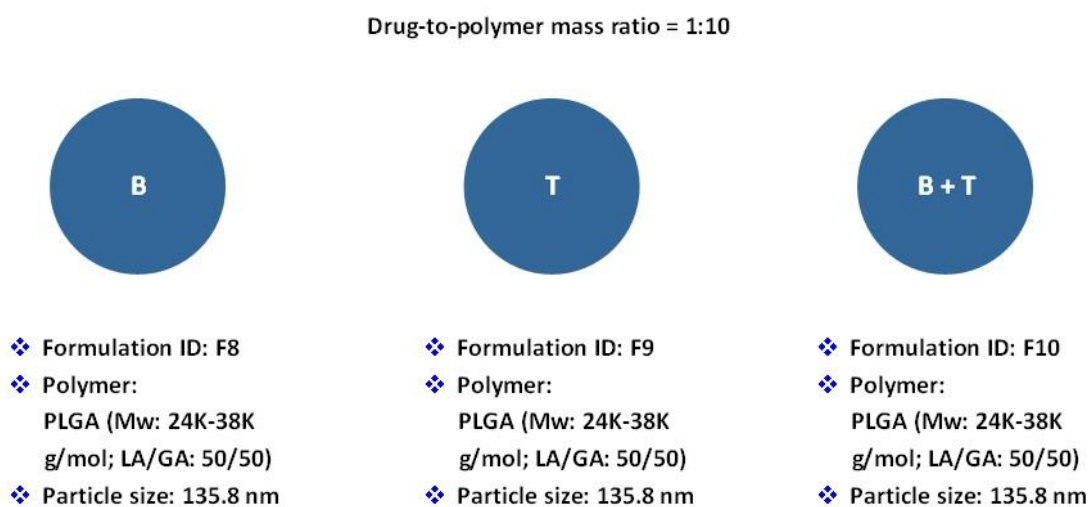
Figure 3.6. The schematic diagram of the 130-140 nm matrix-type ES PLGA (Mw: 24K-38K g/mol, LA/GA: 50/50) particles loaded with Budesonide (B) and/ or Theophylline (T).
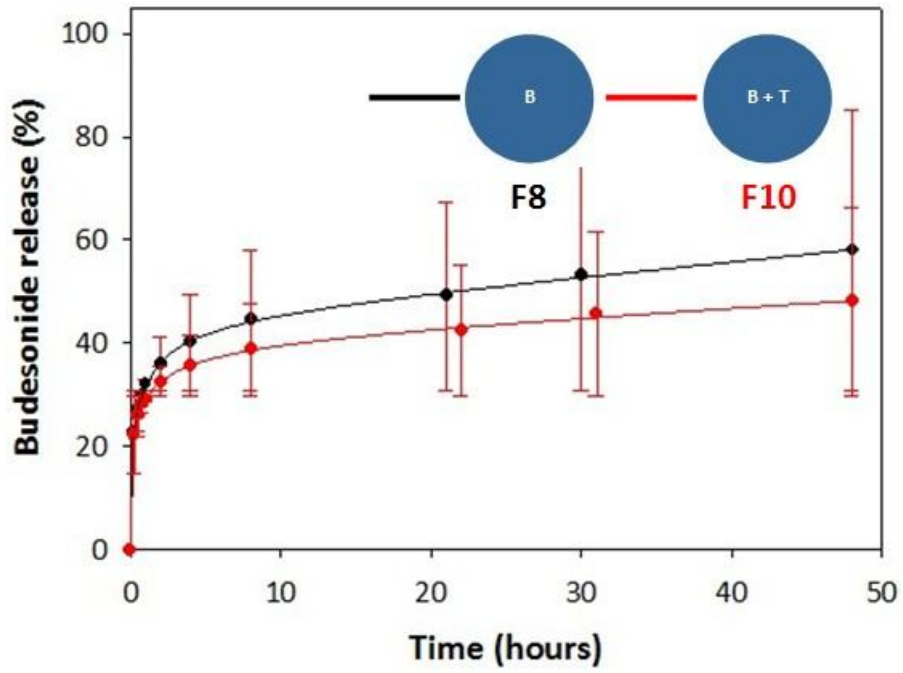
(A) Comparison of release profiles of Budesonide from F8 and F10.
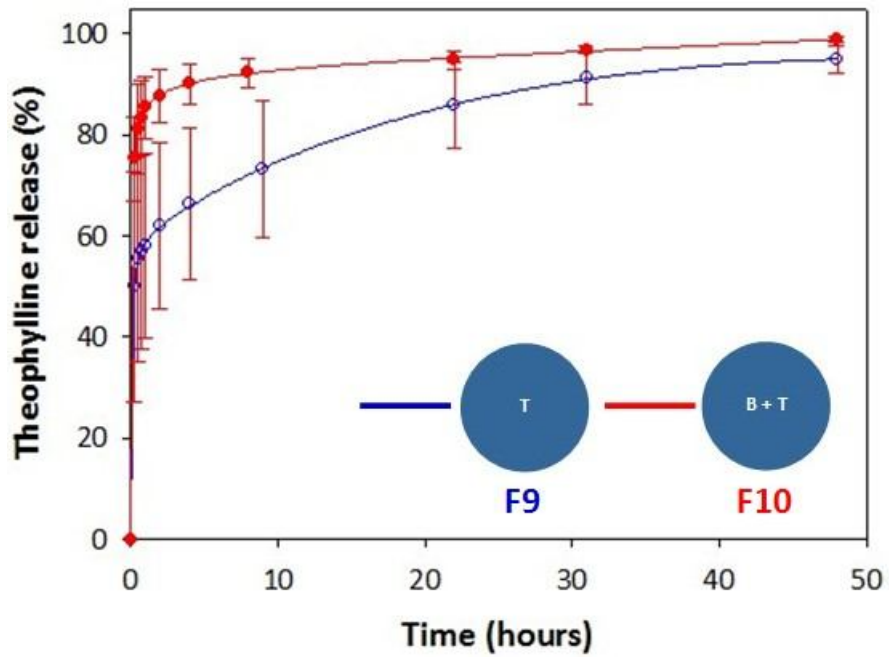
(B) Comparison of release profiles of Theophylline from F9 and F10.

54
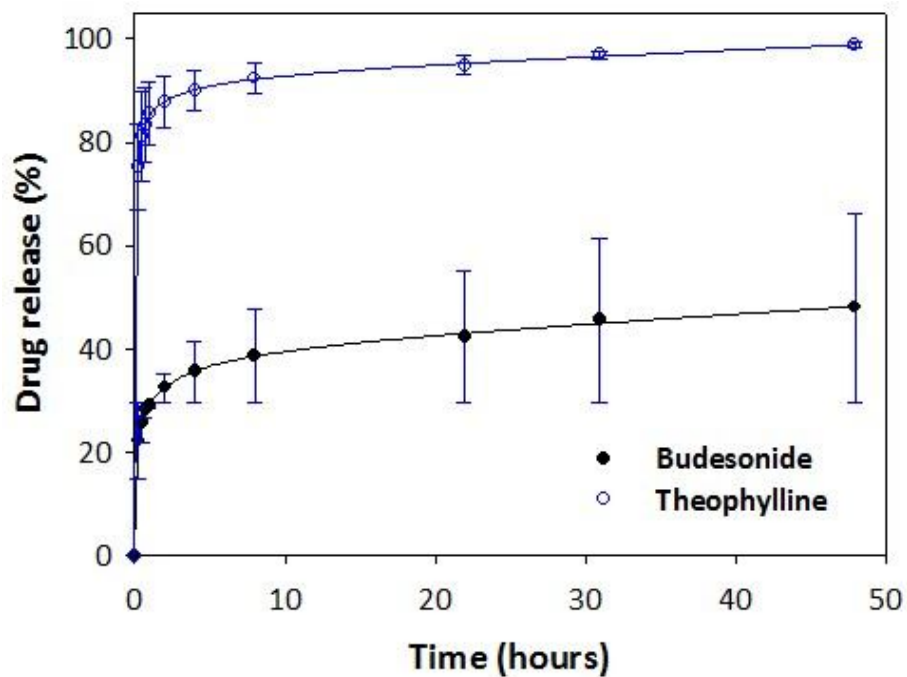
(C) Release profiles of Budesonide and Theophylline from F10.

Figure 3.7. *In vitro* drug release profiles of Budesonide (B) and Theophylline (T) from the 130-140 nm matrix-type ES PLGA (Mw: 24K-38K g/mol, LA/GA: 50/50) particles loaded with Budesonide (F8), Theophylline (F9) and the combination of Budesonide and Theophylline (F10). Duplicate testing with N=2.

3.3 Summary

Matrix-type PLGA nanoparticles (70-80 nm and 130-140 nm in diameter) were produced via the single capillary electrospray (ES) technique along with adequate process parameters determined by the close electrospray system through online measurement of particle size distributions. Two types of PLGAs with same LA/GA ratio (i.e., 50/50) but different molecular weights (i.e., 7,000-17000 g/mol and 24,000-38,000 g/mol) were used for particle generation. *In vitro* drug release testing with the centrifugation method and the previously developed HPLC analytical methods were utilized to study release profiles of Budesonide and Theophylline from the 70-80 nm matrix-type PLGA (Mw: 7,000-17,000 g/mol; LA/GA: 50/50) particles with different drug-to-polymer ratios in order to determine the appropriate amount of model drugs to be loaded in the particles. By using the 130-140 nm PLGA (Mw: 24,000-38,000 g/mol, LA/GA: 50/50) particles, Budesonide and/ or Theophylline were encapsulated in the particles to study how a model drug influenced release behaviors of the other when two model drugs were co-encapsulated in the matrix-type ES PLGA nanoparticles (i.e., F8, F9 and F10). The results suggest that Theophylline release rate was affected by Budesonide while the release rate of Budesonide was not significantly influenced by Theophylline when the two drugs were loaded in a single dosage formulation. The finding could be attributed to the sizes of the void spaces left behind by the released drug molecules. Considering the high Theophylline release rate from formulation F10, further efforts have to be made in order to apply the ES PLGA nanoparticles to extended release of both highly hydrophilic and hydrophobic active ingredients for fixed dose combination therapy. In the mean time, the results and the

conclusions obtained from F1-F10 also demonstrate that the methodology developed for particle generation and characterization of particle size distribution and *in vitro* drug release profiles were feasible and reliable for matrix-type PLGA nanoparticles. The same methodology is therefore applied to the subsequent thesis work to investigate the release profiles of small-molecule model drugs from the core-shell type PLGA nanoparticles produced by the coaxial dual capillary ES technique.

Chapter 4

In vitro Drug Release of Small-molecule
Therapies from Core-shell
Type ES PLGA Particles

4.1 Experiment and Conditions of Core-shell Type ES PLGA Nanoparticles Generated via a Coaxial Dual Capillary Nozzle

Drug release from PLGA particles takes place via a combination of several mechanisms, including detachment of surface-bound drug molecules, drug diffusion through the polymer matrix and erosion of filling materials of the particles [Zarchi et al., 2015]. For matrix-type PLGA nanoparticles, a biphasic drug release profile, wherein there is an initial burst release, is commonly seen. The initial burst release is caused by the surface/ near-surface loading of loaded drugs and is usually much more severe for hydrophilic compounds, leading to potential safety concerns to patients and shorter duration for extended drug release [Almería et al., 2011]. To overcome the issue of the initial burst release of drugs, the coaxial dual capillary electrospray (ES) was proposed in literature and utilized in this research to encapsulate model drugs. Due to the capabilities of the dual capillary ES to generate drug-loaded PLGA particles with desired compositions of particle filling materials, loading configurations of drugs, and internal structures of particles, a systematic investigation by using the particle generation technique was performed to learn how these factors influence drug release behaviors. Key factors for extended release of Theophylline (the highly hydrophilic small-molecule model drug) and the combination of Theophylline and Budesonide (the highly hydrophobic small-molecule model drug) were also identified by looking into the resultant drug release profiles.

For the research purposes, PLGA particles with overall sizes ranging from 380-440 nm (i.e., the 400-nm particles) and 880-1150 nm (i.e., the 1-μm particles) were generated for drug encapsulation in order to improve particle deposition in

alveolar regions of the lung for systemic drug delivery and to slowly release the active ingredients loaded in the particles. Similar to previous sections, ES process parameters to produce PLGA particles with dimensions within desired size ranges were determined by a close electrospray system connected with particle sizing instruments. Herein, two different particle sizers, the SMPS and the OPS, were utilized to size particles smaller and greater than 500 nm, respectively, according to their detectable particle size ranges (SMPS: 3 nm-700 nm; OPS: 100 nm-10 μm). Process parameters of the coaxial dual capillary electrospray (ES) for the thesis work of Chapter 4 are summarized in Table 4.1-4.8 as follows.

Formulation ID		F11	F12	F13
Inner solution	Electric conductivity (μ S/cm)	30	30	30
	Feeding flowrate (μ l/min)	0.5	0.5	0.5
	PLGA (Mw; LA/GA)	54K-69K; 50/50	54K-69K; 50/50	54K-69K; 50/50
	PLGA conc. (mg/ml)	25	25	25
	BUD:PLGA mass ratio	1:10	1:10	-
	THY:PLGA mass ratio	1:10	-	1:10
Outer solution	Electric conductivity (μ S/cm)	30	30	30
	Feeding flowrate (μ l/min)	2.5	2.5	2.5
	PLGA (Mw; LA/GA)	24K-38K; 50/50	24K-38K; 50/50	24K-38K; 50/50
	PLGA conc. (mg/ml)	20	20	20
	BUD:PLGA mass ratio	-	-	1:10
	THY:PLGA mass ratio	-	1:10	-
Spray solvent mixture		Acetonitrile/DMSO (75/25)	Acetonitrile/DMSO (75/25)	Acetonitrile/DMSO (75/25)
Tip-to-collector (TTC) distance (cm)		8.0	8.0	8.0

Table 4.1. Process parameters of the coaxial dual capillary ES for the generation of core-shell PLGA (core: Mw 54K-69K g/mol, LA/GA: 50/50; shell: Mw 24K-38K g/mol; LA/GA: 50/50) composite particles (particle size: 400 nm) loaded with Budesonide (BUD) and Theophylline (THY) in tested configurations (F11: Core loaded with Budesonide and Theophylline; F12: Core loaded with Budesonide, shell loaded with Theophylline; F13: Core loaded with Theophylline, shell loaded with Budesonide).

Formulation ID		F14	F15	F16
Inner solution	Electric conductivity (μS/cm)	30	30	30
	Feeding flowrate (μl/min)	0.5	0.5	0.5
	PLGA (Mw; LA/GA)	50K-75K; 85/15	50K-75K; 85/15	50K-75K; 85/15
	PLGA conc. (mg/ml)	10	10	10
	BUD:PLGA mass ratio	1:10	1:10	-
	THY:PLGA mass ratio	1:10	-	1:10
Outer solution	Electric conductivity (μS/cm)	30	30	30
	Feeding flowrate (μl/min)	2.5	2.5	2.5
	PLGA (Mw; LA/GA)	24K-38K; 50/50	24K-38K; 50/50	24K-38K; 50/50
	PLGA conc. (mg/ml)	20	20	20
	BUD:PLGA mass ratio	-	-	1:10
	THY:PLGA mass ratio	-	1:10	-
Spray solvent mixture		Acetonitrile/DMSO (75/25)	Acetonitrile/DMSO (75/25)	Acetonitrile/DMSO (75/25)
Tip-to-collector (TTC) distance (cm)		8.0	8.0	8.0

Table 4.2. Process parameters of the coaxial dual capillary ES for the generation of core-shell PLGA (core: Mw 50K-75K g/mol, LA/GA: 85/15; shell: Mw 24K-38K g/mol; LA/GA: 50/50) composite particles (particle size: 400 nm) loaded with Budesonide (BUD) and Theophylline (THY) in tested configurations (F14: Core loaded with Budesonide and Theophylline; F15: Core loaded with Budesonide, shell loaded with Theophylline; F16: Core loaded with Theophylline, shell loaded with Budesonide).

Formulation ID		F17	F18	F19
Inner solution	Electric conductivity (μS/cm)	30	30	30
	Feeding flowrate (μl/min)	1.0	1.0	1.0
	PLGA (Mw; LA/GA)	50K-75K; 85/15	50K-75K; 85/15	50K-75K; 85/15
	PLGA conc. (mg/ml)	12.5	12.5	12.5
	BUD:PLGA mass ratio	1:10	1:10	-
	THY:PLGA mass ratio	1:10	-	1:10
Outer solution	Electric conductivity (μS/cm)	30	30	30
	Feeding flowrate (μl/min)	2.5	2.5	2.5
	PLGA (Mw; LA/GA)	50K-75K; 85/15	50K-75K; 85/15	50K-75K; 85/15
	PLGA conc. (mg/ml)	20	20	20
	BUD:PLGA mass ratio	-	-	1:10
	THY:PLGA mass ratio	-	1:10	-
Spray solvent mixture		Acetonitrile/DMSO (75/25)	Acetonitrile/DMSO (75/25)	Acetonitrile/DMSO (75/25)
Tip-to-collector (TTC) distance (cm)		8.0	8.0	8.0

Table 4.3. Process parameters of the coaxial dual capillary ES for the generation of core-shell PLGA (core: Mw 50K-75K g/mol, LA/GA: 85/15; shell: Mw 50K-75K g/mol; LA/GA: 85/15) composite particles (particle size: 400 nm) loaded with Budesonide (BUD) and Theophylline (THY) in tested configurations (F17: Core loaded with Budesonide and Theophylline; F18: Core loaded with Budesonide, shell loaded with Theophylline; F19: Core loaded with Theophylline, shell loaded with Budesonide).

Formulation ID		F20	F21
Inner solution	Electric conductivity (μS/cm)	30	30
	Feeding flowrate (μl/min)	1.0	1.0
	PLGA (Mw; LA/GA)	50K-75K; 85/15	50K-75K; 85/15
	PLGA conc. (mg/ml)	12.5	12.5
	BUD:PLGA mass ratio	-	-
	THY:PLGA mass ratio	1:10	1:10
Outer solution	Electric conductivity (μS/cm)	30	30
	Feeding flowrate (μl/min)	2.5	2.5
	PLGA (Mw; LA/GA)	50K-75K; 85/15	50K-75K; 85/15
	PLGA conc. (mg/ml)	20	20
	BUD:PLGA mass ratio	-	-
	THY:PLGA mass ratio	-	1:4
Spray solvent mixture		Acetonitrile/DMSO (75/25)	Acetonitrile/DMSO (75/25)
Tip-to-collector (TTC) distance (cm)		8.0	8.0

Table 4.4. Process parameters of the coaxial dual capillary ES for the generation of core-shell PLGA (core: Mw 50K-75K g/mol, LA/GA: 85/15; shell: Mw 50K-75K g/mol; LA/GA: 85/15) particles (particle size: 400 nm) loaded with Theophylline (THY) in tested configurations (F20: Theophylline loaded in core; F21: Theophylline loaded in core and shell).

Formulation ID		F20	F22	F23
Inner solution	Electric conductivity (μS/cm)	30	30	30
	Feeding flowrate (μl/min)	1.0	0.5	0.5
	PLGA (Mw; LA/GA)	50K-75K; 85/15	7K-17K; 50/50	24K-38K; 50/50
	PLGA conc. (mg/ml)	12.5	25	25
	BUD:PLGA mass ratio	-	-	-
	THY:PLGA mass ratio	1:10	1:10	1:10
Outer solution	Electric conductivity (μS/cm)	30	30	30
	Feeding flowrate (μl/min)	2.5	2.5	2.5
	PLGA (Mw; LA/GA)	50K-75K; 85/15	7K-17K; 50/50	24K-38K; 50/50
	PLGA conc. (mg/ml)	20	20	20
	BUD:PLGA mass ratio	-	-	-
	THY:PLGA mass ratio	-	-	-
Spray solvent mixture		Acetonitrile/DMSO (75/25)	Acetonitrile/DMSO (75/25)	Acetonitrile/DMSO (75/25)
Tip-to-collector (TTC) distance (cm)		8.0	8.0	8.0

Table 4.5. Process parameters of the coaxial dual capillary ES for the generation of core-shell Theophylline-loaded particles (particle size: 400-450 nm) composed of PLGA with various molecular weights and lactic-to-glycolic ratios. F20: PLGA (Mw: 50K-75K g/mol, LA/GA: 85/15), F22: PLGA (Mw: 7K-17K g/mol, LA/GA: 50/50), F23: PLGA (Mw: 24K-38K g/mol, LA/GA: 50/50).

Formulation ID		F22	F24
Inner solution	Electric conductivity (μ S/cm)	30	30
	Feeding flowrate (μ l/min)	0.5	0.5
	PLGA (Mw; LA/GA)	7K-17K; 50/50	7K-17K; 50/50
	PLGA conc. (mg/ml)	25	25
	BUD:PLGA mass ratio	-	-
	THY:PLGA mass ratio	1:10	1:10
Outer solution	Electric conductivity (μ S/cm)	30	30
	Feeding flowrate (μ l/min)	2.5	2.5
	PLGA (Mw; LA/GA)	7K-17K; 50/50	7K-17K; 50/50
	PLGA conc. (mg/ml)	20	154.64
	BUD:PLGA mass ratio	-	-
	THY:PLGA mass ratio	-	-
Spray solvent mixture		Acetonitrile/DMSO (75/25)	Acetonitrile/DMSO (75/25)
Tip-to-collector (TTC) distance (cm)		8.0	8.0

Table 4.6. Process parameters of the coaxial dual capillary ES for the generation of core-shell PLGA (Mw: 7K-17K g/mol, LA/GA: 50/50) particles with the same core sizes but different shell layer thicknesses to encapsulate Theophylline in the particle cores (F22: 400 nm particles with thinner shell thickness, F24: 1 μm particles with thicker shell thickness).

Formulation ID		F24	F25
Inner solution	Electric conductivity (μS/cm)	30	30
	Feeding flowrate (μl/min)	0.5	0.5
	PLGA (Mw; LA/GA)	7K-17K; 50/50	7K-17K; 50/50
	PLGA conc. (mg/ml)	25	25
	BUD:PLGA mass ratio	-	1:10
	THY:PLGA mass ratio	1:10	1:10
Outer solution	Electric conductivity (μS/cm)	30	30
	Feeding flowrate (μl/min)	2.5	2.5
	PLGA (Mw; LA/GA)	7K-17K; 50/50	7K-17K; 50/50
	PLGA conc. (mg/ml)	154.64	154.64
	BUD:PLGA mass ratio	-	-
	THY:PLGA mass ratio	-	-
Spray solvent mixture		Acetonitrile/DMSO (75/25)	Acetonitrile/DMSO (75/25)
Tip-to-collector (TTC) distance (cm)		8.0	8.0

Table 4.7. Process parameters of the coaxial dual capillary ES for the generation of core-shell PLGA (Mw: 7K-17K g/mol, LA/GA: 50/50) particles (particle size: 1 μm) loaded with Theophylline and/ or Budesonide in the cores of particles (F24: Core loaded with Theophylline; F25: Core loaded with Budesonide and Theophylline).

Formulation ID		F17	F26
Inner solution	Electric conductivity (μS/cm)	30	30
	Feeding flowrate (μl/min)	1.0	1.0
	PLGA (Mw; LA/GA)	50K-75K; 85/15	50K-75K; 85/15
	PLGA conc. (mg/ml)	12.5	12.5
	BUD:PLGA mass ratio	1:10	1:10
	THY:PLGA mass ratio	1:10	1:20
Outer solution	Electric conductivity (μS/cm)	30	30
	Feeding flowrate (μl/min)	2.5	2.5
	PLGA (Mw; LA/GA)	50K-75K; 85/15	50K-75K; 85/15
	PLGA conc. (mg/ml)	20	20
	BUD:PLGA mass ratio	-	-
	THY:PLGA mass ratio	-	-
Spray solvent mixture		Acetonitrile/DMSO (75/25)	Acetonitrile/DMSO (75/25)
Tip-to-collector (TTC) distance (cm)		8.0	8.0

Table 4.8. Process parameters of the coaxial dual capillary ES for the generation of core-shell PLGA (Mw: 50K-75K g/mol, LA/GA: 85/15) composite particles (particle size: 400 nm) encapsulating Budesonide and Theophylline in particle core with different THY-to-PLGA mass ratios.

4.2 Results and Discussion

4.2.1 Effects of Drug Loading Locations of Co-encapsulated Budesonide and Theophylline in Particles on Drug Release

Composite particles (particle size: 400 nm) with three loading conditions (i.e., both Budesonide and Theophylline loaded in the core; Budesonide loaded in the core and Theophylline loaded in the shell; Theophylline loaded in the core and Budesonide loaded in the shell) were produced via the dual capillary ES. Release profiles of

Budesonide and Theophylline were investigated when both loaded in PLGA composite particles for fixed-dose combination therapy. Three PLGA polymers, PLGA (Mw: 24,000-38,000 g/mol, LA/GA: 50/50), PLGA (Mw: 54,000-69,000 g/mol, LA/GA: 50/50) and PLGA (Mw: 50,000-75,000 g/mol, LA/GA: 85/15) were used to produce three types of composite drug-loaded nano-carriers with ES parameters listed in Table 4.1, Table 4.2 and Table 4.3 to encapsulate Budesonide and Theophylline in tested configurations as shown in Figure 4.1.

(A) Drug-to-polymer mass ratio = 1:10

❖ Formulation ID: F11
❖ Polymer (shell):
   PLGA (Mw: 24K-38K g/mol, LA/GA: 50/50)
❖ PLGA (core):
   PLGA (Mw: 54K-69K g/mol, LA/GA: 50/50)
❖ Particle size: 399.5 nm

❖ Formulation ID: F12
❖ Polymer (shell):
   PLGA (Mw: 24K-38K g/mol, LA/GA: 50/50)
❖ PLGA (core):
   PLGA (Mw: 54K-69K g/mol, LA/GA: 50/50)
❖ Particle size: 399.5 nm

❖ Formulation ID: F13
❖ Polymer (shell):
   PLGA (Mw: 24K-38K g/mol, LA/GA: 50/50)
❖ PLGA (core):
   PLGA (Mw: 54K-69K g/mol; LA/GA: 50:50)
❖ Particle size: 399.5 nm

(B) Drug-to-polymer mass ratio = 1:10

❖ Formulation ID: F14
❖ Polymer (shell):
   PLGA (Mw: 24K-38K g/mol, LA/GA: 50/50)
❖ PLGA (core):
   PLGA (Mw: 50K-75K g/mol, LA/GA: 85/15)
❖ Particle size: 399.5 nm

❖ Formulation ID: F15
❖ Polymer (shell):
   PLGA (Mw: 24K-38K g/mol, LA/GA: 50/50)
❖ PLGA (core):
   PLGA (Mw: 50K-75K g/mol, LA/GA: 85/15)
❖ Particle size: 399.5 nm

❖ Formulation ID: F16
❖ Polymer (shell):
   PLGA (Mw: 24K-38K g/mol, LA/GA: 50/50)
❖ PLGA (core):
   PLGA (Mw: 50K-75K g/mol, LA/GA: 85/15)
❖ Particle size: 399.5 nm

(C)   Drug-to-polymer mass ratio = 1:10

- ❖ Formulation ID: F17
- ❖ Polymer (shell):
  PLGA (Mw: 50K-75K g/mol, LA/GA: 85/15)
- ❖ PLGA (core):
  PLGA (Mw: 50K-75K g/mol LA/GA: 85/15)
- ❖ Particle size: 399.5 nm

- ❖ Formulation ID: F18
- ❖ Polymer (shell):
  PLGA (Mw: 50K-75K g/mol, LA/GA: 85/15)
- ❖ PLGA (core):
  PLGA (Mw: 50K-75K g/mol, LA/GA: 85/15)
- ❖ Particle size: 399.5 nm

- ❖ Formulation ID: F19
- ❖ Polymer (shell):
  PLGA (Mw: 50K-75K g/mol, LA/GA: 85/15)
- ❖ PLGA (core):
  PLGA (Mw: 50K-75K g/mol, LA/GA: 85/15)
- ❖ Particle size: 399.5 nm

Figure 4.1. The schematic diagrams of the 400-nm Budesonide (B)-Theophylline (T) loaded core-shell type ES PLGA composite particles in tested drug loading configurations. (A) core: Mw 54K-69K g/mol, LA/GA: 50/50; shell: Mw 24K-38K g/mol, LA/GA: 50/50, (B) core: Mw 50K-75K g/mol, LA/GA: 85/15, shell: Mw 24K-38K g/mol, LA/GA: 50/50, (C) core: Mw 50K-75K g/mol, LA/GA: 85/15; shell: Mw 50K-75K g/mol, LA/GA: 85/15.

With the drug release testing procedures and the HPLC analytical methods of Budesonide and Theophylline developed in Chapter 2, *in vitro* drug release profiles of F11, F12 and F13 are given in Figure 4.2. The configuration effect (i.e., the loading locations of the drugs in the particles) was observed for the case of Budesonide as the release profiles shown in Figure 4.2 (A). With the shortest distance for the influx of the release media and the drug diffusion in the polymer matrix, Budesonide release rate of F13 was highest compared to that of F11 and F12 due to the fastest drug dissolution and the thinnest diffusion barrier thickness. A significant difference in Budesonide release rate was also seen for the cases when it was loaded in the particle core (i.e., F11 and F12). The finding may be explained by the void spaces left behind

after the release of Theophylline loaded in the particle shell, allowing faster infusion of the release media to the cores of the particles for drug dissolution and creating less hindrance for drug release. On the other hand, Theophylline release rates were similar among F11, F12 and F13. Due to the high aqueous solubility and the large diffusion coefficient, release of the core-loaded Theophylline through the void spaces resulted from the released Budesonide originally loaded in the shell (i.e., F13) was as fast as the case when Theophylline was loaded in the particle shell (i.e., F12). Compared to F10, Theophylline release rate was not suppressed by drug carriers with larger particle size, unique core-shell structure, and filling material with higher molecular weight (i.e., F11). Different PLGA materials were thus tested for greater effectiveness of sustained release of Theophylline.
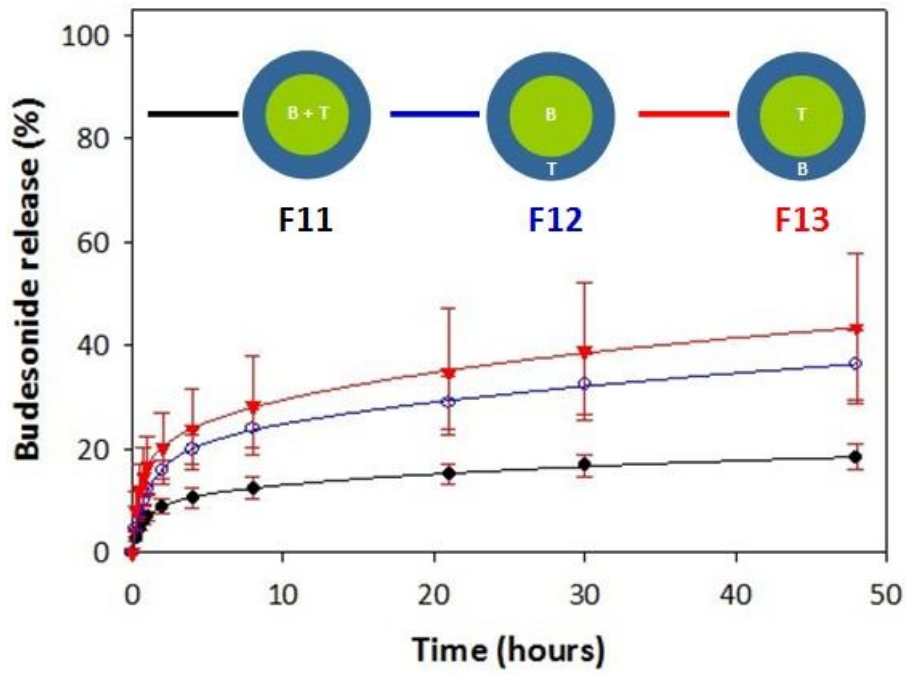
(A)
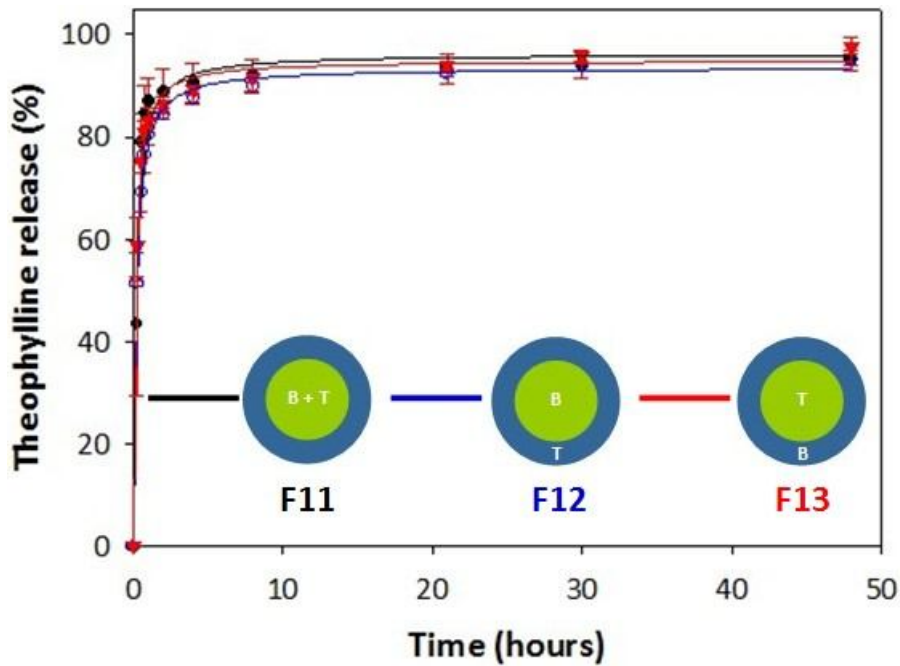
(B)

Figure 4.2. Release profiles of Budesonide (B) and Theophylline (T) from PLGA (core: Mw 54K-69K

g/mol, LA/GA: 50/50; shell: Mw 24K-38K g/mol, LA/GA: 50/50) composite particles (particle size:

400 nm) with both drugs loaded in tested configurations: (A) release profiles of Budesonide, (B)

release profiles of Theophylline. Duplicate testing with N=2.

PLGA (Mw: 50,000-75,000 g/mol, LA/GA: 85/15) was expected to be with slower polymer degradation rate compared to PLGA (Mw: 54,000-69,000 g/mol, LA/GA: 50/50) because of the higher lactic-to-glycolic ratio. Therefore, the polymer could provide greater capabilities for slow release of Theophylline [Makadia and Siegel, 2011]. Accordingly, the 400-nm PLGA (core: Mw 50,000-75,000 g/mol, LA/GA: 85/15; shell: Mw 24,000-38,000 g/mol, LA/GA: 50/50) composite particles (i.e., F14, F15 and F16) and the 400-nm PLGA (core: Mw 50,000-75,000 g/mol, LA/GA: 85/15; shell: Mw 50,000-75,000 g/mol, LA/GA: 85/15) composite particles (i.e., F17, F18 and F19) were generated by ES process parameters listed in Table 4.2 and Table 4.3, respectively. The schematic diagrams of the as-produced nano-particulate formulations are given in Figure 4.1 (B) and Figure (C), respectively, to illustrate detailed drug loading locations of Budesonide and Theophylline in the tested particles. The resultant release profiles of F14 (EE% of Budesonide: 88.1%, EE% of Theophylline: 90.2%), F15 (EE% of Budesonide: 93.6%, EE% of Theophylline: 92.2%) and F16 (EE% of Budesonide: 96.9%, EE% of Theophylline: 97.4%) are displayed in Figure 4.3. Similar to the findings shown in Figure 4.2 (A), the release rate of Budesonide was also determined by its loading locations in the core-shell PLGA nanoparticles. The F16 released Budesonide in the fastest release rate since the majority of Budesonide molecules were loaded in the particle shell. Compared to the case when Budesonide and Theophylline were both loaded in the cores of the particles (i.e., F14), the shell-loaded Theophylline promoted the release rate of core-loaded Budesonide (i.e., F15). On the other hand, the tested PLGA composite drug nano-carrier (particle size: 400 nm) was conducive to slow down the

release rate of Theophylline. In Figure 4.3 (B), Theophylline release rate from F14 was significantly slower than the cases of Theophylline release from F15 and F16 with close to 70% of the encapsulated Theophylline was released during the first hour of the 2-day release testing. Compared to F14, formulation F15 released Theophylline in a higher drug release rate because Theophylline was encapsulated in the shell of particles. The Theophylline release rate from F16 was almost identical with that from F15 because the release rate of the core-loaded Theophylline in F16 was boosted by the shell-loaded Budesonide. The reasons behind the finding have been discussed for the discussions of Theophylline release profiles from F12 and F13 and would not be addressed herein again.
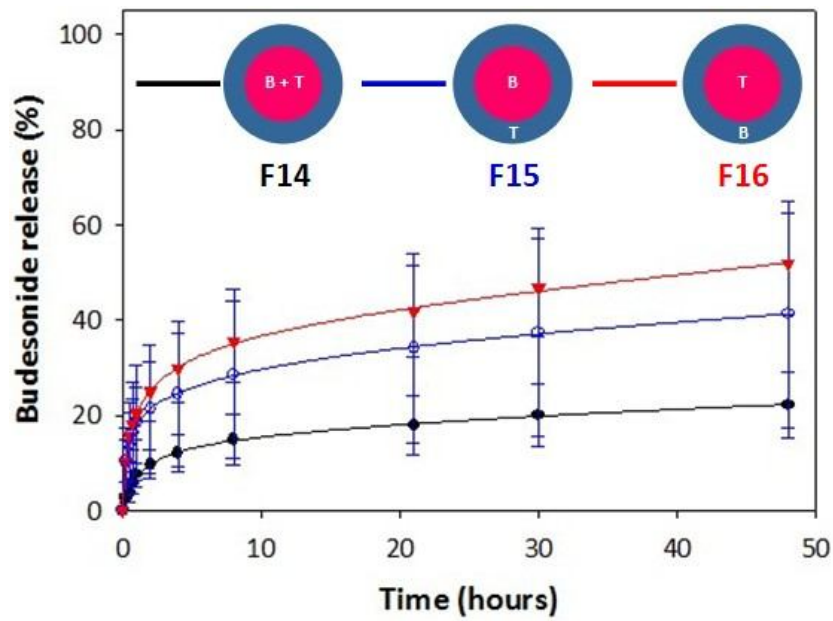
(A)
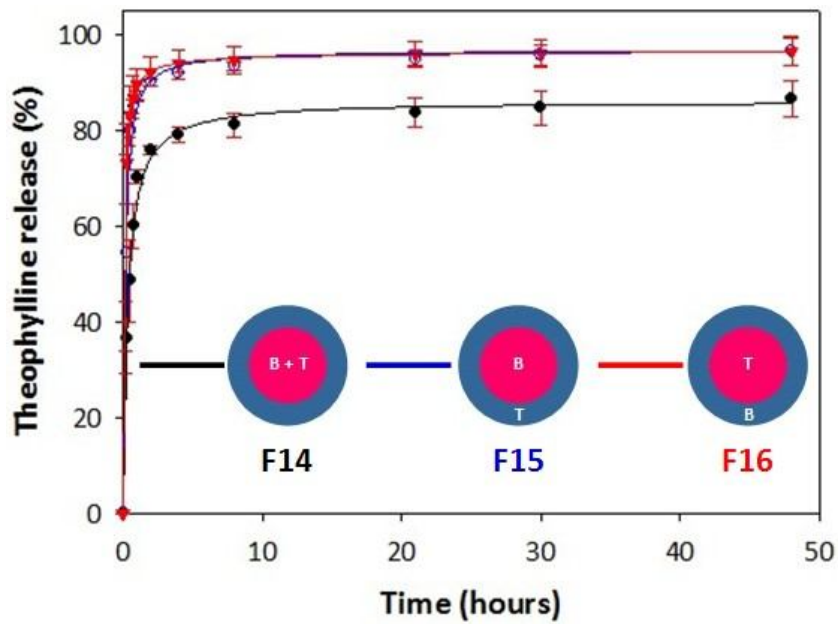
(B)

Figure 4.3. Release profiles of Budesonide (B) and Theophylline (T) from PLGA (core: Mw 50K-75K

g/mol, LA/GA: 85/15; shell: Mw 24K-38K g/mol, LA/GA: 50/50) composite particles (particle size:

400 nm) with both drugs loaded in tested configurations: (A) release profiles of Budesonide, (B)

release profiles of Theophylline. Duplicate testing with N=2.

To further slow down the release rate of Theophylline from the 400-nm PLGA particles, especially for the drug loading configuration when Budesonide and Theophylline were both encapsulated in the core of the particles, the core-shell particles composed of PLGA (Mw: 50,000-75,000 g/mol, LA/GA: 85/15) in core and shell of the particles were produced via the coaxial dual capillary ES process for drug encapsulation. The resultant drug release profiles are depicted in Figure 4.4. Similar to our previous observations in Figure 4.2 (A) and Figure 4.3 (A), release rate of Budesonide from the particles with drugs loaded in the TB configuration (i.e., Theophylline loaded in core, Budesonide loaded in shell) was faster than that from the particles with drugs loaded in the BT configuration (i.e., Budesonide loaded in core, Theophylline loaded in shell) due to the configuration effect. However, Figure 4.4 (A) displays higher Budesonide release rate in F17 than F18, implying high porosity of electrosprayed PLGA (Mw: 50,000 g/mol, LA/GA: 85/15), allowing fast infusion of the release media for fast drug dissolution and drug release. Such an assumption will be proven later via Brunauer-Emmett-Teller (BET) Surface Area Analysis on 400-nm drug-loaded PLGA particles. Figure 4.4 (B) shows equally fast Theophyllind release rates of F17, F18 and F19, suggesting the infusion rate of the release media into the composite nanoparticles was extremely fast possibly due to the high porosity of the particles.
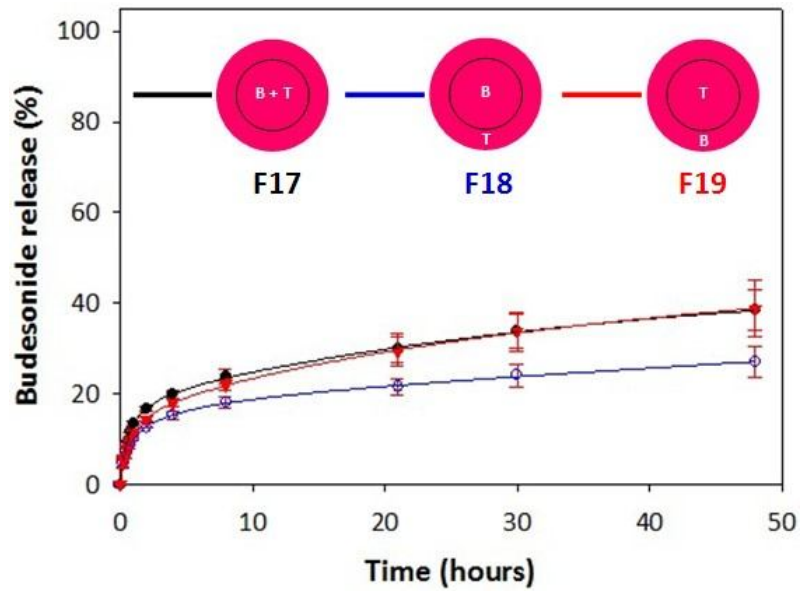
(A)
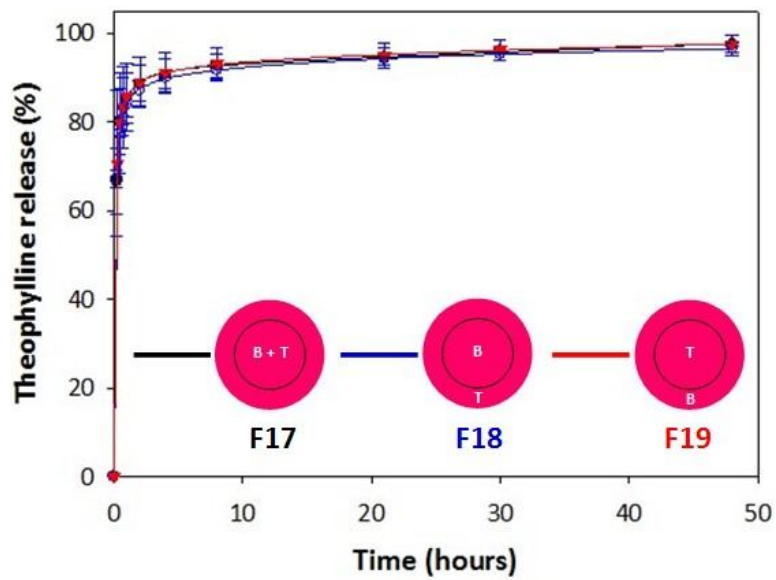
(B)

Figure 4.4. Release profiles of Budesonide (B) and Theophylline (T) from PLGA (core: Mw 50K-75K g/mol, LA/GA: 85/15; shell: Mw 50K-75K g/mol, LA/GA: 85/15) composite particles (particle size: 400 nm) with both drugs loaded in tested configurations: (A) release profiles of Budesonide, (B) release profiles of Theophylline. Duplicate testing with N=2.

Taken all together, *in vitro* drug release behaviors of Budesonide and Theophylline from Budesonide-Theophylline loaded 400-nm PLGA composite particles may be explained by the drug loading locations along with the void spaces in the particle shell left behind by the release of the shell-loaded drug molecules for particles composed of PLGA (Mw: 50,000-75,000 g/mol, LA/GA: 85/15) and PLGA (Mw: 24,000-38,000 g/mol, LA/GA: 50/50) in core and shell, respectively. Size distributions and SEM images of F14, F15 and F16 are shown in Figure 4.5 and Figure 4.6, respectively. The B+T configuration (i.e., Budesonide and Theophylline both loaded in particle core) may be the most capable one to slow down the release rate of Theophylline. However, release behaviors of Budesonide and Theophylline from the 400-nm composite nano-carriers shown in Figure 4.1 (A) and 4.1 (C) may not be explained perfectly. Therefore, effects of particle filling materials on drug release behaviors of Budesonide and Theophylline need to be studied. Due to the challenges of Theophylline slow release observed from release profiles of F11-F19, we first concentrated on Theophylline release from core-shell ES PLGA particles to determine the key factors influencing Theophylline release rate and to learn how to control it. Since the drug loading locations have been proven not to be fully capable of slowing down release rate of Theophylline from Budesonide-Theophylline loaded PLGA composite nanoparticles and not to be sufficient to provide a simplified theory to support the observed findings, the material effect and the particle shell layer thickness effect were subsequently investigated in the following sections for the extended release of Theophylline. Budesonide were then encapsulated together with Theophylline in the PLGA drug carriers capable of suppressing Theophylline release

78

rates to provide formulations that were able to accomplish extended release of both

Budesonide and Theophylline simultaneously.
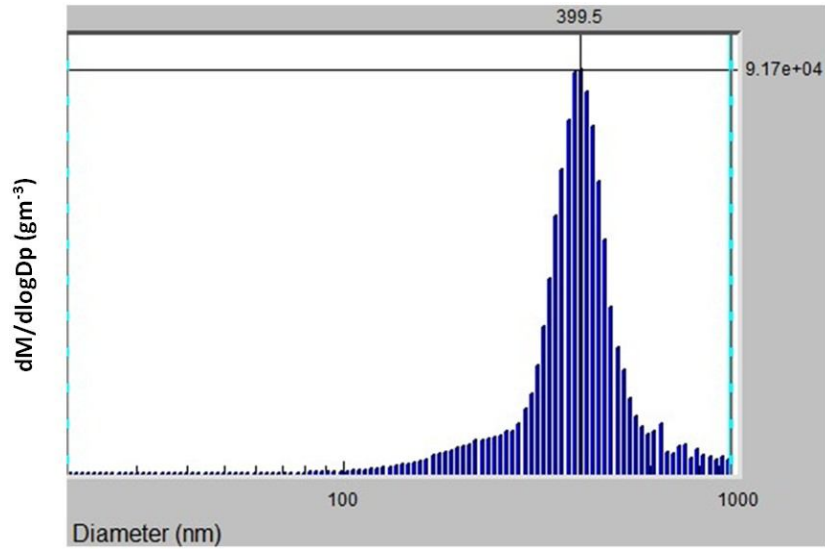
Figure 4.5. Size distributions of F14, F15 and F16 core-shell PLGA nanoparticles (particle size: 400

nm, GSD: 1.40) measured by SMPS.
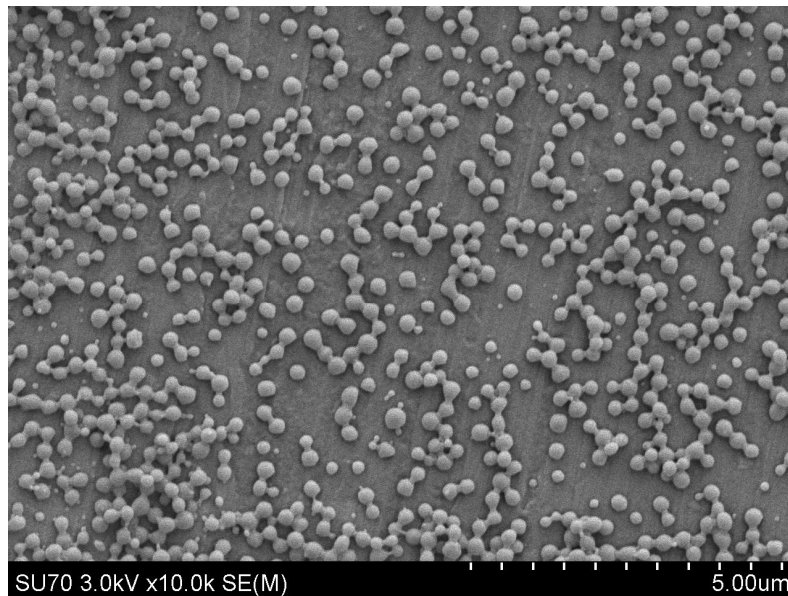
(A)
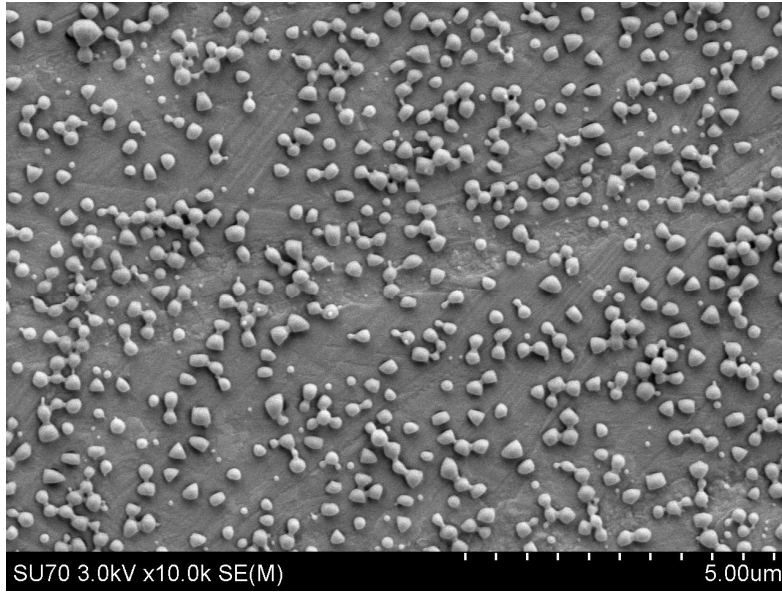
(B)
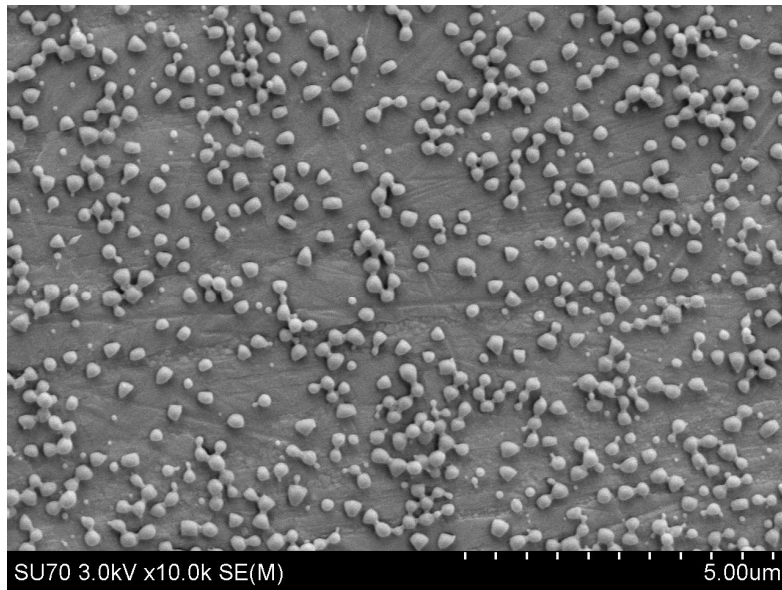
(C)

Figure 4.6. SEM images of 400-nm core-shell PLGA nanoparticles with tested drug loading configurations: (A) F14: core loaded with Budesonide and Theophylline, (B) F15: core loaded with Budesonide, shell loaded with Theophylline, (C) F16: core loaded with Theophylline, shell loaded with Budesonide.

4.2.2 Effects of Loading Locations of Singly Encapsulated Theophylline in Particles on Drug Release

To study the release of Theophylline from core-shell PLGA particles, we first loaded Theophylline in the particle cores only (F20) and in both particle cores and particle shells (F21) with ES process parameters listed in Table 4.4. The PLGA polymer (Mw: 50,000-75,000 g/mol, LA/GA: 85/15) was used as the filler for particle cores and shells. The schematic diagrams of the as-produced nanoparticles are given in Figure 4.7 to illustrate the tested Theophylline loading configurations in the particles. Due to the similar ES process parameters of the outer solutions, size distributions of F20 and F21 were alike and shown in Figure 4.8. SEM images of F20 and F21 are given in Figure 4.9. The above SMPS data and SEM images demonstrate the excellent morphology and uniform size distributions of F20 and F21.

Drug-to-polymer mass ratio = 1:10

❖ Formulation ID: F20
❖ Polymer (shell):
   PLGA (Mw: 50K-75K g/mol,
   LA/GA: 85/15)
❖ PLGA (core):
   PLGA (Mw: 50K-75K g/mol,
   LA/GA: 85/15)
❖ Particle size: 399.5 nm

❖ Formulation ID: F21
❖ Polymer (shell):
   PLGA (Mw: 50K-75K g/mol,
   LA/GA: 85/15)
❖ PLGA (core):
   PLGA (Mw: 50K-75K g/mol,
   LA/GA: 85/15)
❖ Particle size: 399.5 nm
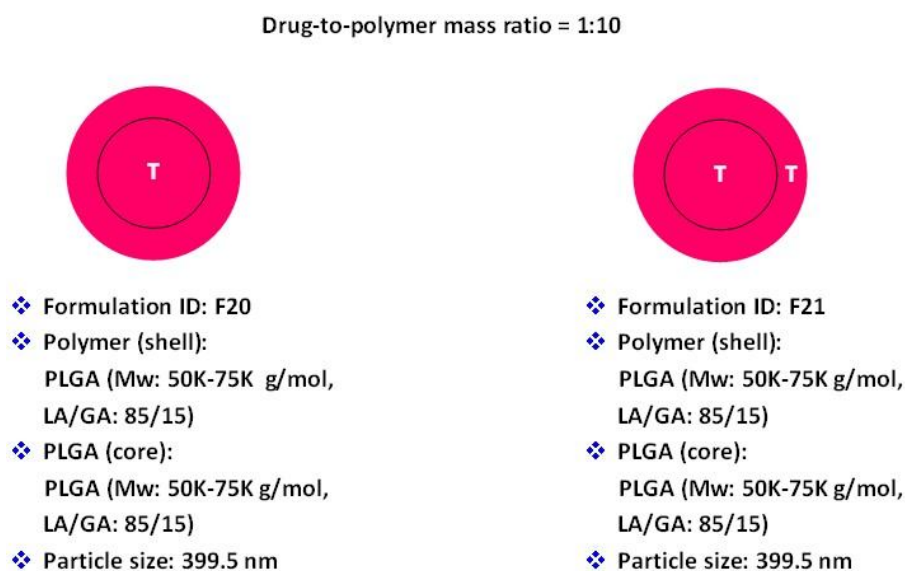
Figure 4.7. The schematic diagrams of the 400-nm Theophylline (T) loaded core-shell type ES PLGA (core and shell: Mw 50K-75K g/mol, LA/GA: 85/15) composite particles in tested drug loading configurations.
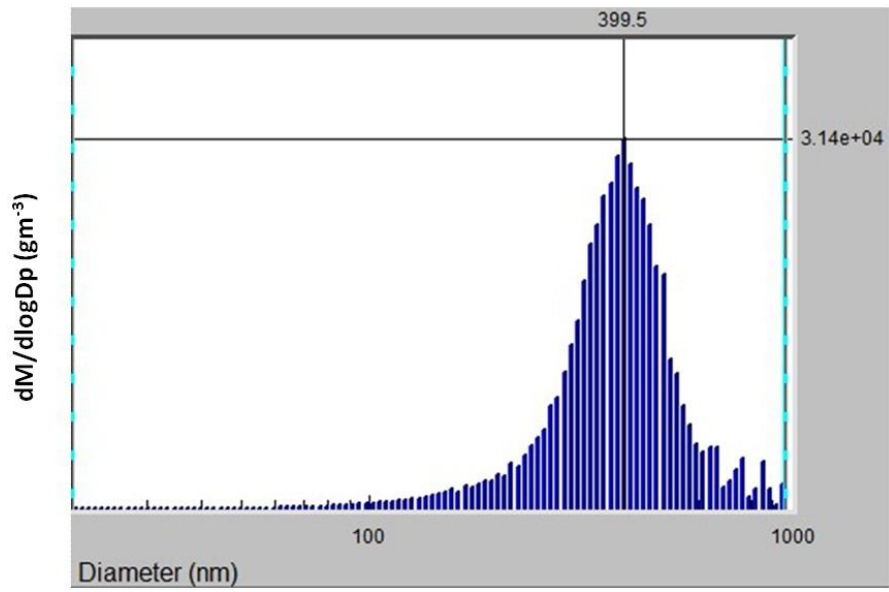
Figure 4.8. Size distributions of F20 and F21 core-shell PLGA particles (particle size: 400 nm, GSD: 1.45) measured by SMPS.
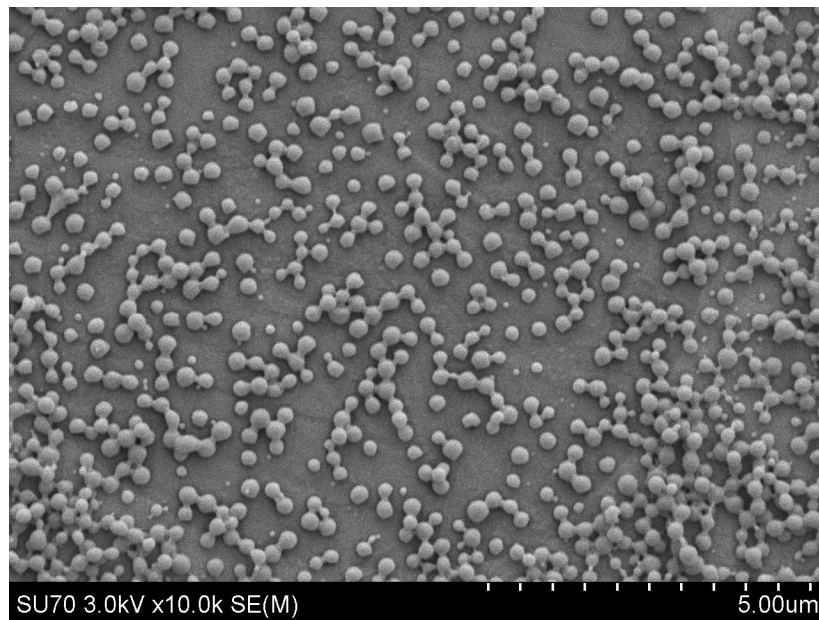
(A)
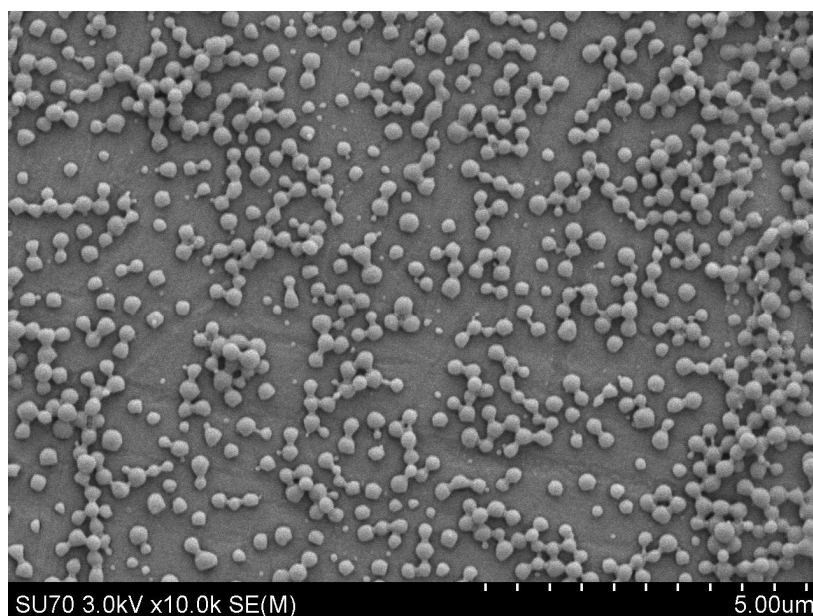
(B)

Figure 4.9. SEM images of the 400-nm core-shell PLGA particles with tested Theophylline loading configurations: (A) F20: Theophylline loaded in the cores, (B) F21: Theophylline loaded in the cores and the shells.

Figure 4.10 shows the resultant release profiles of Theophylline from F20 (EE% of Theophylline: 88.1%) and F21 (EE% of Theophylline: 95.1%). The data evidences that the release rate of Theophylline was increased in the case with Theophylline loaded in both particle cores and shells (F21) compared with the case when Theophylline was loaded in the particle core (F20). The higher Theophylline release rate of F21 was associated with the shorter distance in the core-shell-loaded particles for drug release. The release profiles in Figure 4.10 also suggest that the PLGA formulations prepared under both cases were incapable of effectively slow down the release rate of Theophylline. Approximately 85% of encapsulated Theophylline was released within the 1st hour even in the case when Theophylline

83

was only loaded in the particle cores (i.e., F20). The above finding might be also attributed to the less affinity between Theophylline and the polymer filler [Almería et al., 2011].
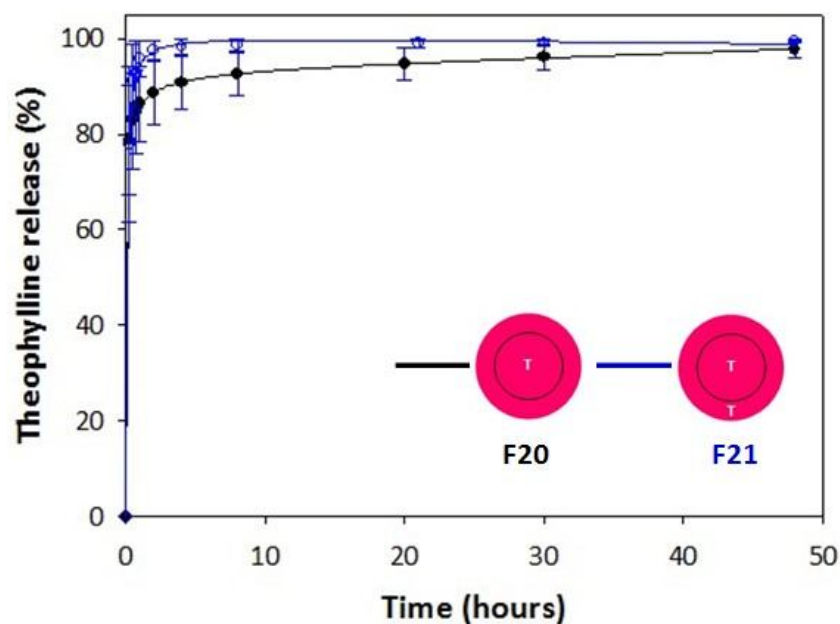
Figure 4.10. Release profiles of Theophylline (T) from PLGA (core: Mw 50K-75K g/mol, LA/GA: 85/15; shell: Mw 50K-75K g/mol, LA/GA: 85/15) composite nanoparticles (particle size: 400 nm): (A) Theophylline loaded in the cores, (B) Theophylline loaded in the cores and the shells. Duplicate testing with N=2.

4.2.3 Effects of Particle Filling Materials on Theophylline and/ or Budesonide Drug Release

To lessen the extent of initial burst release and to decrease the release rate of Theophylline from core-shell composite particles, three types PLGA polymers were applied to produce composites loaded with Theophylline in particle core. As shown in Figure 4.11, three particle formulations (with the size: 400-450 nm) were composed

of PLGA polymers (Mw: 7,000-17,000 g/mol, LA/GA: 50/50; Mw: 24,000-38,000 g/mol, LA/GA: 50/50; and Mw: 50,000-75,000 g/mol, LA/GA: 85/15). Drug encapsulation efficiencies (EE%) of formulation F20, F22 and F23 were 88.1%, 94.4% and 87.7%, respectively. The size distribution data and SEM images of the as-produced nanoparticles are shown in Figure 4.12 and Figure 4.13. Because the same feeding flowrate, electric conductivity and the polymer filling material and its concentration of the outer spray solution were employed to generate formulations F14-F16 and F23, the size distribution of F23 was almost identical with that of F14-F16 and may thus be referred to Figure 4.5. The resultant release profiles of Theophylline from prepared PLGA composites are given in Figure 4.14. Slow release rates of Theophylline were observed when it was encapsulated in particles composed of the PLGA polymer having lower lactic-to-glycolic ratio (i.e., F22 and F23). The above observation confirms the conclusion from literature that great affinity between drug and polymer filler could reduce the release rate of a hydrophilic pharmacologic agent from PLGA particles [Shi et al., 2008; Almería et al., 2011; Cao et al., 2014; Pereira et al., 2015]. It was interesting to notice that the release rate of Theophylline could be further reduced when Theophylline was encapsulated in particles composed of the PLGA polymer with a lactic-to-glycolic ratio of 50:50 but having low molecular weight (7,000-17,000 g/mol) (i.e., formulation F22). The above finding might be explained by the fact that the infusion of release media was impeded by the lower surface porosity and the smaller pore size in the particle matrix composed of PLGA polymers of low molecular weights (BET surface areas of formulations F20 and F22: 3.7056 ± 0.1419 m²/g and 0.6801 ± 0.0658 m²/g, respectively; median pore

width of F20 and F22: 10.934 Å and 7.909 Å, respectively). The above observation implies that, in addition to the LA/GA ratio, the molecular weight of PLGA polymers could be a critical factor for the sustained release of Theophylline from PLGA particles.

<Note> THY-to-polymer mass ratio = 1:10

* Formulation ID: F20
* Polymer (shell):
  PLGA (Mw: 50K-75K g/mol LA/GA: 85/15)
* PLGA (core):
  PLGA (Mw: 50K-75K g/mol, LA/GA: 85/15)
* Particle size: 399.5 nm

* Formulation ID: F22
* Polymer (shell):
  PLGA (Mw: 7K-17K g/mol, L:G = 50:50)
* PLGA (core):
  PLGA (Mw: 7K-17K g/mol, LA/GA: 50/50)
* Particle size: 429.4 nm

* Formulation ID: F23
* Polymer (shell):
  PLGA (Mw: 24K-38K g/mol, LA/GA: 50/50)
* PLGA (core):
  PLGA (Mw: 24K-38K g/mol LA/GA: 50/50)
* Particle size: 399.5 nm
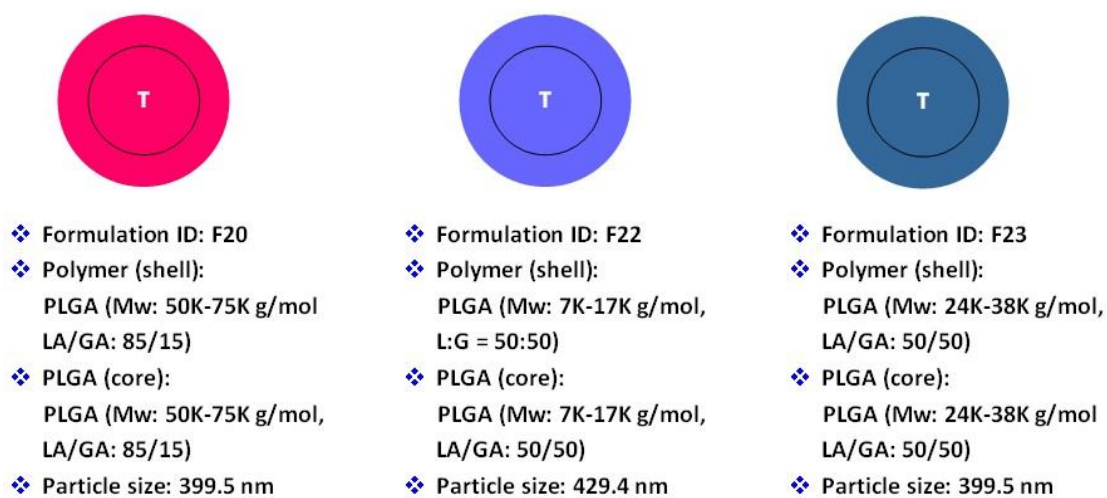
Figure 4.11. The schematic diagrams of Theophylline (T)-loaded ES core-shell PLGA composite particles (particle size: 400-450 nm) composed of PLGA (Mw: 50K-75K g/mol, LA/GA: 85/15), PLGA (Mw: 7K-17K g/mol, LA/GA: 50/50) and PLGA (Mw: 24K-38K g/mol, LA/GA: 50/50).

(A)

SU70 3.0kV x10.0k SE(M)   5.00um
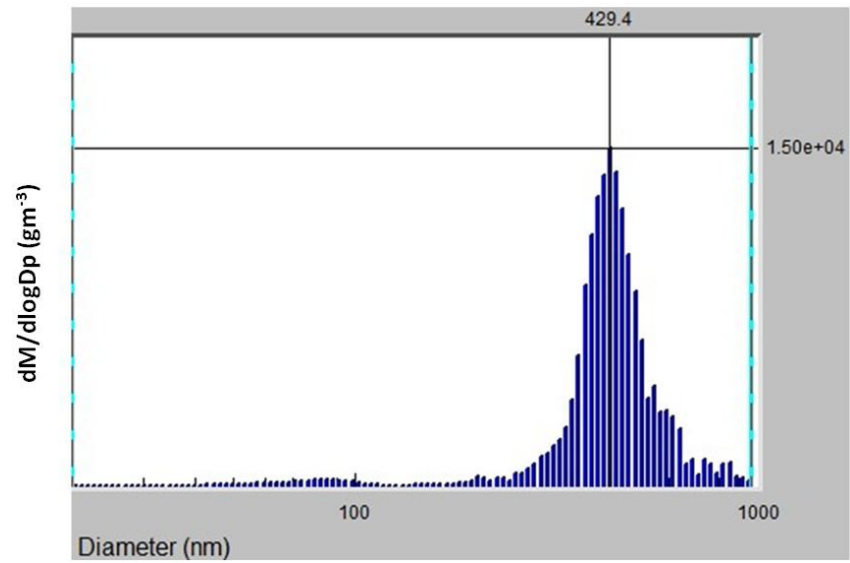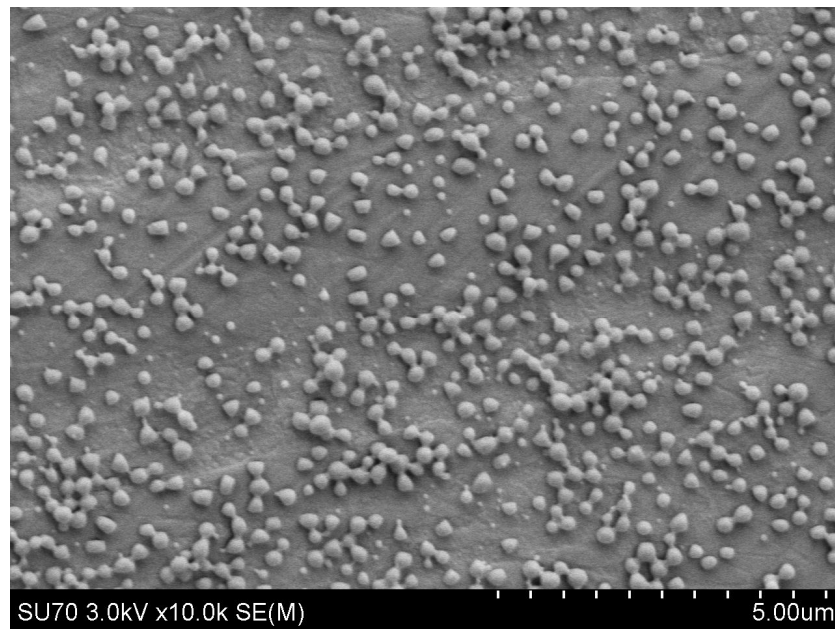
(B)

Figure 4.12. (A) Size distribution and (B) the SEM image of formulation F22 core-shell PLGA

particles (particle size: 429.4 nm, GSD: 1.50) measured by SMPS.
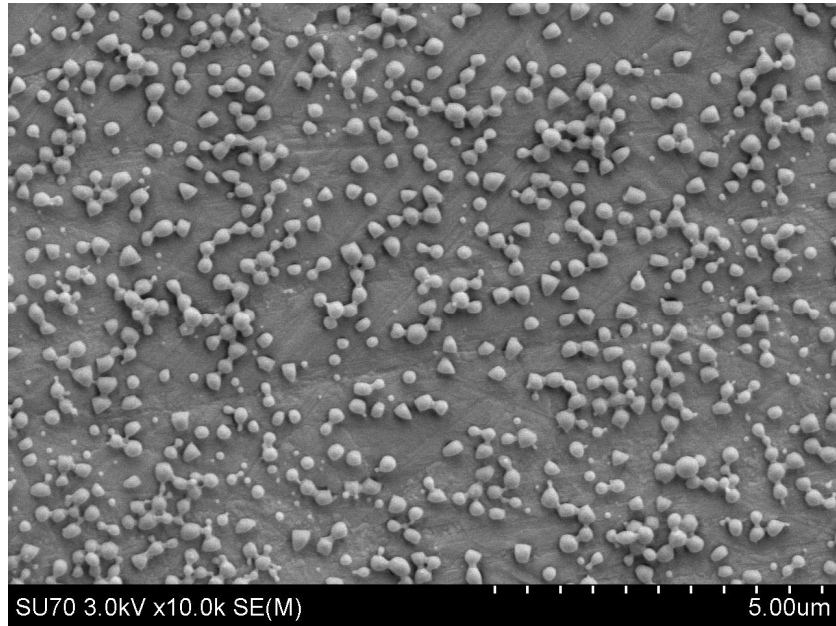
Figure 4.13. The SEM image of formulation F23 core-shell PLGA particles (particle size: 400 nm)
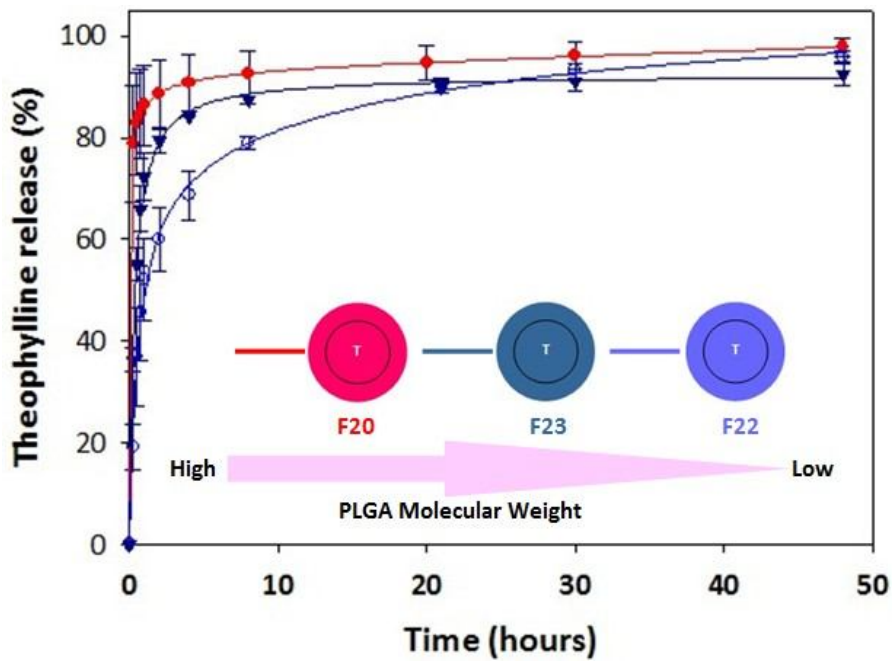
Figure 4.14. *In vitro* drug release profiles of Theophylline (T) from the core regions of the nanoparticles composed of PLGA with various molecular weights and lactic-to-glycolic ratios (particle size: 400-450 nm). F20: PLGA (Mw: 50K-75K g/mol, LA/GA: 85/15), F22: PLGA (Mw: 7K-17K g/mol, LA/GA: 50/50), F23: PLGA (Mw: 24K-38K g/mol, LA/GA: 50/50). Duplicate testing with N=2.

Release profiles of Budesonide and Theophylline from the 400-nm PLGA composite particles given in Section 4.2.1 also allow us to compare drug release behaviors of Budesonide and Theophylline from Budesonide-Theophylline loaded core-shell PLGA composite nanoparticles composed of different filling materials in core or shell of a single particle formulation. Relying on the conclusions just made according to Theophylline release profiles of formulations F20-F23 shown in Figure 4.14, drug release behaviors of selected Budesonide-Theophylline loaded particle formulations with the same drug loading configuration in Section 4.2.1 may be discussed as below. Figure 4.15 depicts release profiles of Budesonide and Theophylline, both loaded in particle cores, from formulations F14 and F17. Due to greater total surface area of PLGA (Mw: 50,000-75,000 g/mol, LA/GA: 85/15) than PLGA (Mw: 24,000-38,000 g/mol, LA/GA: 50/50), the infusion rate of the surrounding release media through the particle shell layer into the particle core was higher for the case of formulation F17 than formulation F14. Budesonide loaded in the cores of formulation F17 was dissolved by the infused release media earlier than that loaded in the cores of formulation F14 for drug release. During drug release, the shell layers of F17 provided lesser resistance due to its greater porosity than formulation F14. In the end, release rates of both Budesonide and Theophylline were higher from formulation F17 than F14.
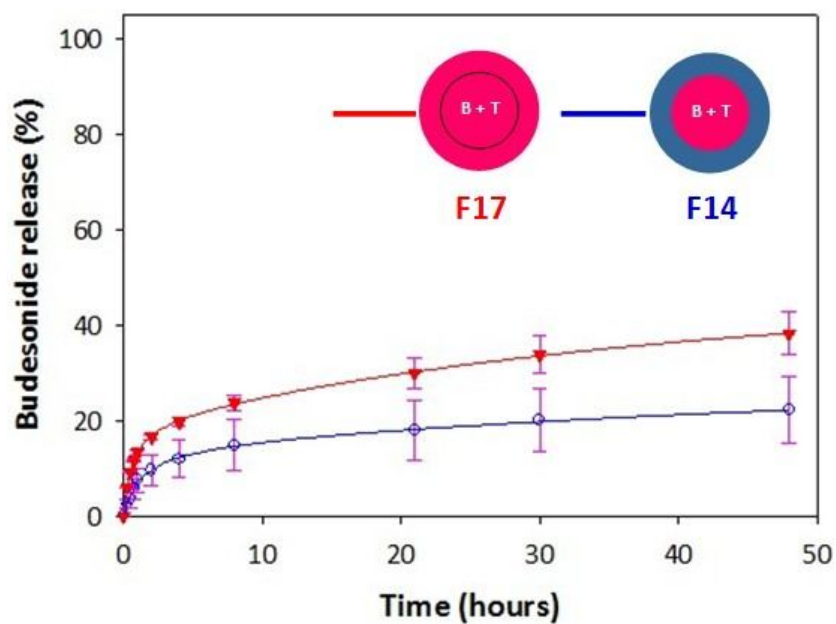
(A)
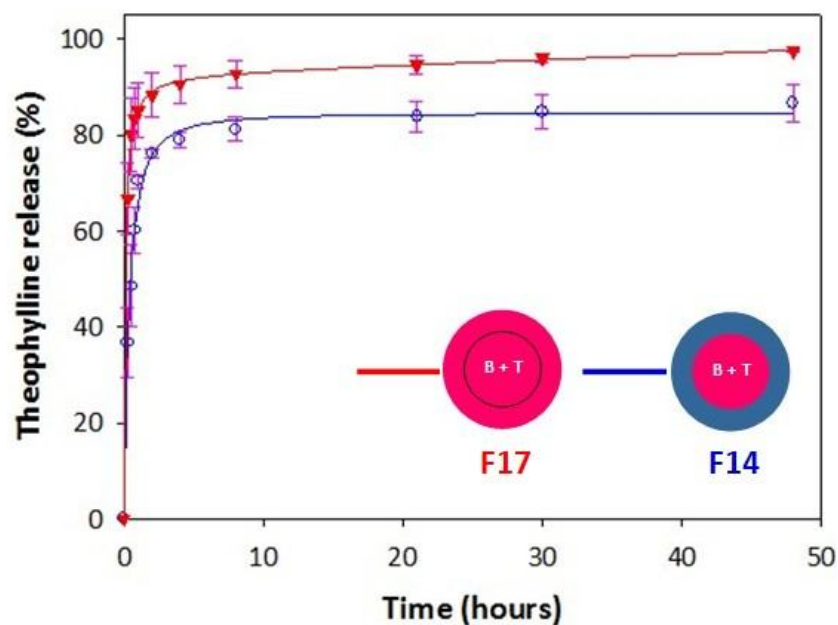
(B)

Figure 4.15. Release profiles of (A) Budesonide and (B) Theophylline from the core regions of PLGA nanoparticles composed of different polymer compositions. Formulation F14: PLGA (Mw 50K-75K g/mol, LA/GA: 85/15) in the cores, PLGA (Mw 24K-38K g/mol, LA/GA: 50/50) in the shells; formulation F17: PLGA (Mw 50K-75K g/mol, LA/GA: 85/15) in both cores and shells. Duplicate testing with N=2.

90

Release profiles of Budesonide and Theophylline from formulations F15 and F18 are given in Figure 4.16. In both cases, Budesonide and Theophylline were encapsulated in core regions and shell regions of PLGA particles (particle size: 400 nm), respectively. Though the infusion rate of release media through the shell layer of F18 was greater than that of F15, the resultant Theophylline release rates were without too much difference because Theophylline was loaded in the cores of both particle formulations. In addition, Theophylline is a highly hydrophilic drug compound with great aqueous solubility. Therefore, release rates from formulations F15 and F18 were both extremely high due to the fast dissolution of Theophylline. However, a significant difference in the Budesonide release rate was observed between formulations F15 and F18. The particle shell of formulation F15 was composed of PLGA (Mw: 24,000-38,000 g/mol, LA/GA: 50/50) with smaller pore size compared to the filling material, i.e., PLGA (Mw: 50,000-75,000 g/mol, LA/GA: 85/15), of the particle shell of formulation F18. Theophylline release from formulation F15 thus caused greater structural disruption on the filling material of the particle shells, leading to greater infusion of the release media into the particle cores and less resistance of diffusion for Budesonide. As a result, Budesonide was released more rapidly when it was loaded in the cores of formulation F15 compared to the case when it was loaded in cores of the formulation F18.
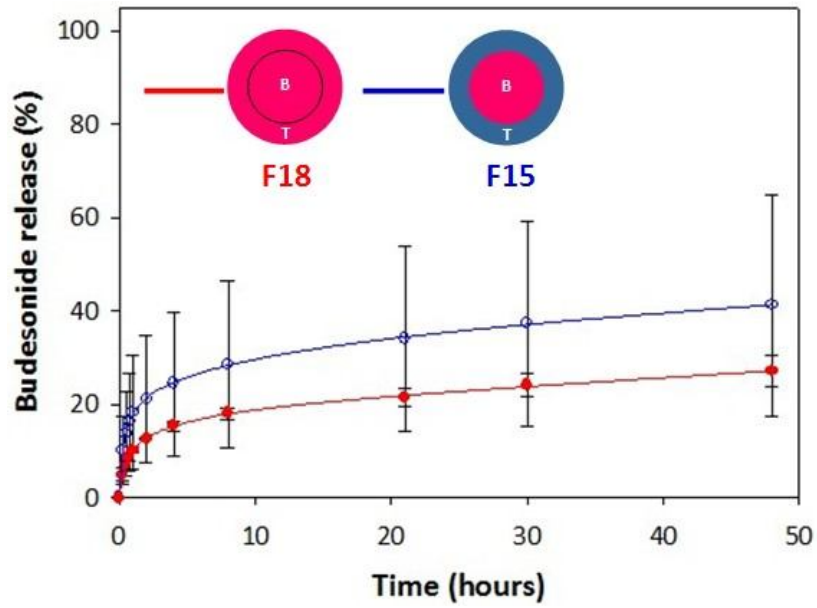
(A)
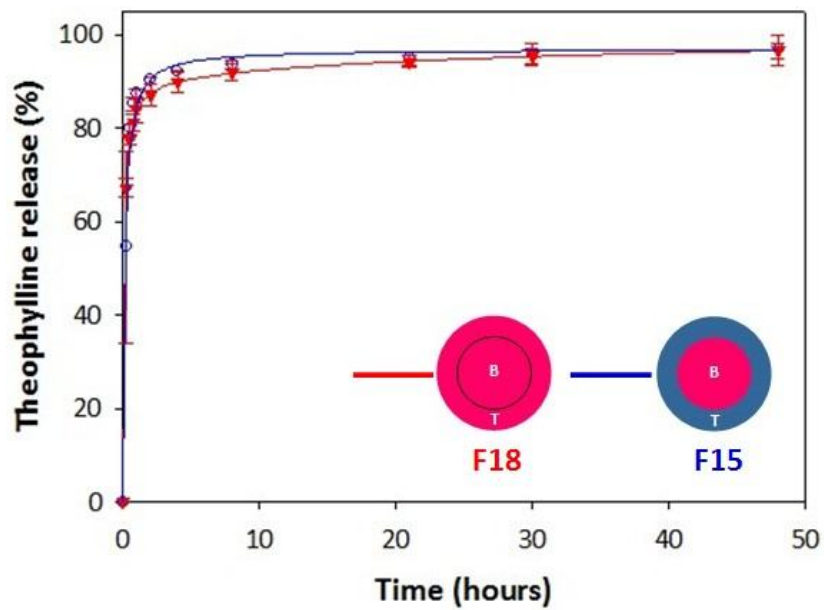
(B)

Figure 4.16. Release profiles of (A) core-loaded Budesonide (B) and (B) shell-loaded Theophylline (T) from the 400-nm core-shell PLGA particles composed of different polymer compositions. Formulation F15: PLGA (Mw 50K-75K g/mol, LA/GA: 85/15) in particle cores, PLGA (Mw 24K-38K g/mol, LA/GA: 50/50) in particle shells; formulation F18: PLGA (Mw 50K-75K g/mol, LA/GA: 85/15) in both particle cores and shells. Duplicate testing with N=2.

Figure 4.17 shows the release profiles of Budesonide and Theophylline from Budesonide-Theophylline loaded composite PLGA particle formulations. Herein, Theophylline and Budesonide were loaded in particle cores and shells, respectively. Fillers of the particle cores were PLGA (Mw: 50,000-75,000 g/mol, LA/GA: 85/15) for both formulations F16 and F19. Fillers of the particle shells were PLGA (Mw: 24,000-38,000 g/mol, LA/GA: 50/50) and PLGA (Mw: 50,000-75,000 g/mol, LA/GA: 85/15) for formulations F16 and F19, respectively. Though the infusion rate of release media through the shell layer of F19 was greater than that through the shell layer of F16, faster release rate of Budesonide from formulation F19 than F16 was not observed as expected. The finding implies that other factors might have offset the effects of the infusion of release media on drug release, which may be attributed to the void spaces in the particle shells created by the release of shell-loaded Budesonide. Because the molecular weight of Budesonide (430.53 g/mol) is larger than that of Theophylline (180.16 g/mol), larger spaces were left behind in the polymer matrix after the release of Budesonide. The void spaces resulted in greater material structural disruption in the shell of formulation F16 than that of F19 because the shells of F16 was composed of PLGA (Mw: 24,000-38,000 g/mol, LA/GA: 50/50) with smaller pore size, which further led to greater influx of the release media for the dissolution and release of Budesonide loaded in particle shells. The extent of material structural disruption in the shell caused by the release of shell-loaded Budesonide also affected the release rate of the core-loaded Theophylline. That is why the Theophylline release rate of formulation F16 was increased to be equally as rapid as that of formulation F19 even though the shells of F19 was composed of the filler (i.e., PLGA: Mw

93

50,000-75,000 g/mol, LA/GA: 85/15) with larger surface porosity and pore size than the filler used to constitute the shells of formulation F16.
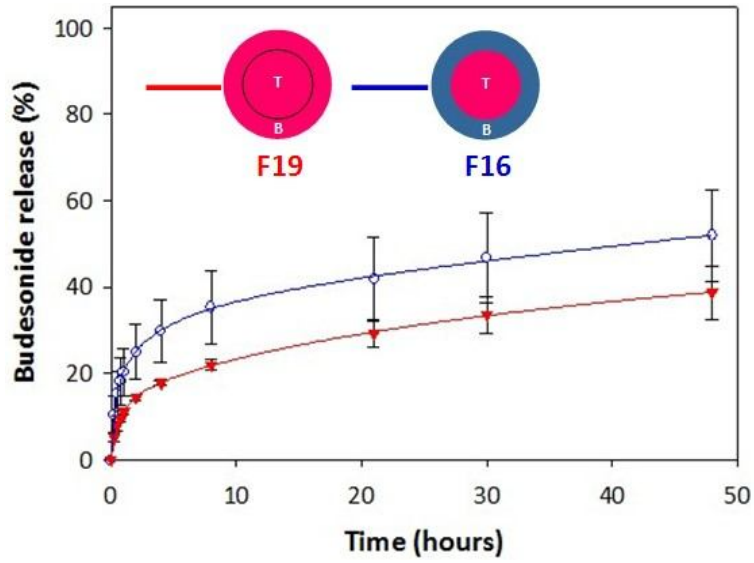
(A)
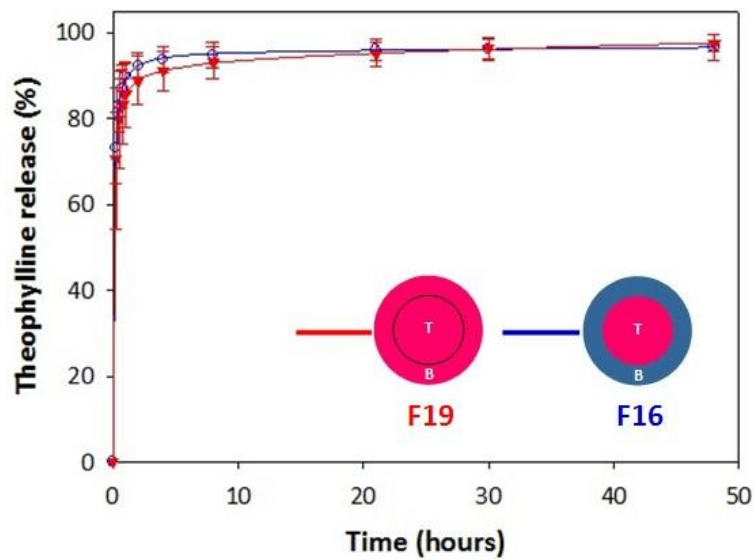
(B)

Figure 4.17. Release profiles of (A) shell-loaded Budesonide (B) and (B) core-loaded Theophylline (T) from PLGA nanoparticles composed of different polymer compositions. Formulation F16: PLGA (Mw 50K-75K g/mol, LA/GA: 85/15) in core, PLGA (Mw 24K-38K g/mol, LA/GA: 50/50) in shell; formulation F19: PLGA (Mw 50K-75K g/mol, LA/GA: 85/15) in both core and shell. Duplicate testing with N=2.

4.2.4   Effects of Particle Shell Layer Thickness on Theophylline Drug Release

According to the results and discussions addressed from Section 4.2.1 to 4.2.3, drug release of Budesonide-Theophylline loaded core-shell PLGA particle composites (particle size: 400-450 nm) was affected by the drug loading locations, the void spaces left behind by the drug loaded in particle shell, and the surface porosity and pore size of the particle filling materials. Through the release profile studies on formulations F20, F22 and F23, the slowest Theophylline release rate was achieved by formulation F22, and the surface porosity and the pore size of the ES nanoparticles were correlated with the molecular weight of PLGA. The formulation F22 released Theophylline in the slowest extended release fashion among the formulations that have been tested so far in Chapter 4 (i.e., formulations F11-F23), which further emphasizes the PLGA (Mw: 7,000-17,000 g/mol, LA/GA: 50/50) was the most capable particle filler for the sustained release of Theophylline.

To investigate the possibility of more reduction on the release rate of Theophylline, composite particles with similar cores but thicker shell thicknesses (i.e., F24) were produced with the ES process parameters listed in Table 4.6. In this part of investigation, PLGA (Mw: 7,000-17,000 g/mol, LA/GA: 50/50) was used as the filler to encapsulate Theophylline in the cores of the prepared particles. By employing the inner solution with the same feeding flowrate, electric conductivity and polymer concentration, core dimensions of formulations F22 and F24 were similar. With the increased PLGA concentration in the outer solution during the coaxial dual capillary ES process, F24 (i.e., particles with greater shell layer thickness than F22) was produced with the SEM image and the size distributions characterized by OPS shown

in Figure 4.18. Given the known mass ratio of PLGA in particle core and shell for F22 and F24 and measured overall particle diameters, the core dimensions may be estimated via the mass conservation. The estimated core diameters of F22 and F24 were both 250 nm. Accordingly, the estimated shell layer thicknesses of F22 and F24 were 90 nm and 360 nm, respectively. Due to the increased PLGA shell thickness, particle size of F24 (i.e., 1 µm) was larger than that of F22 (i.e., 430 nm). The schematic diagram of formulations F22 (EE%: 94.44%) and F24 (EE%: 90.0%) along with their resultant Theophylline release profiles are given in Figure 4.19 (A) and (B), respectively. It is evidenced that a further decrease of Theophylline release rate was accomplished by increasing the thickness of PLGA shell. The above observation is attributed to the extra time required for the release medium infusion into the particle core and the diffusion of Theophylline through the polymer filling matrix. The above finding suggests that particle shell layer thickness is critical for the slow release of Theophylline with PLGA particulate drug carriers no greater than 1 µm in diameter. Encapsulation of Theophylline in the core of lower–molecular-weight PLGA particles with greater shell thickness is an effective strategy to reduce the release rate of Theophylline and may also be applied to co-encapsulate Budesonide and Theophylline for the extended release of both drugs. Relevant research was performed in the following section to prove such a proposed concept.
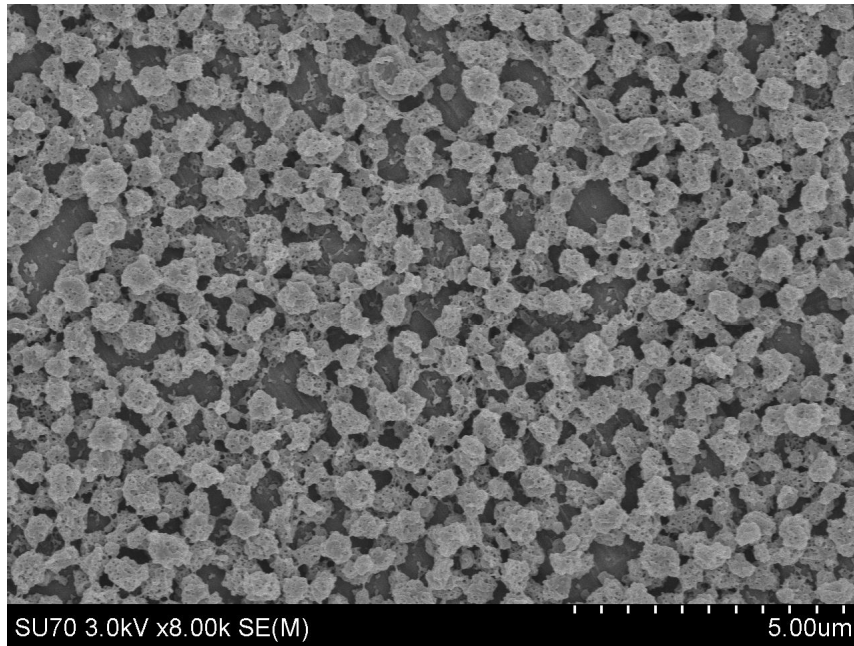
(A)
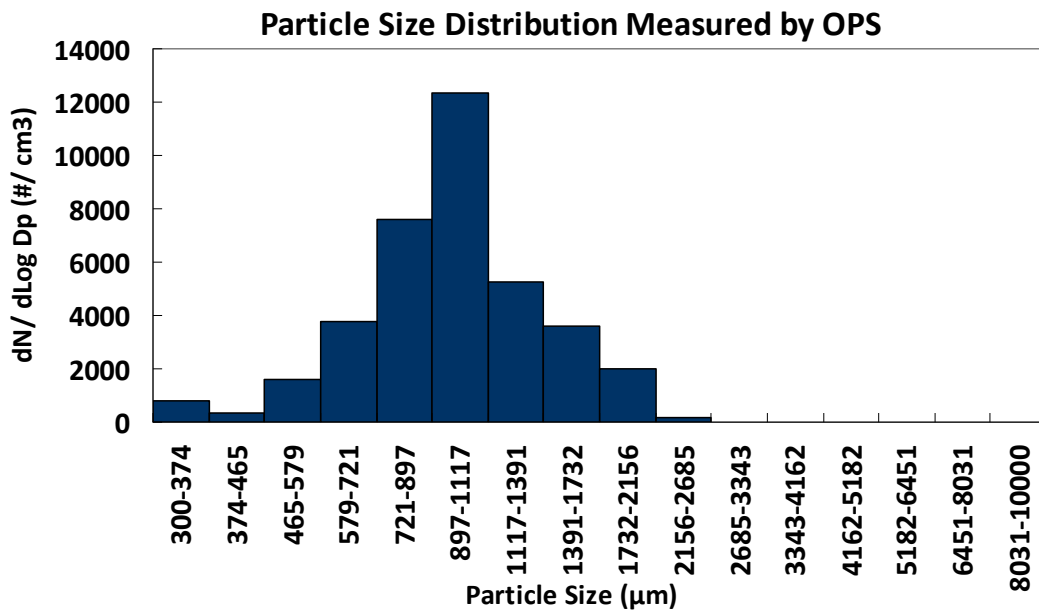
(B)

Figure 4.18. (A) The SEM image and (B) the particle size distribution measured by the OPS of the 1-μm core-shell PLGA (Mw: 7K-17K g/mol, LA/GA: 50/50 in core and shell) particles loaded with Theophylline in the particle cores (i.e., F24).
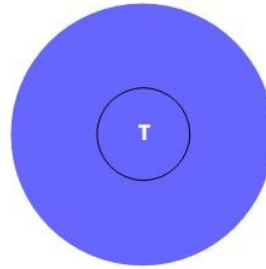
(A)

(B)
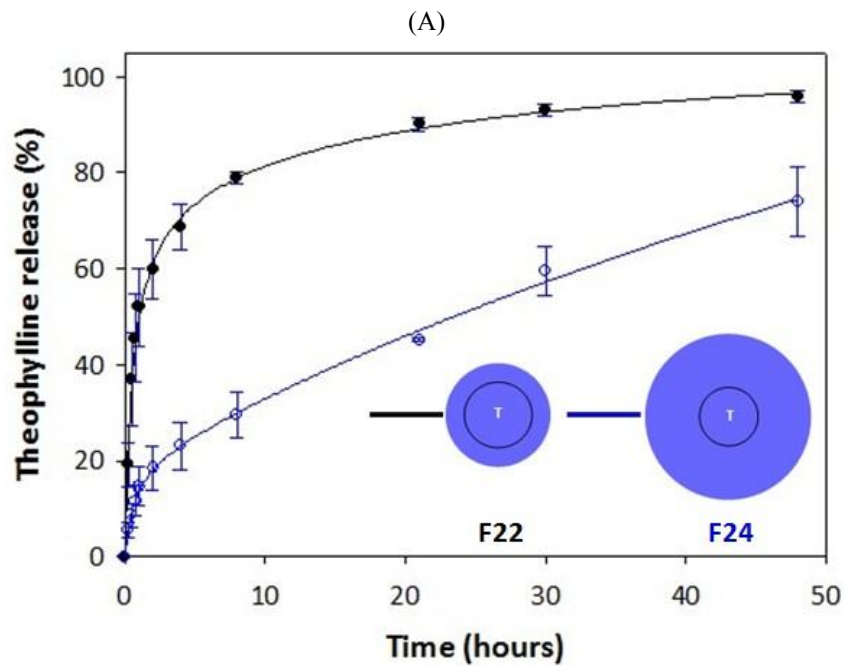
Figure 4.19. (A) The schematic diagrams and (B) the *in vitro* core-loaded Theophylline (T) release profiles of formulations F22 and F24 composed of PLGA (Mw: 7K-17K g/mol, LA/GA: 50/50) in both core and shell with the same core diameters but different shell thicknesses. Duplicate testing with N=2.

4.2.5 Effects of drug combination on release behaviors

To validate the sustained release of both model drugs from particles, we produced core-shell PLGA composite particles (Mw 7,000-17,000 g/mol and LA/GA: 50/50) with the particle diameter of 1 μm by using the ES process parameters consolidated in Table 4.7 to encapsulate both Budesonide and Theophylline in the core of particles (i.e., formulation F25). Schematic diagrams of formulations F24 and F25 are displayed in Figure 4.20 (A) to illustrate the differences of the two formulations studied to compare their drug release behaviors. Figure 4.20 (B) depicts the release profiles of Theophylline from formulations F24 and F25. No significant difference was observed, evidencing that the release rate of Theophylline was not influenced by the presence of Budesonide when both drugs were co-encapsulated in the core of the 1-μm PLGA (Mw: 7,000-17,000 g/mol, LA/GA: 50/50) core-shell particles. In this case, the void spaces left behind after the release of Budesonide did not significantly increase the release rate of Theophylline. The reason could be attributed to the high aqueous solubility of Theophylline, which is associated with the rapid drug dissolution of Theophylline in PBS. Thus, the release of Theophylline in this case was initiated earlier than that of Budesonide, and the release of Budesonide had limited impact on the release of Theophylline when both drugs were loaded in core of the 1-μm particles composed of PLGA (Mw: 7,000-17,000 g/mol, LA/GA: 50/50). On the other hand, formulation F25 also released the core-loaded Budesonide in a controlled fashion. Release profiles of both Budesonide and Theophylline from F25 (EE% of Budesonide: 94.9%, EE% of Theophylline: 92.1%) are given in Figure 4.20 (C) as the finalized fixed-combined particle formulation in this dissertation work

for extended release of both Budesonide and Theophylline from a single dosage formulation. The formulation F25 utilized the same PLGA particle drug carrier for drug encapsulation in the core. Therefore, its particle size distribution measured by the OPS was the same as that of the formulation F24 shown in Figure 4.18 (B). The SEM image of F25 is given in Figure 4.21 for the reference of its particle morphology.

Drug-to-polymer mass ratio = 1:10

❖ Formulation ID: F24
❖ Polymer (shell):
   PLGA (Mw: 7K-17K g/mol, LA/GA: 50/50)
❖ PLGA (core):
   PLGA (Mw: 7K-17K g/mol, LA/GA: 50/50)
❖ Particle size: 890-1120 nm

❖ Formulation ID: F25
❖ Polymer (shell):
   PLGA (Mw: 7K-17K g/mol, LA/GA: 50/50)
❖ PLGA (core):
   PLGA (Mw: 7K-17K g/mol LA/GA: 50/50)
❖ Particle size: 890-1120 nm
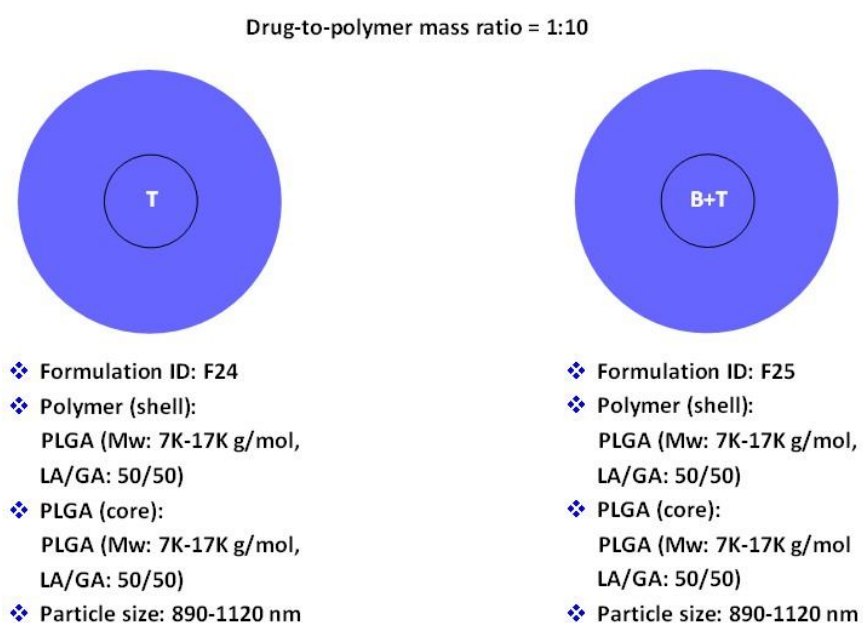
(A)
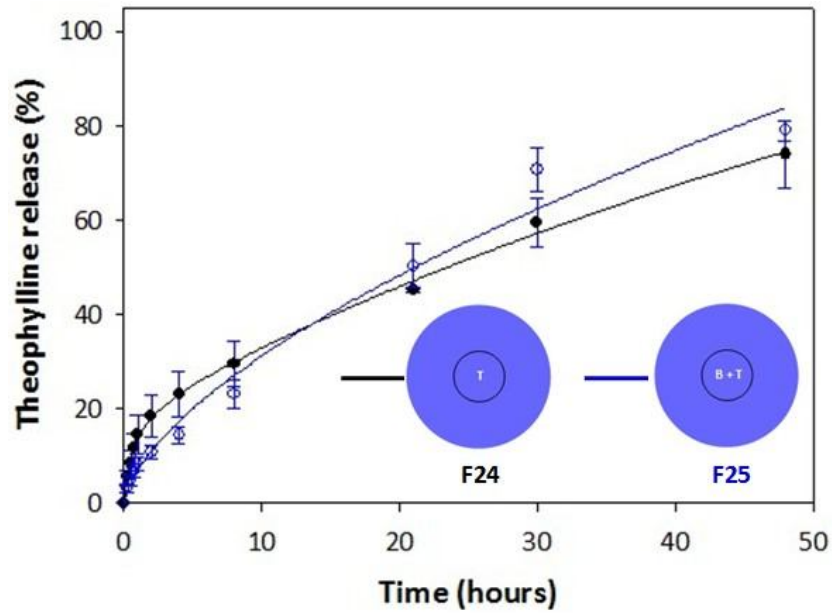
(B)
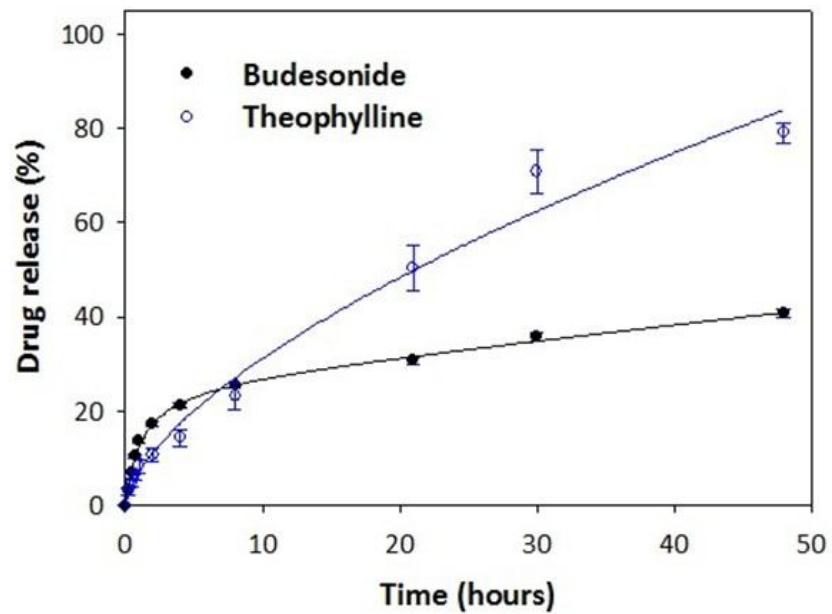
(C)

Figure 4.20. Sustained drug release *in vitro* with the 1-μm core-shell particle formulations composed of PLGA (Mw: 7K-17K g/mol, LA/GA: 50/50) in the core and shell regions: (A) schematic diagrams of formulations F24 and F25, (B) Theophylline (T) release profiles of formulations F24 and F25, (C) release profiles of Budesonide (B) and Theophylline (T) from the fixed-combined formulation F25. Duplicate testing with N=2.
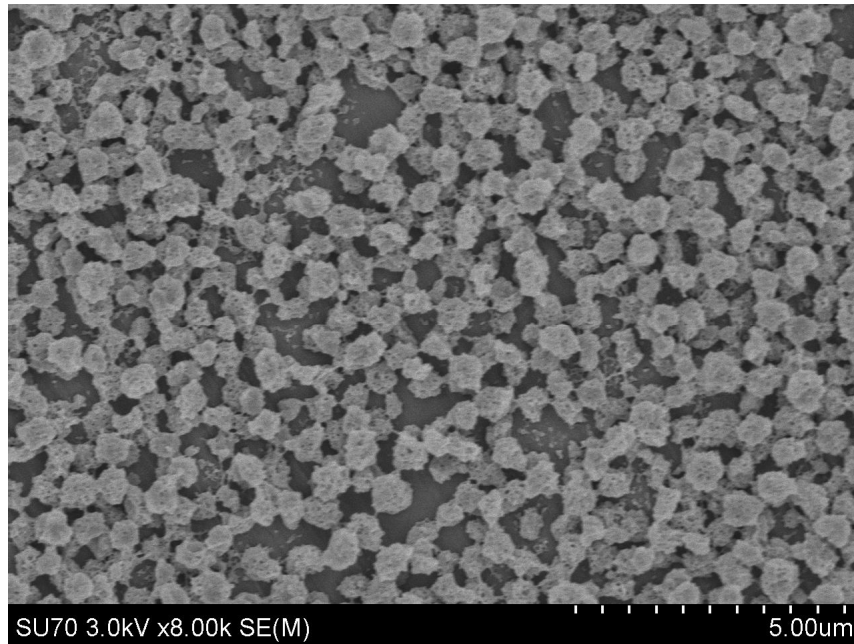
Figure 4.21. The SEM image of particle formulation F25 loaded with both Budesonide and Theophylline in the cores and shells of the particles.

4.2.6 Effects of drug-to-polymer ratio of Theophylline on its release rate from composite particles co-encapsulating Budesonide and Theophylline

As mentioned in previous sections, the drug-to-polymer ratio was set to be 1:10 throughout the present dissertation work to study the effects of particle filling materials, particle shell layer thicknesses and drug loading locations on release profiles of core-shell PLGA particles (particle size: 400 nm and 1000 nm) loaded with Theophylline and/ or Budesonide. F25 has been concluded to be the Budesonide-Theophylline loaded particle formulation capable of providing release profiles of both drugs in a most controlled fashion with the drug-to-polymer ratio of 1:10 throughout this research. However, effects of Theophylline-to-polymer mass ratio on the resultant release profiles of Theophylline when it is loaded together with

Budesonide in particle core are of interest. For the research purpose, PLGA particles (particle size: 400 nm) with the filling materials as PLGA (Mw: 50K-75K g/mol, LA/GA: 85/15) in both core and shell of the particles were generated. Both Budesonide and Theophylline were loaded in the core regions of the drug carriers with the ES process parameters listed in Table 4.8. The Theophylline-to-PLGA mass ratios of 1:10 (i.e., F17) and 1:20 (i.e., F26) were tested while the Budesonide-to-PLGA mass ratio was fixed at 1:10 for both formulations F17 and F26. The resultant release profiles of Budesonide and Theophylline are shown in Figure 4.22. Higher Theophylline release rate of F17 than F26 was observed because greater concentration difference of Theophylline inside and outside the polymer matrix was established in the case of formulation F17 for drug diffusion. On the other hand, Budesonide drug release rates of F17 and F26 were similar because the concentration difference of Budesonide in the polymer matrix and in the surrounding release media at the beginning of the diffusion process was identical for both particle formulations. According to the discussions in previous sections, PLGA (Mw: 50,000-75,000 g/mol, LA/GA: 85/15) is a porous polymeric filler with greater surface porosity and pore size. Due to the lower aqueous solubility of the highly hydrophobic drug compounds and the greater affinity between such drug compounds and the PLGA materials with higher lactic-to-glycolic ratios, the release rates of Budesonide from formulations F17 and F26 were both slow even though both formulations were less than 500 nm in diameter and composed of a PLGA material with high surface porosity and large pore size, which were the factors favorable to infusion of the release media. However, it was surprising that the release rate of core-loaded Theophylline could be decreased by

employing a lower Theophylline-to-PLGA ratio in the nano-particulate formulations. The finding suggests that the loading dose of the hydrophilic pharmacological agents is also crucial for the extended release combination therapy with PLGA particulate drug carriers.
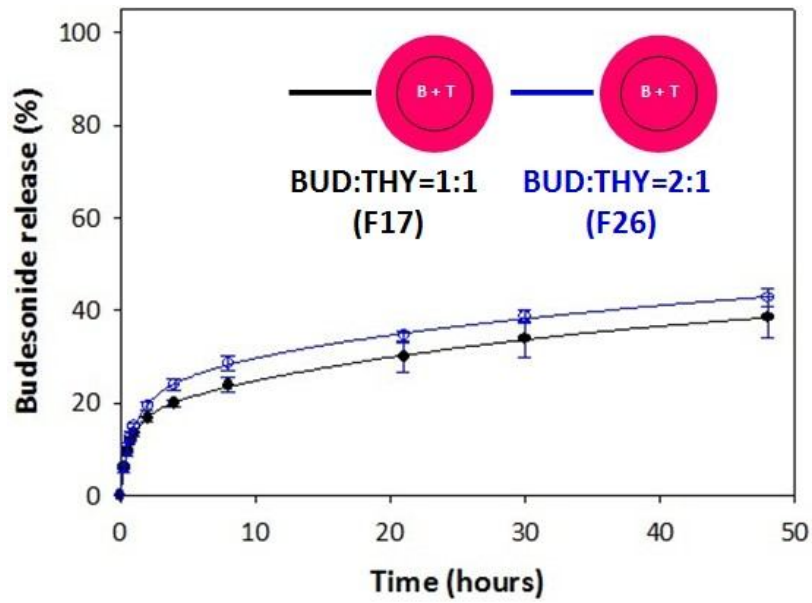
(A)
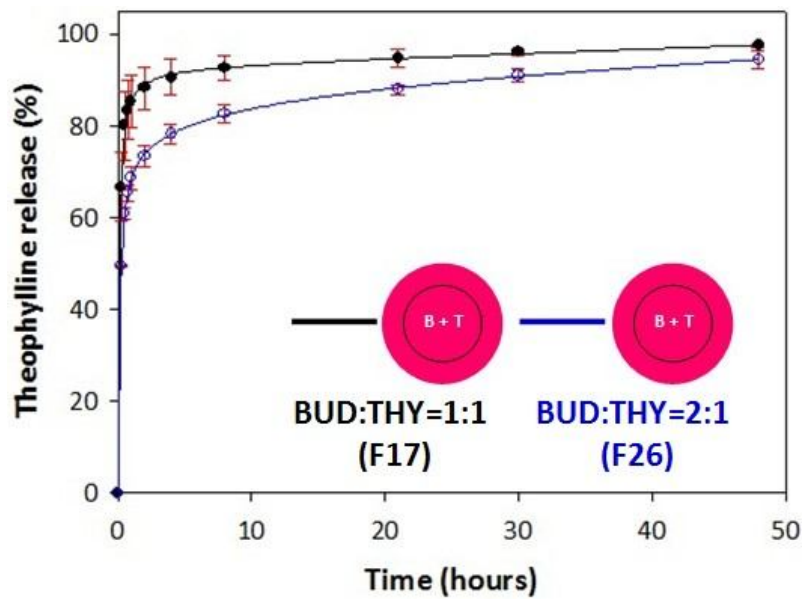
(B)

Figure 4.22. Release profiles of (A) Budesonide and (B) Theophylline from the 400-nm PLGA particles (core and shell: Mw 50K-75 K g/mol, LA/GA: 85/15) loaded with both Budesonide (B) (drug-to-polymer mass ratio at 1:10 for F17 and F26) and Theophylline (T) (drug-to-polymer mass ratio at 1:10 and 1:20 for F17 and F26, respectively) in the cores of the particles. Duplicate testing with N=2.

4.3 Summary

In this part of dissertation work, Theophylline and/ or Budesonide were loaded in core-shell composite PLGA particles with different drug loading configurations. Drug-loaded particles with the sizes of 400 nm and 1 μm were generated via the coaxial dual capillary electrospray (ES) technique. Various PLGA materials, i.e., PLGA (Mw: 7,000-17,000 g/mol, LA/GA: 50/50), PLGA (Mw: 24,000-38,000 g/mol, LA/GA: 50/50), PLGA (Mw: 54,000-69,000 g/mol, LA/GA: 50/50) and PLGA (Mw: 50,000-75,000 g/mol, LA/GA: 85/15) were used as the polymer fillers. The investigation was begun from release profile studies for 400-nm particles loaded with both Budesonide and Theophylline in different loading configurations (i.e., core: Budesonide and Theophylline; core: Budesonide, shell: Theophylline; core: Theophylline, shell: Budesonide). The results demonstrated that release rate of the core-loaded active ingredient was accelerated due to the void spaces left behind by the active ingredient loaded in the shell. Although the drug release rate was affected by the drug loading locations along with the void spaces left behind by the shell-loaded drug molecules, such a theory could not comprehensively explain the reasons behind the differences of release profiles of Budesonide and Theophylline from formulations F11-F19. Via the release profile characterizations of the core-loaded Theophylline from 400-nm particles (i.e., formulations F20, F22 and F23) composed of PLGA (Mw: 7,000-17,000 g/mol, LA/GA: 50/50), PLGA (Mw: 24,000-38,000 g/mol, LA/GA: 50/50) and PLGA (Mw: 50,000-75,000 g/mol, LA/GA: 85/15), the PLGA with lower molecular weight was confirmed to be effectively slowing down the release rate of Theophylline, achieving a 35% decrease in drug release within the first hour of the

2-day release testing according to release profiles of F20 and F22. The finding was attributed to the greater surface porosity and larger pore sizes of particles composed of PLGA materials with higher molecular weights, which was confirmed by the results of BET surface area analysis. The further decrease of Theophylline drug release rate was realized by loading Theophylline in core of the thick-shell particles (particle size: 1 μm) composed of PLGA (Mw: 7,000-17,000 g/mol, LA/GA: 50/50). The presence of Budesonide co-encapsulated with Theophylline in the core of the thick-shell PLGA particles did not influence the release rate of Theophylline. According to the literature reviews, this is a unique research providing effective strategies for extended release of Theophylline, a highly hydrophilic compound, from PLGA particulate drug carriers with the diameters no greater than 1 μm. No chemical reactions, such as polymer cross-linking during the drug encapsulation process or surface modification on particulate drug carriers, were involved in our methodology, suggesting its simplicity for simultaneous encapsulation of a highly hydrophilic agent and a highly hydrophobic agent for extended drug release as a small-molecule combination therapy. Formulation F25 could be promising for prevention and treatment of symptoms and blockage of airways caused by asthma with the slowly released combination of Budesonide and Theophylline. The delivery of Budesonide to the alveolar region with the 1-μm PLGA particle formulations can also minimize the immuno suppression that is usually resulted from deposition of steroid pharmaceutical aerosols at the upper airways for treating asthma.

Chapter 5

In vitro Drug Release of Small and Large-molecule Therapies from Core-shell Type ES PLGA Particles

5.1 Experiment and Conditions of Core-shell type ES PLGA Nanoparticles Generated via a Coaxial Dual Capillary Nozzle

Multiple drugs can induce synergistic therapeutic effects to achieve better biological outcomes. Combination therapy with multiple drugs administrated has become an important treatment modality in many disease categories, such as cancer, cardiovascular disease and infectious disease [Center for Drug Evaluation and Research, 2013].

Cancer arises from a loss of normal cellular growth control, which is caused by either uncontrolled cell growth or loss of a cell's ability to undergo apoptosis. The disrupted balance of cell growth and cell death leads to uncontrolled cell proliferation and eventually forms a tumor. Tumors which tend to invade nearby tissues, enter blood streams and metastasize to different sites of the human body are malignant tumors, also known as "cancer." With defense mechanisms against medicine, such as over expression of drug efflux pumps, enhancement of self-repairing ability, increase of drug metabolism, and expression of altered drug targets, the combination cancer therapy targeting multiple pathologic processes is considered the future for treatment of cancer for its intrinsic heterogeneous complexity [Cao et al., 2014]. Since the administration time, dose and sequence of different drugs are crucial to achieve greatest efficacy and tolerable toxicity to cancer patients, sequential drug release in a controlled fashion is thus important to combination cancer therapy [Yanping et al., 2017; Lee and Nan, 2012].

Micro- and nano-particles with multi-layered structures have attracted many people's attention for their capabilities of sequentially-extended drug release of more

than one active ingredient form the drug carriers [Lee et al., 2011]. Hybrid polymeric micelles with the core and envelope structure have been employed to co-encapsulate a conventional small-molecule chemotherapeutic agent Doxorubicin (Dox) and a small-molecule anti-angiogenesis agent Combretastatin (Com). Rapid release of Combretastatin (Com) loaded within the lipid envelope vascular collapse. The resultant intra-tumoral trapped nanoparticles endowed the drug carriers with longer duration for the subsequent slow release of the Doxorubicin (Dox) to kill tumor cells by inducing their apoptosis [Sengupta et al., 2005]. The anticancer effectiveness was reported to be significantly superior to physical mixtures of the two drugs or even the liposomal drug formulations. Inspired by the finding, the co-encapsulation of a conventional small-molecule chemotherapeutic agent and Bovine Serum Albumin (BSA, as a model drug of the monoclonal antibodies used for inhibition of the tumor angiogenesis) with the ES core-shell PLGA composite particles was conducted to investigate the resultant drug release profiles for their potential applications of sequential drug release against cancer. Molecular structure and selective physicochemical properties of Paclitaxel (PTX) and Bovine Serum Albumin (BSA) are summarized in Figure 5.1 [HUO et al., 2015; Drug Bank Website].
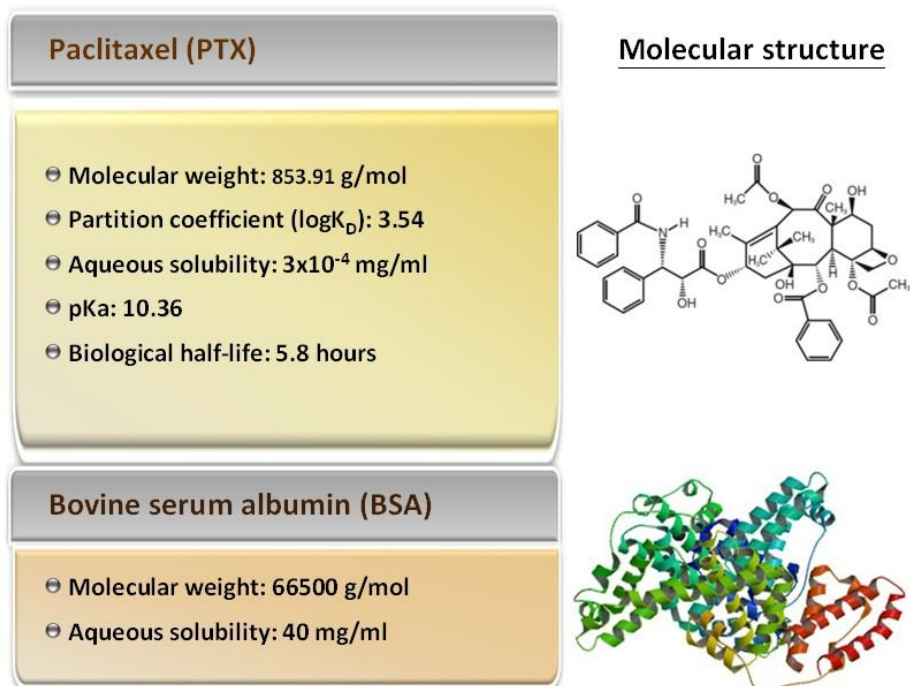
Figure 5.1. Molecular structures and selective physiological properties of Paclitaxel and Bovine Serum Albumin.

In chapter 5, PLGA (Mw: 7,000-17,000 g/mol, LA/GA: 50/50) was selected as the particle filling material for its excellent capability for extended release of the hydrophilic model drug (i.e, Theophylline) according to the results of our previous investigation in Chapter 4. PLGA particles with overall sizes ranging from the diameters of 400 nm and 880-1150 nm were utilized to encapsulate Bovine Serum Albumin and/ or Paclitaxel to study their *in vitro* drug release profiles. Process parameters of the coaxial dual capillary electrospray (ES) to generate the tested particle formulations are summarized in Table 5.1-5.3. Due to the lower solubility of BSA and PTX in Acetonitrile, the volumetric ratio of Acetonitrile-to-DMSO in the spray solvent mixture used in Chapter 5 was lowered from 75:25 to 50:50 in order to dissolve PTX. The co-solvent method, i.e., the micro-emulsion of BSA aqueous

solution in the polymer solution, was utilized for the encapsulation of BSA in ES core-shell particles. The BSA-to-PLGA ratio was set to be 1:50 for the highest BSA concentration to be encapsulated into PLGA particles and to be detectable by an appropriate protein assay. Accordingly, the PTX-to-PLGA ratio was set to be 2:10 in order to shorten the ES process time to minimize the extent of emulsion phase separation while PTX was still detectable by HPLC.

	Formulation ID	F27	F28
Inner solution	Electric conductivity (μ S/cm)	30	30
	Feeding flowrate (μ l/min)	0.5	0.5
	PLGA (Mw; LA/GA)	7K-17K; 50/50	7K-17K; 50/50
	PLGA conc. (mg/ml)	25	25
	PTX:PLGA mass ratio	1:5	-
	BSA:PLGA mass ratio	-	1:50
Outer solution	Electric conductivity (μ S/cm)	30	30
	Feeding flowrate (μ l/min)	2.5	2.5
	PLGA (Mw; LA/GA)	7K-17K; 50/50	7K-17K; 50/50
	PLGA conc. (mg/ml)	154.64	154.64
	PTX:PLGA mass ratio	-	-
	BSA:PLGA mass ratio	-	-
Spray solvent mixture		Acetonitrile/DMSO (50/50)	Acetonitrile/DMSO (50/50)
Tip-to-collector (TTC) distance (cm)		8.0	8.0

Table 5.1. Process parameters of the coaxial dual capillary ES for the generation of the core-shell PLGA (Mw: 7K-17K g/mol, LA/GA: 50/50) composite particles (particle size: 1 μm) singly encapsulating Paclitaxel (PTX) or Bovine Serum Albumin (BSA) in the cores of the particles.

Formulation ID		F28	F29	F30
Inner solution	Electric conductivity (μS/cm)	30	30	30
	Feeding flowrate (μl/min)	0.5	0.5	0.5
	PLGA (Mw; LA/GA)	7K-17K; 50/50	7K-17K; 50/50	7K-17K; 50/50
	PLGA conc. (mg/ml)	25	25	25
	PTX:PLGA mass ratio	-	-	-
	BSA:PLGA mass ratio	1:50	1:50	1:50
Outer solution	Electric conductivity (μS/cm)	30	30	30
	Feeding flowrate (μl/min)	2.5	2.5	2.5
	PLGA (Mw; LA/GA)	7K-17K; 50/50	7K-17K; 50/50	-
	PLGA conc. (mg/ml)	154.64	20	-
	PTX:PLGA mass ratio	-	-	-
	BSA:PLGA mass ratio	-	-	-
Spray solvent mixture		Acetonitrile/DMSO (50/50)	Acetonitrile/DMSO (50/50)	Acetonitrile/DMSO (50/50)
Tip-to-collector (TTC) distance (cm)		8.0	8.0	8.0

Table 5.2. Process parameters of the coaxial dual capillary ES for the generation of PLGA (Mw: 7K-17K g/mol, LA/GA: 50/50) composite particles with different shell layer thicknesses to encapsulate Bovine Serum Albumin (BSA) in the cores of the particles.

Formulation ID		F29	F31	F32
Inner solution	Electric conductivity (μS/cm)	30	30	30
	Feeding flowrate (μl/min)	0.5	0.5	0.5
	PLGA (Mw; LA/GA)	7K-17K; 50/50	7K-17K; 50/50	7K-17K; 50/50
	PLGA conc. (mg/ml)	25	25	25
	PTX:PLGA mass ratio	-	1:5	1:5
	BSA:PLGA mass ratio	1:50	1:50	-
Outer solution	Electric conductivity (μS/cm)	30	30	30
	Feeding flowrate (μl/min)	2.5	2.5	2.5
	PLGA (Mw; LA/GA)	7K-17K; 50/50	7K-17K; 50/50	7K-17K; 50/50
	PLGA conc. (mg/ml)	20	20	20
	PTX:PLGA mass ratio	-	-	-
	BSA:PLGA mass ratio	-	-	1:50
Spray solvent mixture		Acetonitrile/DMSO (50/50)	Acetonitrile/DMSO (50/50)	Acetonitrile/DMSO (50/50)
Tip-to-collector (TTC) distance (cm)		8.0	8.0	8.0

Table 5.3. Process parameters of the coaxial dual capillary ES for the generation of the core-shell type

PLGA (Mw: 7K-17K g/mol, LA/GA: 50/50) composite particles (particle size: 430 nm) loaded with

Bovine Serum Albumin (BSA) and/ or Paclitaxel (PTX) (F29: Core loaded with BSA; F31: Core

loaded with BSA and PTX; F32: Core loaded with PTX, shell loaded with BSA).

5.2 Release Profile Studies for PLGA Particles Loaded with One Single Agent

It is essential to learn drug release behaviors of an active ingredient from a

single dosage formulation before studying its release kinetics when it is

co-encapsulated with the other active ingredient within a single dosage formulation.

Hence, PLGA (Mw: 7,000-17,000 g/mol, LA/GA: 50/50) particles (particle size: 1 μm)

loaded with either Bovine Serum Albumin (BSA) or Paclitaxel (PTX) were generated

via process parameters of the coaxial dual capillary ES listed in Table 5.1 for this

purpose. The schematic diagrams of the as-produced particle formulations are shown

in Figure 5.2. According to the release profile of PTX shown in Figure 5.3 (A), less than 40% of the loaded drug was released within the first 8 hours of the 2-day release testing, which may be attributed to the hydrophobicity of PTX. The highly hydrophobic property of PTX led to slow drug dissolution and therefore slow rate of diffusion for drug release through the particles with thick shell layers. On the other hand, release rate of BSA, according to Figure 5.3 (B), was only slightly higher than that of PTX even though the aqueous solubility of BSA is much larger than that of PTX. The diffusion coefficient of BSA is significantly smaller than that of PTX. Therefore, the resultant release rate of BSA was not greatly higher than that of PTX and could be well controlled by the 1-μm core-shell particles composed of PLGA with lower surface porosity and smaller pore size, i.e., the PLGA (Mw: 7,000-17,000 g/mol, LA/GA: 50/50). The above findings conclude that extended release of both drug compounds can be realized by the ES core-shell PLGA particles with a drug individually loaded in core.

PTX-to-PLGA mass ratio = 1:5
BSA-to-PLGA mass ratio = 1:50

❖ Formulation ID: F27
❖ Polymer (shell):
  PLGA (Mw: 7K-17K g/mol,
  LA/GA: 50/50)
❖ PLGA (core):
  PLGA (Mw: 7K-17K g/mol,
  LA/GA: 50/50)
❖ Particle size: 890-1120 nm

❖ Formulation ID: F28
❖ Polymer (shell):
  PLGA (Mw: 7K-17K g/mol,
  LA/GA: 50/50)
❖ PLGA (core):
  PLGA (Mw: 7K-17K g/mol,
  LA/GA: 50/50)
❖ Particle size: 890-1120 nm

Figure 5.2. Schematic diagrams of drug-loaded ES core-shell PLGA (Mw: 7K-17K, LA/GA: 50/50) composite particle formulations (particle size: 1 μm) loaded with Paclitaxel (P) or Bovine Serum Albumin (BSA) in core of the particles.

(A)

117
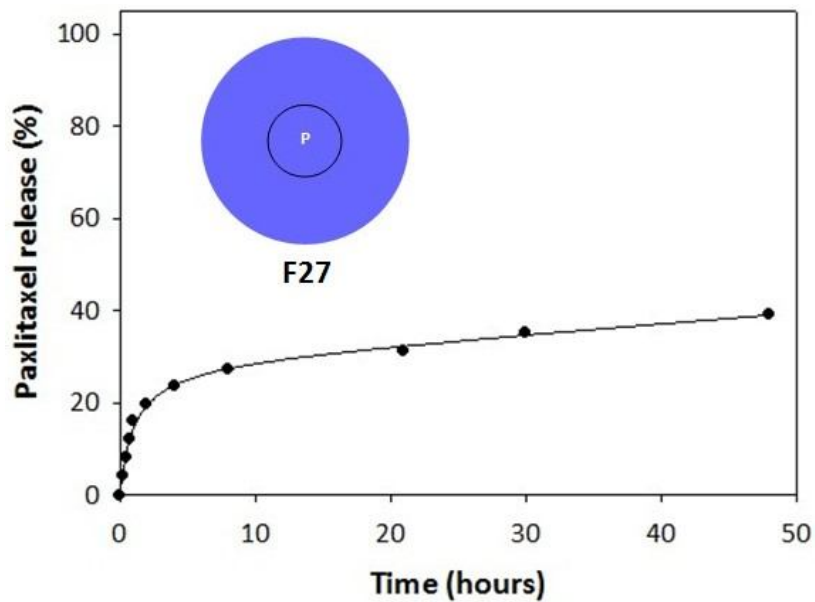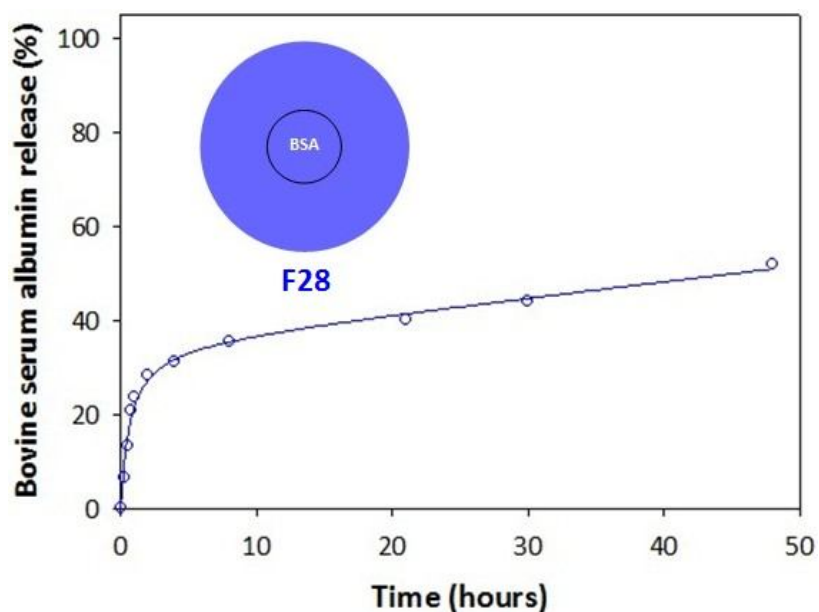
(B)

Figure 5.3. *In vitro* release profiles of (A) Paclitaxel (P) and (B) Bovine Serum Albumin (BSA) from

the cores of the 1-μm core-shell PLGA (Mw: 7K-17K g/mol, LA/GA: 50/50) particles with thick shell

layers.

5.3 Effects of Particle Shell Layer Thickness on BSA Drug Release

The effectiveness of particle shell thickness on the extended release of

hydrophilic small-molecule pharmacologic agent has been demonstrated by

investigating release profiles of Theophylline from core-shell PLGA (Mw:

7,000-17,000 g/mol, LA/GA: 50/50) particles (particle size: 400 nm and 1 μm) loaded

with Theophylline in particle core. Herein, the effect of particle shell thickness on

release behaviors of the core-loaded BSA was also investigated. PLGA particles

without shell layers and PLGA particles with shell layers but different in their

thicknesses were generated via process parameters of the coaxial dual capillary ES

technique listed in Table 5.2. PLGA (Mw: 7,000-17,000 g/mol, LA/GA: 50/50) was

the particle filler for its lower surface porosity and smaller pore size. Schematic diagrams of the prepared particle formulations (i.e., F28-F30) and the resultant BSA release profiles are given in Figure 5.4 (A) and (B), respectively. The BSA release profiles from PLGA (Mw: 7,000-17,000 g/mol, LA/GA: 50/50) particles with different shell layer thicknesses evidences that the release rate of core-loaded BSA was significantly decreased by gradually increasing the shell thickness of the particles. The differences of BSA release profiles between formulations F28, F29 and F30 were attributed to the slower permeation of surrounding release media through particle shell and longer distance for drug diffusion for the particle formulations with greater shell layer thicknesses. Considering the promise of sequential drug release in cancer therapy, we focused on the *in vitro* release behaviors of BSA and PTX from 400-nm core-shell PLGA (Mw: 7,000-17,000 g/mol, LA/GA: 50/50) particles for their potential biopharmaceutical applications in the following sections in this chapter.

Drug-to-PLGA mass ratio = 1:50

❖ Formulation ID: F30
❖ Polymer (shell):
  N/A
❖ PLGA (core):
  PLGA (Mw: 7K-17K g/mol, LA/GA: 50/50)
❖ Particle size: 249.4 nm

❖ Formulation ID: F29
❖ Polymer (shell):
  PLGA (Mw: 7K-17K g/mol, LA/GA: 50/50)
❖ PLGA (core):
  PLGA (Mw: 7K-17K g/mol, LA/GA: 50/50)
❖ Particle size: 429.4 nm

❖ Formulation ID: F28
❖ Polymer (shell):
  PLGA (Mw: 7K-17K g/mol, LA/GA: 50/50)
❖ PLGA (core):
  PLGA (Mw: 7K-17K g/mol, LA/GA: 50/50)
❖ Particle size: 890-1120 nm

(A)

(B)

Figure 5.4. Evaluation of the effect of particle shell layer thickness on release profiles of core-loaded BSA from PLGA (Mw: 7K-17K g/mol, LA/GA: 50/50) particles with various shell thicknesses: (A) schematic diagrams of tested particle formulations with different shell thicknesses, (B) *in vitro* BSA release profiles from particle formulations listed in (A).

5.4 Effects of Drug Combination on Release Behaviors

Similar to the research in extended release of fixed-combined Budesonide (the hydrophobic small-molecule model drug) and Theophylline (the hydrophilic small-molecule model drug) with PLGA particulate drug carriers, release profiles of core-loaded Bovine Serum Albumin (BSA, a model drug of protein biologics for the inhibition of tumor angiogenesis) were also investigated with or without Paclitaxel loaded together in the particle cores. According to BSA release profiles of the tested formulations F28, F29 and F30 given in Figure 5.4 (B) with different shell layer

thickness and accordingly different particle diameters, the 400-nm core-shell PLGA

(Mw: 7,000-17,000 g/mol, LA/GA: 50/50) particles were chosen to be the drug

carriers used for the relatively faster BSA release rate of F29 (around 40% of the

loaded BSA released within the first 4 hours of the release testing) than F28 and the

better sustained release profile for BSA from F29 than F30. Furthermore, the 400-nm

core-shell PLGA drug carriers are also more suitable for cancer therapy compared to

the 1-μm PLGA particles for their smaller particle sizes to accumulate in malignant

tumors. By using the ES process parameters listed in Table 5.3, the 400-nm core-shell

PLGA (Mw: 7,000-17,000 g/mol, LA/GA: 50/50) particle formulation loaded with

both Paclitaxel together with Bovine Serum Albumin (i.e., formulation F31) was

produced as the schematic diagram shown in Figure 5.5. To study the effects of

co-encapsulated Paclitaxel on release of Bovine Serum Albumin, the resultant Bovine

Serum Albumin release profile of formulation F31 was compared with that of

formulation F29 and shown in Figure 5.6. Faster BSA release rate from F31 was

observed, implying that the release rate of Bovine Serum Albumin was enhanced by

the presence of Paclitaxel when both drugs were loaded in the core of 400-nm PLGA

(Mw: 7,000-17,000 g/mol, LA/GA: 50/50) particles. The finding could be associated

with the void spaces in particle cores left behind after the release of Paclitaxel.

Compared to the effects of Budesonide (the hydrophobic small-molecule model drug)

on the release behaviors of Theophylline (the hydrophilic small-molecule model drug)

when both drugs were loaded in particle core (Section 4.2.5), release of the

hydrophobic small-molecule model drugs, i.e., Paclitaxel, in this case left behind

pores with larger sizes due to the larger molecular weight of Paclitaxel than

Budesonide. The release rate of Bovine Serum Albumin, the hydrophilic large-molecule model drug, was slower than that of Theophylline (the hydrophilic small-molecule model drug in Chapter 4). In the end, the void spaces left behind by the released Paclitaxel induced more rapid release media infusion, which accelerated the release rate of the co-encapsulated Bovine Serum Albumin in particle cores. Around 50% of the loaded BSA was released within the first 4 hours of the release testing suggests that F31 could be used for sequential release of Bovine Serum Albumin and Paclitaxel, which will be further discussed in the following sections.
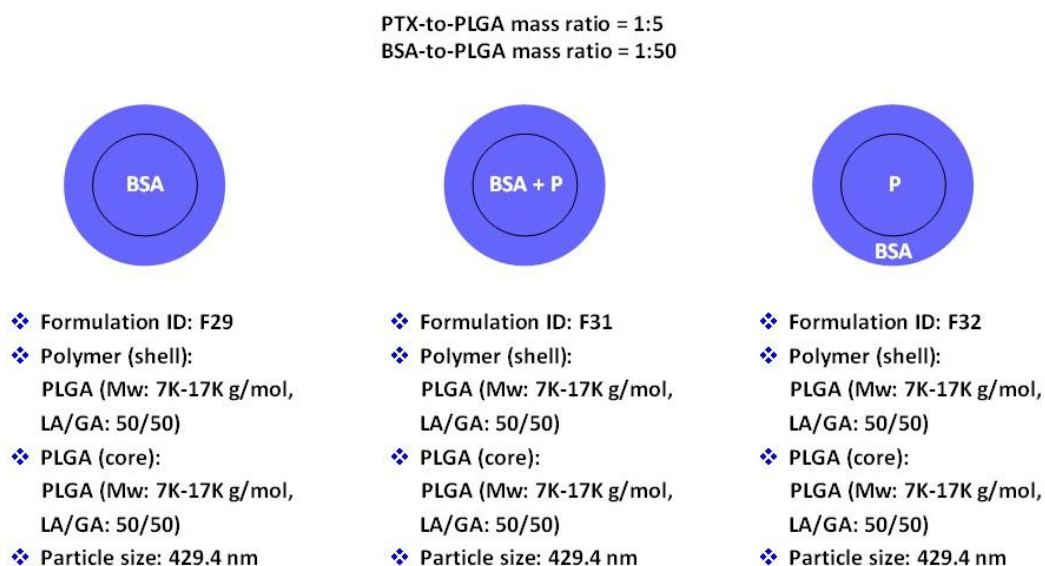
Figure 5.5. Schematic diagrams of the 400-nm core-shell PLGA (Mw: 7K-17K g/mol, LA/GA: 50/50) particle formulations loaded with Bovine Serum Albumin (BSA) and/ or Paclitaxel (PTX) in various tested drug loading configurations.
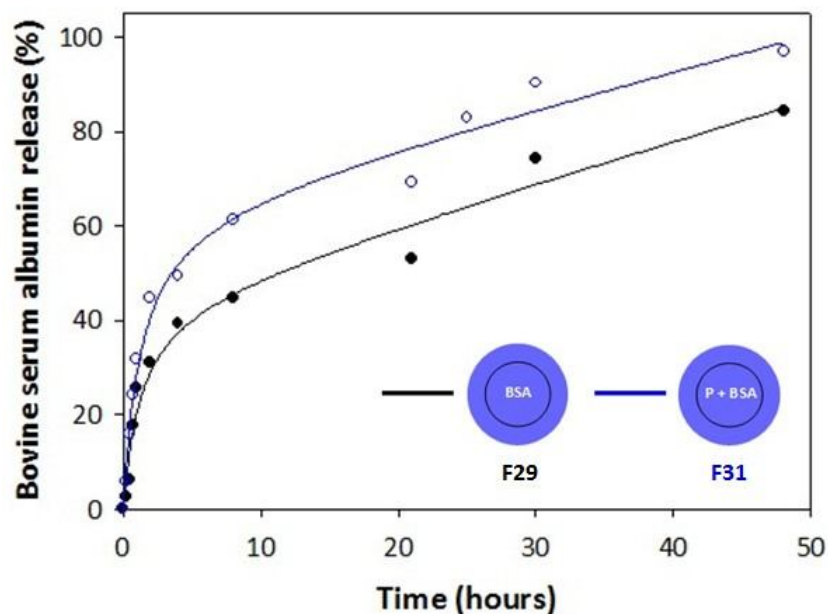
Figure 5.6. *In vitro* Bovine Serum Albumin (BSA) release profiles from the 400-nm core-shell PLGA (Mw: 7K-17K g/mol, LA/GA: 50/50) particle formulations loaded with Bovine Serum Albumin (BSA) and/ or Paclitaxel (PTX) in particle cores.

5.5 Sequential Drug Release of Fixed-dose Combination of BSA and PTX from PLGA Particles

To investigate the sequential release of Bovine Serum Albumin (BSA) and Paclitaxel (PTX) from the 400-nm core-shell PLGA (Mw: 7,000-17,000 g/mol, LA/GA: 50/50) particles, two particle formulations with designated drug loading configurations, i.e., F31 and F32 illustrated in Figure 5.5 , were generated via the ES process parameters listed in Table 5.3. The resultant PTX and BSA release profiles displayed in Figure 5.7 depict very limited variance in release behaviors of PTX and BSA between formulations F31 and F32. For formulation F32, release of shell-loaded Bovine Serum Albumin should create large void spaces that further improved the infusion of the release media to the particle core. However, the extent of the enhanced

release media infusion was insufficient to rapidly dissolve the core-loaded Paclitaxel since its aqueous solubility is extremely low (3×10^{-4} mg/ml). Therefore, the Paclitaxel release rate from F32 was slightly higher than that from F31 without too much difference. On the other hand, release rate of BSA was not appreciably increased by loading BSA in the particle shell (i.e., F32) as expected. The shell layer thickness (90 nm) of the 400-nm core-shell PLGA drug carrier was not thick enough to provide a barrier to the infusion of the release media and the diffusion of BSA. As a result, BSA release rates of F31 and F32 were almost identical without too much difference.
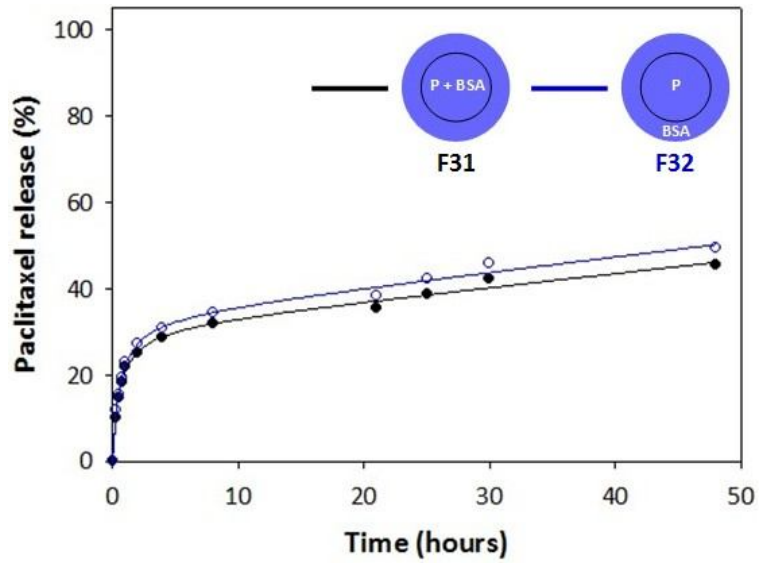
(A)
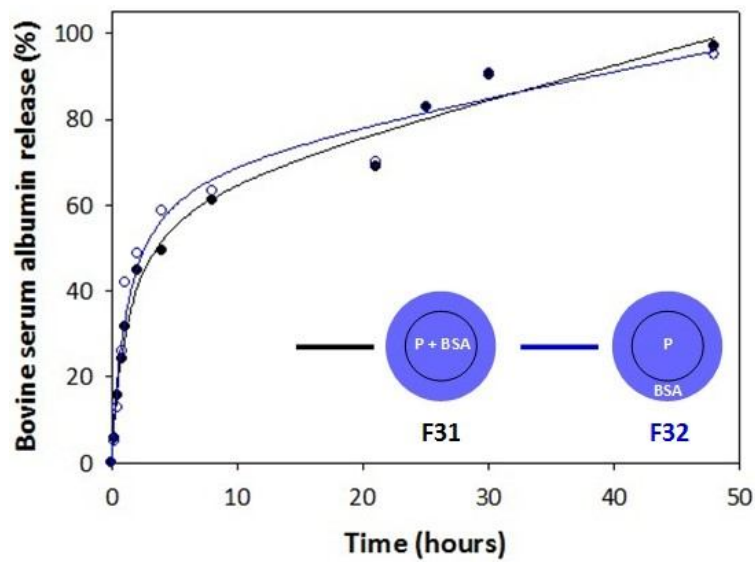
(B)

Figure 5.7. Release profiles of (A) Paclitaxel (P) and (B) Bovine Serum Albumin (BSA) from the 400-nm core-shell PLGA (Mw: 7K-17K g/mol, LA/GA: 50/50) composite particles loaded with Paclitaxel and Bovine Serum Albumin in tested drug loading configurations (F31: Core loaded with Paclitaxel and Bovine Serum Albumin; F32: Core loaded with Paclitaxel, shell loaded with Bovine Serum Albumin).

The overall release profiles of PTX and BSA from formulations F31 and F32 are given in Figure 5.8, concluding that both particle formulations were capable of sequentially releasing BSA first and then the PTX. The relatively faster release rate of BSA suggested that both formulations are able to more rapidly release monoclonal antibodies in the first place for the inhibition of tumor angiogenesis. The slower, but continuous, release of PTX unremittingly inhibits the cell division process for greater anti-cancer outcomes. As a conclusion, both formulations F31 and F32 could be promising for cancer therapy by sequential drug release.
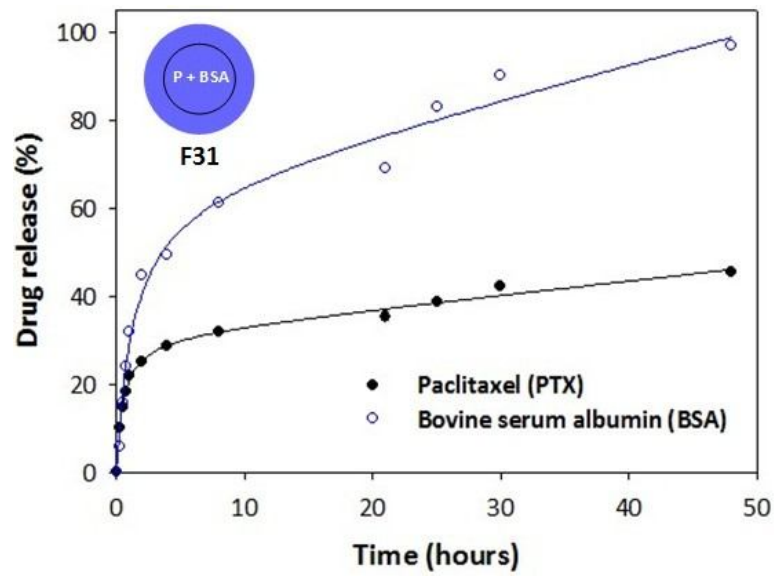
(A)
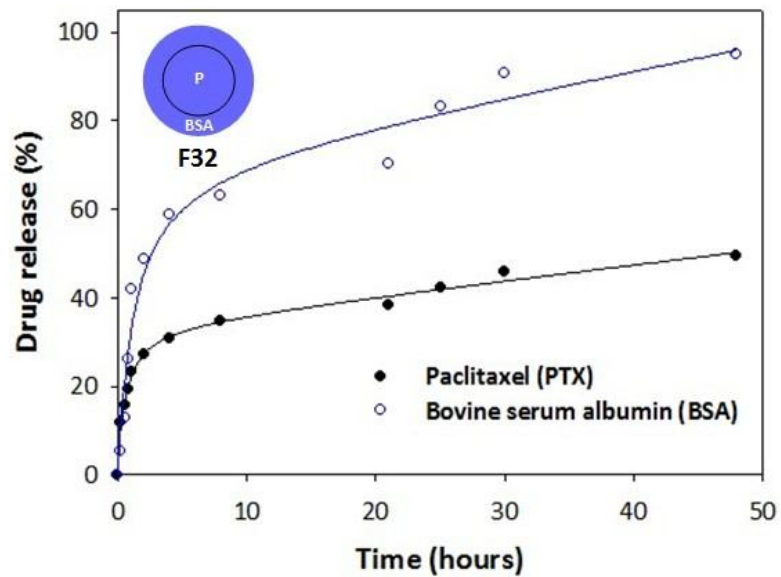
(B)

Figure 5.8. Release profiles of Paclitaxel (P) and Bovine Serum Albumin (BSA) from the 400-nm core-shell PLGA (Mw: 7K-17K g/mol, LA/GA: 50/50) composite particles loaded with Paclitaxel and Bovine Serum Albumin in tested drug loading configurations: (A) formulation F31, (B) formulation F32.

5.6 Summary

In this part of dissertation work, PLGA (Mw: 7,000-17,000 g/mol, LA/GA: 50/50) was selected as the particle filling material for its lower porosity and smaller pore sizes according to the results previously addressed in Chapter 4. Core-shell particles with the sizes of 400 nm and 1 μm were produced by the coaxial dual capillary ES to encapsulate Bovine Serum Albumin (BSA, the hydrophilic model drug of monoclonal antibodies) and/ or Paclitaxel, (PTX, the hydrophobic small-molecule chemotherapeutic agent). Release profiles of PTX and BSA singly loaded in the core of the 1-μm PLGA particles demonstrated that both drugs can be slowly released from the particulate core-shell particles used in this part of research. Particles with different shell layer thicknesses were also generated with BSA loaded in the core to study the effect of shell thickness on release behaviors of BSA. Results confirmed that release rate of BSA was associated with the particle shell thickness. Thicker particle shell layer decreased the release rate of BSA by prolonging the time for infusion of the release media to particle cores and the distance for the diffusion of BSA molecules to be released to the release media. Considering the BSA release rate of F29, the 400-nm core-shell PLGA particles were chosen as the drug carrier to study whether the BSA release behavior would be influenced by the presence of PTX in the same location within the particles. The increased release rate of core-loaded BSA was reported when PTX was co-encapsulated with BSA in core of the particles. The reason behind the observation was explained by greater infusion of the release media caused by the void spaces left behind by the release of PTX. Due to the appreciably larger molecule weight of BSA than small-molecule hydrophilic agents, greater infusion of the release

media had chances to accelerate the dissolution process for drug diffusion. Though the formulation F31 has demonstrated its capability of sequential drug release of BSA and PTX already, release profiles of the formulation F32 were further investigated to learn whether the release rate of BSA could be further enhanced by loading BSA in the shell region of the 400-nm core-shell particles. The results indicated that both release rates of PTX and BSA was not accelerated by loading BSA in particle shell, which was attributed to the extreme hydrophobicity of PTX and the fast dissolution of BSA. Through this part of the study, it was evidenced that the release rate of BSA can be tailored by the particle shell thickness, and the sequential release of BSA and PTX can be realized by the core-shell PLGA nanoparticles produced by the dual capillary ES technique as a potential pharmaceutical particle formulations for treating Metastatic Breast Cancer.

Chapter 6

Conclusions

6.1 Overall Summary

Effective drug concentration at the site of action for a sufficient duration is crucial in order to provide greater biological outcomes. Such a concept can be realized through the application of extended release formulations to drug delivery systems. Furthermore, the extended release formulations are also favorable to enhance the safety, the convenience and the compliance of the drug products for patients. Due to the capabilities of drug combinations to direct at multiple therapeutic targets for improved biological outcomes, the application of combination therapy has become an important therapeutic approach in many disease settings. Fixed-dose combinations (FDCs) offer an alternative to the patients requiring multiple therapies to manage their diseases for the simplified medication regimen and the improved patient compliance. Similar to the conventional monotherapy, maintaining blood levels of all released active ingredients from pharmaceutical dosages to be within the therapeutic window for longer period of time is important to assure the greatest efficacy and the minimized side effects to patients.

PLGA is a biodegradable polymeric material that has been approved by U.S. FDA and EMA and widely applied to extended drug release for its excellent biocompatibility and innocuous degradation products for minimal safety concerns. For the capabilities of fabricating PLGA particles with a myriad of filling material compositions, drug loading configurations, internal structures and sizes, the coaxial dual capillary electrospray (ES) technique was chosen to generate drug-loaded PLGA core-shell particles (particle size: 400 nm and 1 μm in diameter) to study factors influencing the resultant drug release behaviors of the loaded hydrophilic and/ or

hydrophobic model drug compounds. Key factors were also identified for most efficiently slowing down release rates of the hydrophilic model drugs. Drug release behaviors of all tested particle formulations were learned from their *in vitro* drug release profiles characterized by HPLC and the NanoOrange Protein Assay for small-molecule model drugs (Budesonide, Theophylline and Paclitaxel) and Bovine Serum Albumin (BSA, the model drug of monoclonal antibodies), respectively. Drug release testing was performed in 10 ml PBS (0.02 M, pH 7.4) as the release media at 36.5 ^{o}C. *In vitro* drug release studies of matrix-type PLGA (Mw: 7,000-17,000 g/mol, LA/GA: 50/50) nanoparticle formulations (particle size: 70-80 nm, produced by the single capillary ES) loaded with Budesonide at different Budesonide-to-PLGA ratios were performed to determine the drug-to-polymer ratio to be 1:10 for all tested particle formulations in Chapter 3 and Chapter 4 (except for formulations F17 and F26). Differently, the PTX-to-PLGA and the BSA-to-PLGA mass ratios were set at 1:5 and 1:50, respectively, for all tested particle formulations in Chapter 5 considering the aqueous solubility of BSA and the phase separation issue happening during the ES process. The major findings of the present dissertation work are summarized as below:

Part 1 In vitro release profile studies on Theophylline (the hydrophilic small-molecule model drug) and/ or Budesonide (the hydrophobic small-molecule model drug) from core-shell PLGA particles:

1. According to Theophylline release profiles of formulations F20 and F21, the release rate of Theophylline from the 400-nm core-shell PLGA (Mw: 50,000-75,000 g/mol, LA/GA: 85/15) particle formulations loaded with

Theophylline in the core can be increased by additionally loading Theophylline in particle shell. The finding suggests that the drug-loaded core-shell PLGA nanoparticles could be applied to repeat-action formulations to maintain the blood level of an active pharmaceutical ingredient with a short half-life within its therapeutic window for longer period of time.

2. The molecular weight and the lactic-to-glycolic ratio of PLGA are crucial for the sustained release of Theophylline. It is evidenced that the release rate of the core-loaded Theophylline is lower when Theophylline is loaded in the cores of the 400-nm particles composed of PLGA with a lower molecular weight and a lower LA/GA ratio because of the lower porosity and the smaller pore sizes of the particle filling material.

3. Release behaviors of Budesonide and Theophylline from core-shell PLGA particles co-encapsulating both drugs cannot be explained simply by the drug loading locations within the particles. Void spaces in the particle shell layers left behind by the release of the shell-loaded drug molecules can induce greater infusion of the release media and therefore accelerate the release rate of the core-loaded drug molecules.

4. The particle shell layer thickness is essential to sustained release of Theophylline. By using PLGA (Mw: 7,000-17,000 g/mol, LA/GA: 50/50) as the particle filler, the Theophylline release rate can be significantly decreased by core-shell particles with thicker shell layers.

5. The release rate of the core-loaded Theophylline from the 1-μm PLGA (Mw: 7,000-17,000 g/mol, LA/GA: 50/50) particles is not affected by the presence of

Budesonide loaded in particle cores. As a result, the 1-μm drug-loaded PLGA particle formulations co-encapsulating Budesonide and Theophylline in the cores are capable of slowly releasing both loaded drugs as a promising fixed-dose combination extended release formulation.

Part 2 In vitro release profile studies on Bovine Serum Albumin (the hydrophilic large-molecule model drug) and/ or Paclitaxel (the hydrophobic small-molecule model drug) from core-shell PLGA particles:

1. Sustained release of Bovine Serum Albumin (BSA) can be realized by the encapsulation of BSA in the cores of PLGA (Mw: 7,000-17,000 g/mol, LA/GA: 50/50) particles. The BSA release rate is also affected by the thickness of the particle shell layers. It is reported that the release rate of BSA is lower from the core-shell PLGA particles with greater shell thicknesses.

2. The presence of Paclitaxel (PTX) in the particle core accelerates the release rate of the core-loaded BSA when both compounds are co-encapsulated in the cores of the 400-nm PLGA (Mw: 7,000-17,000 g/mol, LA/GA: 50/50) particles. The finding implies the potential applications of the as-produced PTX-BSA loaded particle formulations to sequential release of a protein and a small-molecule conventional chemotherapeutic compound for combination cancer treatment.

3. The loading locations of BSA do not impact the performance of sequential drug release of the PTX-BSA loaded core-shell PLGA (Mw: 7,000-17,000 g/mol, LA/GA: 50/50) particles (particle size: 400 nm) when PTX is loaded in particle cores. The observation may be associated with the insufficient shell thickness and

the extremely low aqueous solubility of PTX.

6.2 Future Work

The present dissertation work is an exploratory study demonstrating one of the possible strategies for *in vitro* extended release and/ or sequential release of the fixed-dose combinations containing a highly hydrophobic small-molecule agent with a highly hydrophilic small-molecule or a hydrophilic large-molecule agent from PLGA particles. Due to the therapeutic effectiveness of the selected model drugs, the as-produced particle formulations could be potential for therapeutics of inhalation diseases and malignant tumors. However, more efforts are needed to study the feasibilities of the as-produced drug-loaded PLGA particles for the treatment of the aforementioned diseases:

1. The mixing of core-shell PLGA particles loaded with one drug individually could also be a strategy of fixed-dose combination therapy. Relevant particle formulation generation tasks and *in vitro* drug release testing should be conducted to study the resultant drug release profiles and their differences from the release profiles of core-shell PLGA particles co-encapsulating a hydrophilic and a hydrophobic model drug.

2. Phosphate buffered saline simulates only limited aspects of physiological fluids, the pH and the ionic strength. It is well established that drug release in PBS is different from that in protein-containing media. Release testing should be further performed in media containing proteins at a concentration relevant to the target site of actions in the human body. The pH and the osmotic pressure effects should

135

also be studied to confirm extended release of the drug-loaded particles can be achieved under the physiological environment of the target tissues.

3. The incapability of the electrospray (ES) to completely remove the solvents used in the process has been addressed in literature. To minimize the safety concerns of the residual solvent in the prepared PLGA particles, content of residual solvent should be identified before proceeding with the subsequent cell, animal, or even human studies.

4. From the view points of pharmaceutics, controlling drug release rate is meaningful when the active pharmaceutical ingredient is stable. That is why the stability of the small-molecule and the large-molecule model compounds during the release testing should be investigated in order to provide effective therapeutic outcomes to patients.

5. A simple and reliable process for mass production of the drug-loaded particles is the prerequisite for their real applications to disease treatment. That is why the multi-notched ES nozzle should be utilized to generate drug-loaded core-shell PLGA particles with greater mass throughput. The resultant *in vitro* drug release profiles should be studied for the performances of the as-produced PLGA particle formulations in extended and sequential drug release.

6. It is suggested that the cell and/ or animal studies should be conducted with the as-produced drug-loaded PLGA particles from this thesis work to further look into the safety and efficacy of the extended release and the sequential release particulate formulations.

References

Abdel-Mottaleb, M.M.A. and Lamprecht, A. Standardized in vitro drug release test for colloidal drug carriers using modified USP dissolution apparatus I, Drug Development and Industrial Pharmacy 37 (2) (2011) 178-184.

Ali, H, Weigmann, B., Neurath, M.F., Collnot, E.M., Windbergs, M., Lehr, C.-M. Budesonide loaded nanoparticleswith pH-sensitive coating for improved mucosal targeting in mouse models of inflammatory bowel diseases, Journal of Controlled Release 183 (2014) 167-177.

Almería, B., Fahmy, T.M., Gomez, A. A multiplexed electrospray process for single-step synthesis of stabilized polymer particles for drug delivery, Journal of Controlled Release 154 (2011) 203–210.

Anselmo, A.C., Mitragotri, S. An overview of clinical and commercial impacts of drug delivery systems, Journal of Controlled Release 190 (28) (2014) 15-28.

Bai, M.Y., Liu, S.Z. A simple and general method for preparing antibody-PEG-PLGAsub-micron particles using electrospray technique: An in vitro studyof targeted delivery of cisplatin to ovarian cancer cells, Colloids and Surfaces B: Biointerfaces 117 (2014) 346–353.

Bai, M.Y., Yang, H.C. Fabrication of novel niclosamide-suspension using an electrospray system to improve its therapeutic effects in ovarian cancer cells in vitro, Colloids and Surfaces A: Physicochem. Eng. Aspects 419 (2013) 248– 256.

Banker, G.S. & Rhodes, C.T. (Eds.). (2002). *Modern Pharmceutics*. New York: Marcel Dekker, Inc.

Barnes, P.J. Scientific rationale for inhaled combination therapy with long-acting β_2-agonists and corticosteroids, Eur Respir J 19 (2002) 182–191.

Beletsi, A., Panagi, Z., Avgoustakis, K. Biodistribution properties of nanoparticles based on mixtures of PLGA with PLGA–PEG diblock copolymers, International Journal of Pharmaceutics 298 (2005) 233–241.

Betageri, G.V., Kadajji, V.G., Venkatesan, N. Approaches for dissolution testing of novel drug delivery systems, American Pharmaceutical Review 14 (6) (2011) 38-44.

Bispo, M.S., Veloso, M.C.C., Pinheiro, H.L.C., De Oliveira, R.F.S., Reis, J.O.N., and De Andrade, J.B. Simultaneous Determination of Caffeine, Theobromine, and Theophylline by High-Performance Liquid Chromatography, Journal of Chromatographic Science 40 (2002) 45-48.

Bock, N., Dargaville, T.R., Woodruff, M.A. Electrospraying of polymers with therapeutic molecules: State of the art, Progress in Polymer Science 37 (2012) 1510–1551.

Cal, K., Sollohub, K. Spray Drying Technique. I: Hardware and Process Parameters, Journal of Pharmaceutical Sciences, 99 (2) (2010) 575-586.

Cao, Y., Wang, B., Wang, Y. and Lou, D. Polymer-controlled core–shell nanoparticles: a novel strategy for sequential drug release, RSC Advances 4 (2014) 30430-30439.

Chen, D.R., Pui, D.H.Y. and Kaufman, S.L. Electrospraying of conducting liquids for monodisperse aerosol generation in the 4 nm TO 1.8 μm diameter range, J. Aerosol Sci. 26 (6) (1995) 963-977.

Cho, Y.W., Lee, J., Lee, S.C., Huh K.M., Park, K. Hydrotropic agents for study of in vitro paclitaxel release from polymeric micelles, Journal of Controlled Release 97 (2004) 249– 257.

Danhier, F, Ansorena, E, Silva, J.M., Coco, R., Le Breton, A., Préat, V. PLGA-based nanoparticles: An overview of biomedical applications, Journal of Controlled Release 161 (2012) 505-522.

Davis, M.E., Chen, Z. and Shin, D.M. Nanoparticle therapeutics: an emerging treatment modality for cancer, Nature Reviews Drug Discovery 7 (2008) 771-782.

Enayati, M., Ahmad, Z., Stride, E. and Edirisinghe, M. One-step electrohydrodynamic production of drug-loaded micro- and nanoparticles, J. R. Soc. Interface 7 (2010) 667-675.

Ernst, O., Zor, T. Linearization of the Bradford Protein Assay, Journal of Visualized Experiments (2010) DOI: 10.3791/1918.

Fonseca, C., Simo˜es, S., Gaspar, R. Paclitaxel-loaded PLGA nanoparticles: preparation, physicochemical characterization and in vitro anti-tumoral activity, Journal of Controlled Release 83 (2002) 273–286.

Guan, Y., Zhou, Y., Sheng, J., Jiang, Z.Y., Jumahan, H. and Hu, Y. Preparation of ALA-loaded PLGA nanoparticles and its application in PDT treatment, J Chem Technol Biotechnol (2015) DOI 10.1002/jctb.4697.

Gupta, M., Bhargava, H.N. Development and validation of a high-performance liquid chromatographic method for the analysis of budesonide, Journal of Pharmaceutical and Biomedical Analysis 40 (2006) 423–428.

Guterres, S.S., Beck, R.C.R., Pohlmann, A.R. Spray-drying technique to prepare innovative nanoparticulated formulations for drug administration: a brief overview, Brazilian Journal of Physics 39 (1A) (2009) 205-209.

Hao, S., Wang, Y., Wang, B., Deng, J., Zhu, L., Cao, Y. Formulation of porous poly(lactic-co-glycolic acid) microparticles by electrospray deposition method for controlled drug release, Materials Science and Engineering C 39 (2014) 113-119.

HEYDER, J., GEBHART, J., RUDOLF, G., SCHILLER, C.F., and STAHLHOFEN, W. DEPOSITION OF PARTICLES IN THE HUMAN RESPIRATORY TRACT IN THE SIZE RANGE 0.005-15 μm, J. Aerosol Sci. 17 (5) (1986) 811-825.

HUO, M., ZHU, Q., WU, Q., YIN, T., WANG, L., YIN, L., ZHOU, J. Somatostatin Receptor-Mediated Specific Delivery of Paclitaxel Prodrugs for Efficient Cancer Therapy, JOURNAL OF PHARMACEUTICAL SCIENCES 104 (2015) 2018-2028.

Jaworek, A., Sobczyk, A.T. Electrospraying route to nanotechnology: An overview, Journal of Electrostatics 66 (2008) 197–219.

Kanakal, M.M., Abdul Majid, A.S., Sattar, M.Z.A, Ajmi, N.S. and Abdul Majid, A.M.S. Buffer-Free High Performance Liquid Chromatography Method for the Determination of Theophylline in Pharmaceutical Dosage Forms, Tropical Journal of Pharmaceutical Research January 13 (1) (2014) 149-153.

Kerimoğlu, O., Alarçin, E. Poly(lactic-co-glycolic acid) based drug delivery devices for tissue engineering and regenerative medicine, ANKEM Derg 26 (2) (2012) 86-98.

Lee, J.H. and Nan A. Combination Drug Delivery Approaches in Metastatic Breast Cancer, Journal of Drug Delivery 2012 (2012) Article ID 915375.

Lee, Y.H., Bai, M.Y., Chen, D.R. Multidrug encapsulation by coaxial tri-capillary electrospray, Colloids and Surfaces B: Biointerfaces 82 (2011) 104-110.

Lee, Y.H., Mei, F., Bai, M.Y., Zhao, S., Chen, D.R. Release profile characteristics of biodegradable-polymer-coated drug particles fabricated by dual-capillary electrospray, Journal of Controlled Release 145 (2010) 58–65.

Leonard, F., Ali, H., Collnot, E.M., Crielaard, B.J., Lammers, T., Storm, G., and Lehr, C.M. Screening of Budesonide Nanoformulations for Treatment of Inflammatory Bowel Disease in an Inflamed 3D Cell-Culture Model, ALTEX 29 (3) (2012) 275-285.

Makadia, H.K. and Siegel, S.J. Poly Lactic-co-Glycolic Acid (PLGA) as Biodegradable Controlled Drug Delivery Carrier, Polymers (Basel) September 1; 3 (3) (2011) 1377–1397.

Mei, F., Chen, D.R. Operational Modes of Dual-capillary Electrospraying and the Formation of the Stable Compound Cone-jet Mod, Aerosol and Air Quality Research 8 (2) (2008) 218-232.

Mu, L., Feng, S.S. Fabrication, characterization and in vitro release of paclitaxel (Taxol®) loaded poly (lactic-co-glycolic acid) microspheres prepared by spray drying technique with lipid / cholesterol emulsifiers, Journal of Controlled Release 76 (2001) 239–254.

Muthu, M.S. Nanoparticles based on PLGA and its co-polymer: An overview, Asian Journal of Pharmaceutics 3 (4) (2009) 266-273.

Nagavarma, BVN., Hemant, K.S.Y., Ayaz, A., Vasudha, L.S., Shivakumar, H.G. Different Techniques for preparation of polymeric nanoparticles-A review, Asian Journal of Pharmaceutical and Clinical Research 5 (3) (2012) 16-23.

Naikwade, S.R. and Bajaj, A.N. Development of a validated specific HPLC method for budesonide and characterization of its alkali degradation product, Canadian Journal of Analytical Sciences and Spectroscopy 53 (3) (2008) 113-122.

Nair, L.S., Laurencin, C.T. Polymers as Biomaterials for Tissue Engineering and Controlled Drug Delivery, Adv Biochem Engin/Biotechnol 102 (2006) 47–90.

O'Donnell, P.B., McGinity, J.W. Preparation of microspheres by the solvent evaporation technique, Advanced Drug Delivery Reviews 28 (1997) 25–42.

Olson, B.J. Assays for Determination of Protein Concentration, Curr Protoc Pharmacol (2016) doi: 10.1002/cpph.3.

Oprea, A.M., Nistor, M.T., Popa, M.I., Lupusoru, C.E., Vasile, C. In vitro and in vivo theophylline release from cellulose/chondroitin sulfate hydrogels, Carbohydrate Polymers 90 (2012) 127– 133.

Ozeki, T., Tagami, T. Drug/polymer nanoparticles prepared using unique spray nozzles and recent progress of inhaled formulation, Asian Journal of Pharmaceutical Sciences 9 (2014) 236-243.

Park, C.H., Lee, J. Electrosprayed Polymer Particles: Effect of the Solvent Properties, Journal of Applied Polymer Science 114 (2009) 430–437.

Patel, R.P., Patel, M.P. and Suthar, A.M. Spray drying technology: an overview, Indian Journal of Science and Technology 2 (10) (2009) 44-47.

Pereira, M.C., Hill, L.E., Zambiazi, R.C., Mertens-Talcott, S., Talcott, S., Gomes, C.L. Nanoencapsulation of hydrophobic phytochemicals using poly (DL-lactide-co-glycolide) (PLGA) for antioxidant and antimicrobial delivery applications: Guabiroba fruit (Campomanesia xanthocarpa O. Berg) study, LWT - Food Science and Technology 63 (2015) 100-107.

Popa, V. & Dumitriu, S. (Eds.). (2013), P.596-598. *Polymeric Biomaterials (Structure and Function), Volume 1.* Boca Raton, FL: Taylor & Francis Group.

Rezvanpour, A., Attia, A.B.E., and Wang, C.H. Enhancement of Particle Collection Efficiency in Electrohydrodynamic Atomization Process for Pharmaceutical Particle Fabrication, Ind. Eng. Chem. Res. 49 (2010) 12620–12631.

Rytting, E., Nguyen, J., Wang, X. & Kissel, T. Biodegradable polymeric nanocarriers for pulmonary drug delivery, Expert Opin. Drug Deliv. 5 (6) (2008) 1-11.

Sah, E and Sah, H. Recent Trends in Preparation of Poly(lactide-co-glycolide) Nanoparticles by Mixing Polymeric Organic Solution with Antisolvent, Journal of Nanomaterials, Volume 2015 (2015), Article ID 79460.

Schubert, S., Delaney, J.T. Jr and Schubert, U.S.. Nanoprecipitation and nanoformulation of polymers: from history to powerful possibilities beyond poly(lactic acid), Soft Matter 7 (2011) 1581–1588.

Sengupta S., Eavarone, D., Capila I., Zhao G., Watson N., Kiziltepe T. and Sasisekharan R. Temporal targeting of tumour cells and neovasculature with a nanoscale delivery system, NATURE 436 (28) (2005) 568-572.

Shendge, R.S., Sayyad, F.J. Formulation development and evaluation of colonic drug delivery system of budesonide microspheres by using spray drying technique, Journal of Pharmacy Research 6 (2013) 456-461.

Shi, K., Cui, F., Yamamoto, H., Kawashima, Y. Optimized preparation of insulin-lauryl sulfate complex loaded poly (lactide-co-glycolide) nanoparticles using response surface methodology, Pharmazie 63 (2008) 721-725.

Sipai, A.B.M., Vandana, Y., Mamatha, Y., Prasanth, V.V. Liposomes: An overview, Journal of Pharmaceutical and Scientific Innovation 1 (1) (2012) 13-21.

Smyth, H.D.C. & Hickey, A.J. (Eds.). (2011). *Controlled Pulmonary Drug Delivery*. New York: Springer-Verlag.

Sridhar, R. and Ramakrishna, S. Electrosprayed nanoparticles for drug delivery and pharmaceutical applications, Biomatter 3 (3) (2013) e24281-1 – e24281-12.

Sundaran, S., Buvaneswari, Muralidharan, S., Saji, M., Rajendran, SD. & Sankar, S. A reliable reverse phase high performance liquid chromatography method for a frequently prescribed Bronchodilator-Theophylline, Asian Journal of Pharmaceutical and Clinical Research 6 (2) (2013) 30-32.

Ungaro F., d' Angelo, I., Miro, A., La Rotonda, M.I. and Quaglia, F. Engineered PLGA nano- and micro-carriers for pulmonary delivery: challenges and promises, Journal of Pharmacy and Pharmacology 64 (2012) 1217-1235.

Valo, H, Peltonen, L., Vehvila¨inen, S., Karjalainen, M., Kostiainen, R., Laaksonen, T., and Hirvonen, J. Electrospray Encapsulation of Hydrophilic and Hydrophobic Drugs in Poly(L-lactic acid) Nanoparticles, Small 5 (15) (2009) 1791-1798.

Wang, Y., Wei, Y., Zhang, X., Xu, M., Liu, F., Ma, Q., Cai, Q., Deng, X. PLGA/PDLLA core–shell submicron spheres sequential release system: Preparation, characterization and promotion of bone regeneration in vitro and in vivo, Chemical Engineering Journal 273 (2015) 490–501.

Xie, J., Jiang, J., Davoodi, P., Srinivasan, M.P, Wang, C.H. Electrohydrodynamic atomization: A two-decade effort to produce and process micro-/nanoparticulate materials, Chemical Engineering Science 125 (2015) 32–57.

Xie, J., Lim, L.K., Phua, Y., Hua, J, Wang, C.H. Electrohydrodynamic atomization for biodegradable polymeric particle production, Journal of Colloid and Interface Science 302 (2006) 103–112.

Yang, W.W. and Pierstorff, E. Reservoir-Based Polymer Drug Delivery Systems, Journal of Laboratory Automation 17 (1) (2012) 50–58.

Yanping Ding, Shishuai Su, Ruirui Zhang, Leihou Shao, Yinlong Zhang, Bin Wang, Yiye Li, Long Chen, Qun Yu, YanWu, Guangjun Nie. Precision combination therapy for triple negative breast cancer via biomimetic polydopamine polymer core-shell nanostructures, Biomaterials 113 (2017) 243-252.

Zarchi, A.A.K., Abbasi, S., Faramarzi, M.A., Gilani, K., Ghazi-Khansari, M., Amani, A. Development and optimization of N-Acetylcysteine-loaded poly(lactic-co-glycolic acid) nanoparticles by electrospray, International Journal of Biological Macromolecules 72 (2015) 764–770.

Zambito, Y., Pedreschi, E., Colo, G.D. Is dialysis a reliable method for studying drug release from nanoparticulate systems?—A case study, International Journal of Pharmaceutics 434 (2012) 28– 34.

Zhang, L., Chan, J.M., Gu, F.X., Rhee, J.W., Wang, A.Z., Radovic-Moreno, A.F., Alexis, F., Langer, R., and Farokhzad, O.C. Self-Assembled Lipid Polymer Hybrid Nanoparticles: A Robust Drug Delivery Platform, ACS Nano 2 (8) (2008) 1696-1702.

Guidance for Industry: Codevelopment of Two or More New Investigational Drugs for Use in Combination, U.S. Department of Health and Human Services Food and Drug Administration Center for Drug Evaluation and Research (CDER) (2013).

United States pharmacopeia 35 (2012) 2394-2396.